universität wien

MASTERARBEIT / MASTER'S THESIS

Titel der Masterarbeit / Title of the Master's Thesis

"Investigation and characterization of traffic related (nano)particles from road runoffs along the river Wien."

verfasst von / submitted by

Armin Rohr, BSc

angesstrebter akademischer Grad / in partial fulfillment of the requirements for the degree of

Master of Science (MSc)

Wien, 2021 / Vienna 2021

Studienkennzahl lt. Stduienblatt / Degree programme as it appears on The student record sheet:	UA 066 815
Studienrichtung lt. Studienblatt / Degree programme as it appears on the student record sheet:	Masterstudium Erdwissenschaften
Betreut von / Supervisor:	Univ.-Prof. Dr. Thilo Hofmann

Acknowledgements

First, I want to thank Univ.-Prof. Dr. Thilo Hofmann and Dr. Frank von der Kammer, M.A. for giving me the opportunity to work on such a rewarding project and for sharing their knowledge and expertise. Many thanks also to Frédéric Loosli for his menthorship, inspiration and sharing his knowledge which supported the development of my scientific way of thinking during the whole study. I also want to thank Wolfgang Obermaier for sharing his lab experience especially during the development of the digestion protocol and Vesna Micic Batka for performing the SEM analysis but also all other members from the EDGE working group which are all very caring and always supportive. On a personal level I want to thank my girlfriend Bianca and my whole family for always supporting me and empower me during my life.

Graphical Abstract

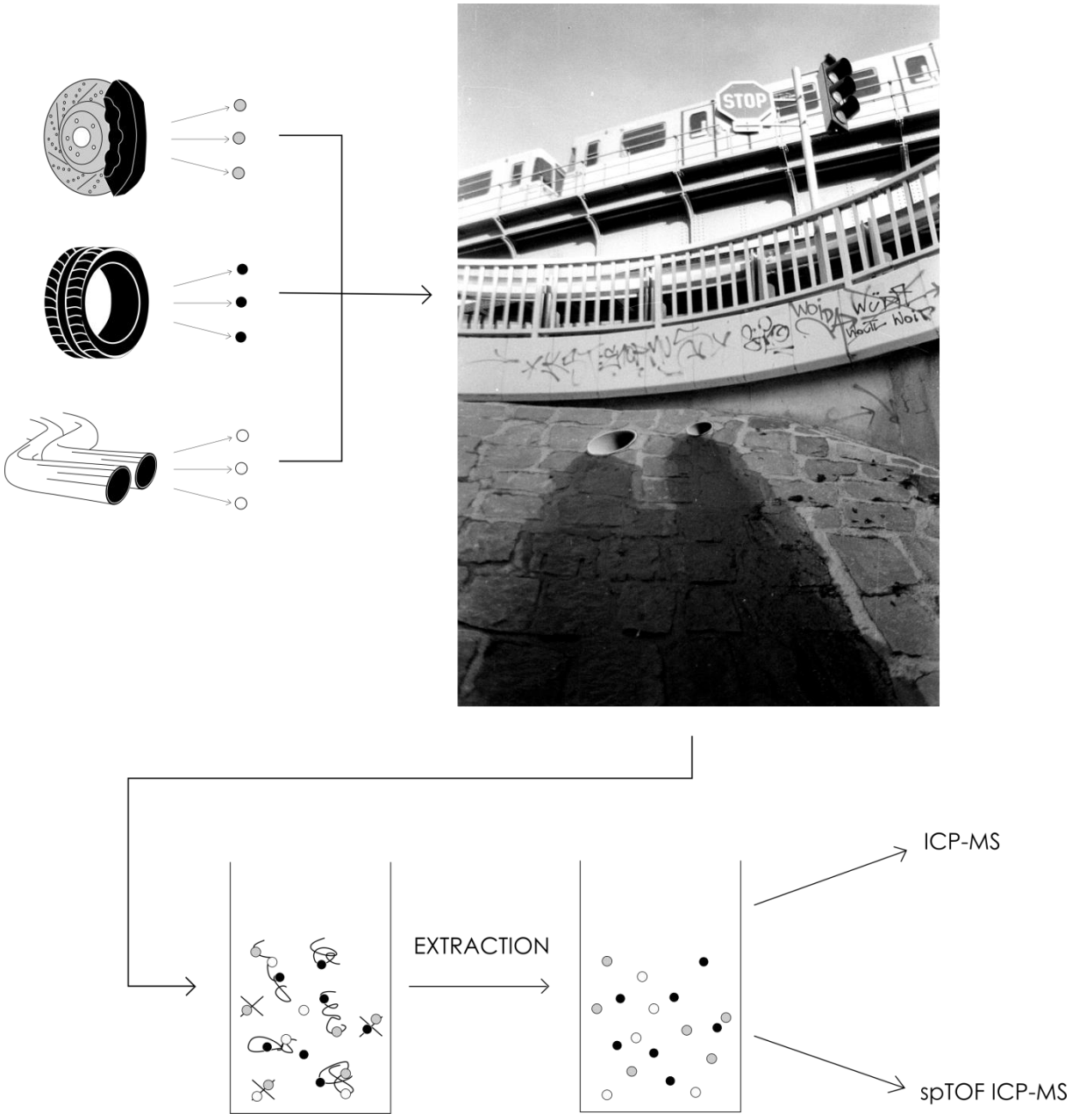

Abstract

Individual traffic is a major source of pollution, especially in urbanized areas where a high and continuously growing population density leads to an increasing volume of vehicles. As a result, emissions of traffic related particles (TRPs) are becoming increasingly important and significant as they may become a threat to health of organisms under uncontrolled release. Heavy metal containing particles are getting emitted by road traffic and some are deposed on road surfaces after they go airborne. During rain events deposed TRPs, in addition to particles in air, are eluted and getting transported in road runoff. TRPs may thus end up in roadside soils, surface water sediments, surface waters and wastewater treatment plants (WWTPs). TRPs are mainly produced through exhaust emissions as well as tire wear and brake wear from vehicles and contain a certain number of heavy metals.

The aim of this study is to determine the concentrations of TRPs in road runoff sediments and waters. Therefore, samples of road runoff waters and sediments were taken at accessible spots at a road runoff system of Vienna's west exit along the river Wien, with a measured traffic frequency up to 500 vehicles per 15min (Snizek+Partner Verkehrsplanungs GmbH).

Particles from waters and sediments were extracted using 5 dispersing agents. Indeed, in addition to ultra-purified water (UPW) particle extractions were also performed using 1mM $Na_4P_2O_7$ (Sodium Pyrophosphate), 1mM $Na_2C_2O_4$ (Sodium Oxalate), as well as with the two surfactants 1% Sodium Dodecyl Sulfate (SDS) and 1% FL-70. Suspensions with theoretical size cut-off of 10µm and 1µm particle were obtained by centrifugation. Waters and soil suspensions were analyzed to determine the distribution (size but also spatial distribution) of heavy metal containing TRPs.

Firstly, extracted suspensions and reference tire material have been total digested and metal concentrations of suspensions were measured by conventional inductively coupled plasma mass spectrometry (ICP-MS). It permits to evaluate the effect of the extraction agents on the extracted particles but also the spatial distribution of the TRPs between different sampling spots. Metal concentration in suspensions was also compared to published data of element concentration in local topsoil and upper crust. Multi element-single particle ICP-MS (ME-spICP-MS) was performed to get a better understanding on the element associations within extracted particles.

Potential TRPs were characterized on their chemical fingerprint and element mass ratios. Applied mass ratios were La/Ce, Ba/Sb, Ba/Pb, Sb/Pb and Cr/Mn which were chosen as this metal associations appear especially in brake and tire wear particles but may occur also naturally (e.g., clay minerals) with different and constant mass ratios. Catalyst products have also been determined by ME-spICP-MS and were defined by the presence of rhodium (Rh), palladium (Pd), platinum (Pt) as well as cerium (Ce).

Morphologies of dispersed colloids were observed through scanning electron microscopy (SEM).

Results show a significant change of chemical compositions in the analyzed sediment samples against the natural background likely caused through the exposure to road traffic emissions. Potential TRPs could have been identified on their chemical fingerprint and mass ratio in both runoff waters and sediments samples. Different extraction protocols show variations in particle concentrations but a constant trend for one certain extraction protocol on delivering enhanced metal concentrations cannot be observed. The applied method to quantify TRPs in road runoff offers new insights for the identification of tire- and brake wear as well as catalyst particles in natural matrices. Also, during this study a protocol to digest sediments containing tire rubber was developed.

Kurzfassung

Individualverkehr spielt eine bedeutende Rolle in Sachen Umweltverschmutzung, insbesondere in urbanen Gebieten, in denen eine hohe und stetig wachsende Bevölkerungsdichte zu einem steigenden Fahrzeugaufkommen führt. Infolgedessen werden partikuläre Emissionen aus dem Straßenverkehr (TRPs) Emissionen immer bedeutender, da sie bei unkontrollierter Freisetzung die Gesundheit von Organismen gefährden können. Schwermetallhaltige Partikel werden durch den Straßenverkehr emittiert, bevor sich infolgedessen eine Vielzahl an emittierten Partikeln auf Straßenoberflächen ablagert. Bei Regen werden die abgelagerten TRPs zusätzlich zu den Partikeln in der Luft eluiert und über den Straßenabfluss weitertransportiert. Dadurch können TRPs so in Böden am Straßenrand, in Oberflächengewässern sowie deren Sedimenten und in Kläranlagen landen. Hauptquellen durch die TRPs erzeugt werden sind Abgasemissionen sowie Reifen- und Bremsenabrieb von Fahrzeugen.
Ziel dieser Studie ist es, die Konzentrationen von TRPs in Sedimenten und Gewässern des Straßenabflusses zu bestimmen. Dazu wurden an zugänglichen Stellen eines Straßenabflusssystems der Wiener Westausfahrt entlang des Wienflusses (Verkehrsfrequenz: ~500 Fahrzeugen pro 15min laut Snizek+Partner Verkehrsplanungs GmbH), Proben von Straßenabflusswasser und Sedimenten genommen.
Partikel wurden mit fünf unterschiedlichen Reagenzen aus Wasser und Sedimenten extrahiert. So wurden neben Reinstwasser (UPW) auch Partikelextraktionen mit 1mM Na4P2O7 (Natriumpyrophosphat), 1mM Na2C2O4 (Natriumoxalat), sowie mit den beiden Tensiden 1% Natriumdodecylsulfat (SDS) und 1% FL-70 durchgeführt. Durch Zentrifugation wurden Suspensionen mit einer theoretischen Trenngrenze von 10µm und 1µm Partikelgröße gewonnen. Wasser und Sedimentsuspensionen wurden analysiert, um die Verteilung (Größe, aber auch räumliche Verteilung) der schwermetallhaltigen TRPs zu bestimmen. Extrahierte Suspensionen und Referenz-Reifenmaterial wurden aufgeschlossen und die Metallkonzentrationen der Suspensionen mittels konventioneller ICP-MS gemessen. Dies ermöglicht es, die Wirkung der Reagenzen auf die extrahierten Partikel, aber auch die räumliche Verteilung der TRPs zwischen verschiedenen Probenahmestellen, zu bewerten. Die Metallkonzentrationen in den Suspensionen wurden, anhand veröffentlichter Daten, mit derer lokaler Oberböden und der oberen Erdkruste verglichen. Multi-Element-Einzelpartikel-ICP-MS (ME-spICP-MS) wurde durchgeführt, um Aufschluss über Metalassoziationen in den extrahierten Partikeln zu erhalten. Potenzielle TRPs wurden anhand ihres chemischen Fingerabdrucks und Massenverhältnisse charakterisiert. Angewandte Massenverhältnisse waren La/Ce, Ba/Sb, Ba/Pb, Sb/Pb und Cr/Mn, da sie gleichzeitig in Brems- und Reifenabriebpartikeln aber auch konstant in der Natur (z.B. Tonminerale) vorkommen. Katalysatorprodukte wurden ebenfalls mittels ME-spICP-MS bestimmt und durch die Anwesenheit von Rhodium (Rh), Palladium (Pd), Platin (Pt) sowie Cer (Ce) definiert. Morphologien der dispergierten Kolloide wurden mittels Rasterelektronenmikroskopie (SEM) beobachtet.
Ergebnisse zeigen eine signifikante Veränderung der chemischen Zusammensetzung in den untersuchten Sedimentproben gegenüber dem natürlichen Hintergrund, die sehr wahrscheinlich durch die Belastung von Straßenverkehrsemissionen verursacht wurde. Potenzielle TRPs konnten anhand ihres chemischen Fingerabdrucks und ihres Massenverhältnisses sowohl im Abflusswasser- als auch in den Sedimentproben nachgewiesen werden. Verschiedene Extraktionsverfahren weissen eindeutige Variationen in den Partikelkonzentrationen auf. Jedoch konnte so weit nicht beobachtet werden, dass ein bestimmtes Extraktionsverfahren, erhöhte Partikelkonzentrationen betreffend aller beobachteten Metalle, gleichzeitig begünstigt. Die angewandte Methode zur Quantifizierung von TRPs in Straßenabflüssen bietet neue Erkenntnisse zur Identifizierung von Reifen- und Bremsenabrieb, sowie von Katalysatorpartikeln in natürlicher komplexer Matrix. Außerdem wurde im Rahmen dieser Studie ein Verfahren zum Aufschluss von reifengummihaltigen Sedimenten entwickelt.

Abstract

Il traffico è una delle principali fonti di inquinamento, soprattutto nelle aree urbanizzate dove una densità di popolazione elevata e in continua crescita porta a un maggiore numero di veicoli. Di conseguenza, le emissioni di particelle legate al traffico (TRPs) stanno aumentando e rappresentano una minaccia per la salute degli organismi in caso di rilascio incontrollato. Alcune particelle contenenti metalli pesanti ed emesse dal traffico cittadino si depositano sulle superfici stradali dopo essere state trasportate dall'aria. In particolare durante gli eventi di pioggia i TRP depositati, oltre alle particelle in aria, vengono eluiti e trasportati nel deflusso stradale finendo così nei suoli stradali, nei sedimenti delle acque superficiali, nelle acque superficiali e negli impianti di trattamento delle acque reflue (WWTP).

Questo studio mira a determinare le concentrazioni di TRPs prodotti principalmente attraverso le emissioni di scarico, l'usura dei pneumatici e dei freni dei veicoli nei sedimenti e nelle acque di deflusso stradale. A questo scopo sono stati prelevati campioni di acque e sedimenti di deflusso stradale in punti accessibili in un sistema di deflusso dell'uscita ovest di Vienna (lungo il fiume Wien) con una frequenza di traffico misurata fino a 500 veicoli per 15 minuti (Snizek+Partner Verkehrsplanungs GmbH).

Le particelle sono state estratte dalle acque e dai sedimenti utilizzando 5 agenti disperdenti: oltre all'acqua ultra-purificata (UPW) le estrazioni di particelle sono state eseguite anche con 1mM Na_4P_2O7 (pirofosfato di sodio), 1mM $Na_2C_2O_4$ (ossalato di sodio), così come con i due tensioattivi 1% Sodium Dodecyl Sulfate (SDS) e 1% FL-70. Le sospensioni con cut-off dimensionale teorico di 10µm e 1µm di particelle sono state ottenute per centrifugazione. Le acque e le sospensioni del suolo sono state analizzate per determinare la dimensione e la distribuzione spaziale dei TRP contenenti metalli pesanti.

In primo luogo, le sospensioni estratte e il materiale di riferimento del pneumatico sono stati sottoposti a digestione totale e le concentrazioni di metallo delle sospensioni sono state misurate mediante spettrometria di massa a plasma accoppiato induttivamente (ICP-MS). Questo permette di valutare l'effetto degli agenti di estrazione sulle particelle estratte, ma anche la distribuzione spaziale dei TRP tra diversi punti di campionamento. La concentrazione di metalli nelle sospensioni è stata anche confrontata con i dati pubblicati sulla concentrazione di elementi nel topsoil locale e nella crosta superiore. Multi element single particle ICP-MS (ME-spICP-MS) è stata eseguita per ottenere una migliore comprensione delle associazioni di elementi all'interno delle particelle estratte.

I potenziali TRP sono stati caratterizzati sulla loro impronta digitale chimica e sui rapporti di massa degli elementi. I rapporti di massa applicati (La/Ce, Ba/Sb, Ba/Pb, Sb/Pb e Cr/Mn) sono stati scelti perché queste associazioni di metalli appaiono soprattutto nelle particelle di usura dei freni e degli pneumatici, ma possono verificarsi anche in natura (ad esempio, minerali di argilla) con rapporti di massa diversi e costanti. I prodotti del catalizzatore sono stati determinati anche da ME-spICP-MS e sono stati definiti dalla presenza di rodio (Rh), palladio (Pd), platino (Pt) e cerio (Ce). Le morfologie dei colloidi dispersi sono state osservate attraverso la microscopia elettronica a scansione (SEM).

I risultati mostrano un cambiamento significativo delle composizioni chimiche nei campioni di sedimenti analizzati rispetto al fondo naturale dovuto probabilmente all'esposizione alle emissioni del traffico stradale. Potenziali TRPs sono stati identificati in base alla loro impronta chimica e al rapporto di massa sia nelle acque di deflusso che nei campioni di sedimenti. Diversi protocolli di estrazione mostrano variazioni nelle concentrazioni di particelleTuttavia, finora non è stato possibile ottenere un aumento delle concentrazioni con nessun protocollo, per quanto riguarda tutti i metalli osservati. Il metodo applicato per quantificare TRPs nel deflusso stradale offre nuove intuizioni per l'identificazione di pneumatici e usura dei freni, così come le particelle di catalizzatore in matrici naturali. Inoltre, durante questo studio è stato sviluppato un protocollo per digerire i sedimenti contenenti gomma da pneumatici.

List of Figures

List of Tables

Abbreviations

CO_2 ..... Carbon dioxide
CSV ..... Comma-seperated values
DI ..... Deionized water
DLS ..... Dynamic light scattering
EC ..... European comission
EDX ..... Energy-dispersive X-ray microanalysis
ENM ..... Engineered nanomaterial
HCl ..... Hydrochloric acid
HF ..... Hydrofluoric acid
H_5F_2N ..... Ammonium bifluoride
HNO_3 ..... Nitric acid
H_2O_2 ..... Hydrogen peroxide
HV ..... High voltage
ICP-MS ..... Inductively coupled plasma mass spectrometry
ICP-TOFMS ..... Inductively coupled plasma-time of flight mass spectrometer
INM ..... Incidental nanomaterial
NM ..... Nanomaterial
NNM ..... Natural nanomaterial
NOCl ..... Nitrosyl chloride
NOM ..... Natural organic matter
PGE ..... Platinum group elements
PM_{10} ..... Particles which pass through a size-selective inlet with a 50% efficiency (by mass) cutoff at 10µm aerodynamic diameter
$PM_{2.5}$ ..... Particles which pass through a size-selective inlet with a 50% efficiency (by mass) cutoff at 2.5µm aerodynamic diameter
PE ..... Polyethylene
PFA ..... Perfluoralkoxy
PP ..... Polypropylene
PSD ..... Partice Size Distribution
SEM ..... Scanning electron microscope
SDS ..... Sodium dodecyl sulfate
SPP ..... Sodium pyrophosphate
SOM ..... Soil organic matter
SOx ..... Sodium oxalate
TOC ..... Total organic carbon
TRP ..... Traffic related particulates
TWC ..... Three-way catalists
UPW ..... Ultra pure water
WWTP ..... Wastewater treatment plant

Table of Content

1. Introduction

The aquatic environment is very vulnerable and could easily get damaged through anthropogenic pollution sources (Häder et al., 2020). Anthropogenic inorganic pollution is mainly caused through release of heavy metals in high concentrations into the environment which can be a threat to the health of organisms (Mohammed et al., 2011). Next to industrial waste dumping as one of the main anthropogenic inorganic pollution sources (Häder et al., 2020) additional sources of heavy metal contamination through anthropogenic activities are of significant relevance such as incidental (nano) materials (INMs) released through road traffic emissions (Grigoratos and Martini, 2014). Material that gets emitted from road traffic goes airborne and may be deposed on road surfaces. During rain events such materials may get transported into surface waters, surface water sediments, roadside soils and wastewater treatment plans (WWTPs) through road runoffs (Li et al., 2005). Previous studies frequently reported that traffic related particles (TRPs) such as emitted brake dust and tire wear contain significant amounts of heavy metals (Boulter, 2006; Thorpe and Harrison, 2008; Puisney et al., 2018). Within cities road runoff usually gets collected with domestic wastewater in combined sewer systems and then treated in municipal WWTPs (Reemtsma et al., 2006). Nevertheless, in case of combined sewer overflow or in separate sewer systems, road runoff may be discharged without or with only partial treatment (Baur et al., 2020) and thus heavy metal containing TRPs can be released into surface waters.

Emitted TRPs are categorized according to their production source into two main classes. The first class is exhaust TRPs which are the final product of incomplete fuel combustion, lubricant volatilization as well automotive catalysts particles. The second class includes non-exhaust TRPs, primarily generated through tire and brake wear (Grigoratos et al., 2014; Folens et al., 2018). Overall, it is estimated that approximately 40-50% by mass of generated brake wear particles and only 0.1-10% of tire wear particles are emitted as PM_{10} (Garg et al., 2000; Sanders et al., 2003; Mosleh et al., 2004; Wik and Dave., 2009; Kukutshová et al., 2011; Harrison et al., 2012; Kumar et al., 2013) while there is a general agreement that exhaust related emissions can be classified as $PM_{2.5}$. It was suggested that non-exhaust related particles contribute to both the fine and the coarse mode of PM_{10} (Boulter, 2006; Dahl et al., 2006; Gustafsson et al., 2008; Kukutshová et al., 2011; Harrison et al., 2012). Elevated metal and metal oxide contents in road runoffs caused by road traffic emissions have been reported for fine particle fractions with a particle sizes below 1µm to the size of nanomaterials (NMs) (Helmreich et al., 2010; Sutherland et al., 2012; Charters et al., 2015; Hilliges et al., 2017; Folens et al., 2018; Lanzerstorfer, 2018;

Baur et al, 2019). Since TRPs contain metals that may be a threat on the health of organisms after exposure of toxic concentrations (IARC, 1989; Varrica et al., 2013), policy and health organizations should be alerted to observe metal concentrations in road runoffs which may be elevated due to the emission of TRPs. To do so it may require scientifically developed methods and protocols which are designed to extract, detect, and characterize TRPs that are embedded in complex natural matrices.

Meanwhile several methods have been developed to extract fine particulates and certain NMs from soils and aquatic samples e.g., centrifugation, cloud point- and aqueous colloidal-extraction (Hartmann et al., 2013; von der Kammer et al., 2012; Tang et al., 2009). To assess metal concetration spectrometry techniques are routine tools (Lee et al,2014). Metal concentrations in sediments and waters may be determined by the analysis of total dissolved metal concentrations after total digestion of TRPs and their embedded matrix with conventional ICP-MS (Falciani et al, 2000) and a comparison against the natural background. In addition, infomation on element association on a particle level may be investigated by multi element-single particle-inductively coupled plasma-mass spectrometry (ME-sp-ICP-MS). Such technique may be a promising approach to investigate TRPs' chemical fingerprints (Praetorius et al., 2017).

Detection and quantification of TRPs in the environment is hampered by 1.) heteroaggregation of TRPs with natural colloids (*e.g.*, clays, natural organic matter (NOM), *etc*). 2.) the heterogeneity (size distribution, chemical compositions, surface chemistry, etc) of TRPs and 3.) INMs as released TRPs in road runoff waters and sediments are often embedded in matrices with NNMs having similar chemical composition which complicates their detection (Montaño et al., 2014).

Thus, specific extraction protocols to extract TRPs from natural matrices and well-defined chemical fingerprints of TRPs need to get developed for a detection and characterization of TRPs in road runoffs.

2. State of knowledge

2.1. Detection of TRPs in natural matrices

Detection, quantification, and characterization of INMs such as TRPs in environmental systems is limited by their heteroaggregation, resulting in their spread over a wide particle size distribution (PSD) (Labille et al., 2015; Praetorius et al., 2014; Therezien et al., 2014; Wang et al., 2015) and due to the coexistence of NNMs such as clay minerals that could appear to have similar elemental compositions (Montaño et al, 2014). Hence dispersing NMs into their primary particles is a prerequisite to enable analysis of NM primary particle sizes (Tuoriniemi et al. 2014, Wagner et al. 2014, Baalousha et al. 2016). Increasing electrostatic repulsion between NMs within aggregates by altering the suspension pH using an indifferent electrolyte may break them apart into smaller aggregates and/or into primary particles (Baalousha 2009, Loosli et al. 2013). Alternatively, particle dispersing agents have been shown to disperse metal oxide NNMs and NOM from soils more efficiently by increasing NNM surface charge (Hall et al. 1996, Pronk et al. 2011, Regelink et al. 2014, Tatzber et al. 2007). Previous studies used sodium pyrophosphate (SPP), sodium oxalate (SOx), sodium dodecyl sulfate (SDS) and FL-70 as dispersing agents (Hall et al., 1996; Fujitake et al., 1998; Loosli et al, 2018; Baur et al., 2019). Next to chemical treatments, sonication over a certain time is a commonly used method to release heteroaggregation between NMs physicaly within suspensions (Li et al., 2012). Generating a certain particle size cutoff by size separation through centrifugation or filtration finally enables the analysis of NMs with selected sizes (Tang et al., 2009; Bakshi et al., 2014). Furthermore, possibilities of NM detection obviously are depending on the extraction size cutoff, meaning, the particle size cutoff introduced by the extraction method must meet the requirements of the detection technique in terms of lower and upper size limits. Anyway, for emitted exhaust related TRPs and brake wear particles sizes below 10µm are suggested in previous studies (Baur et al., 2019; Grigoratos et al., 2014). Tire wear particles may also be found as particulates with a size below 10µm although it is known that only about 10% of emitted tire particles by mass are released as PM_{10} (Grigoratos et al., 2014).

To get overall information about PSD, dynamic light scattering (DLS) is commonly used. Nevertheless, DLS is unable to distinguish different particle types or particle composition, is based towards larger particles and has limited capabilities to resolve multi-modal or polydisperse distributions correctly (Xing et al., 2016). Furthermore, DLS is unable to analyse

primary particles within aggregates (Xing et al., 2016). Zeta (ζ) potential, a factor that is related to the surface charge of NMs and influences particle agglomeration, can be determined by Laser-Doppler Anemometry in most commercially available DLS instruments (Helmenstine, 2019). Because it is not possible to differentiate between NNMs and TRPs by a DLS analysis alone, other measurement methods are applied, by which it is possible to get information about the chemical compositions of NMs e.g., scanning electron microscopy (SEM) and transmission electron microscopy (TEM) coupled with analytical tools such as Energy-dispersive X-ray analysis (EDX) (Wang et al., 2019). A common method for NM detection is the time-resolved single particle inductive coupled plasma-mass spectrometry (spICP-MS) (von der Kammer et al., 2012). Through spICP-MS it is possible to get information about the number concentration and size distribution of particles that have at least a diameter above 10nm (Au, Ag) to 80nm (Ti, Si) depending on the respective element, the isotopic abundance of the selected isotope and the mass fraction of the isotope in the particle (Lee et al., 2014). Nevertheless, in time-resolved mode on conventional quadrupole and sector-field ICP-MS spectometers measureing multiple isotopes at the same time can not be practiced, which means a direct distinction between potential TRPs and NNMs is rarely possible. Therefore time-of-flight (TOF) based ICP-MS spectrometers allow particle measurements of several isotopes in one single particle event simultaneously which is the prerequisite for the distinction between TRPs and NNMs through single-particle multi-element fingerprinting (spMEF) and which can be performed by ICP-TOFMS as described by Praetorius et al. (2017) for the distinction of Cerium containing ENMs and NNMs.

For the chemical characterization of TRPs, trace metals are chosen through frequently reported inorganic sources as colloids containing Fe, Pb, Cu, Ba, Sb, Zn, Cr, Mn, Zr, Cd and Ni particles are released by brake linings during braking manoeuvres (Boulter, 2006; Thorpe and Harrison, 2008; Folens et al., 2018; Puisney et al., 2018). Tire wear particles are characterized by predominantly Zn as it is an important additive during the tire vulcanization process and in lower amounts W, Fe, Ti, Cu, Cr, Te and Mo (Adachi et al., 2004; Boulter, 2006; Thorpe and Harrison, 2008; Apeagyei et al., 2011; Harrison et al., 2012). Ce is used as tracer for both exhaust and non exhaust TRPs as it appears in the form of CeO_2 which is known as the most insoluble oxide under ambient conditions and is used as an oxygen storage and combustion catalyst, for optical polishing and as fuel additive (von der Kammer et al., 2012). Finally, Pt, Pd and Rh particles will be investigated and used as source for emissions from automotive catalytic converters which is often be mentioned as the main source of environmental pollution through platinum group elements (PGEs) (Domesle, 1997; Folens et al., 2018).

2.2. Behavior of NMs in natural matrices

The preparation for effective NM extraction from natural matrices obviously requires the necessary background knowledge, as there are several factors that need to be considered. Basically, the stability, fate, and transformations of NMs is strongly influenced by the water properties (pH, ionic strength, electrolytes valency, etc.), the NM intrinsic properties (surface chemistry and charge, size, shape) and the presence of aquagenic compounds (such as colloids) (Baalousha, 2009; Philippe and Schaumann, 2014; Loosli et al., 2015). A theoretical model on the colloid stability was developed by Derjaguin, Landau, Verwey and Overbeek (DLVO) to understand the interactions between colloidal particles and their agglomeration behavior (Derjaguin, 1939; Derjaguin and Landau, 1941; Verwey and Overbeek, 1948). Briefly explained, in the DLVO theory the stability of particles may be estimated based on the potential of interaction between particles (particle free energy). The interaction potential, which is a function of the particles sepraration distance, is approximated in the DLVO theory by being equal to the sum of the van der Waals *(VvdW)* and the double layer *(Vdl)* interactions (Eq.1).

Eq.1. Interaction potential $$V(h) = V_{vdW}(h) + V_{dl}(h)$$

The van der Waals interactions are due to the interaction of rotating and fluctuating dipoles (permanent or induced) of atoms and molecules. They refer to Keesom, Debye and London forces and are most of the time attractive intermolecular interactions. Van der Waals forces are short-range distance forces. The second interaction considered in the DLVO theory is the double layer interaction which are due to the overlap of the diffuse part of the charged particle double layers. Double layer interactions can be attractive or repulsive forces depending on the nature of the charge of the particles and are influenced by the particles charges in natural matrices, where NMs are often associated with natural organic matter (NOM) and have the ability to form larger heteroaggregates through organo-mineral interactions (Buffle et al., 1998; Cornelis et al., 2014). When (nano)particles interact with NOM the stability of these particles is strongly dependent on the particle intrinsic properties (size, surface charge, etc), the NOM physicochemical properties (chemical composition, structural charge, molecular weight, etc) and concentration (i.e. influence of the particle surface coverage, osmotic pressure, etc) and the water systems properties (pH, ionic strength, etc) (Colvin 2003, Ju-Nam and Lead 2008, Klaine et al. 2008, Nowack and Bucheli 2007, Wiesner et al. 2006). The zeta (ζ) potential is related to the surfaces charge of particles and does provide indication on such colloid stability. ζ potential

values will be suggested as ±0–10 mV highly unstable particles, ±10–20 mV relatively stable particles and ±20–30 mV moderately stable and>± 30 mV highly stable particles (Bhattacharjee, 2016).

2.3. Aims and Hypotheses

Overall, the aim of this study is to detect and quantify the amount of emitted TRPs in Vienna's road runoff waters and road runoff exposed sediments by applying a multi method approach. Insights are meant to confirm that road runoffs favor the transport of a high number of TRPs during rain events. This will affirm, that in future, road departments and policy should consider the release of TRPs in the design of road runoff systems to avoid impending contamination. Also, findings and results generated during this study should facilitate the approach of future studies focused on investigating released TRPs distributed and embedded in environmental matrices.

Hypotheses 1

We expect that TRPs may change compositions of heavy metals in sediments that are exposed to road runoffs along the river Wien. Thus, concentrations of trace metals reported to be present in certain TRPs may be elevated in the taken samples compared against the natural background (Kreiner, 2004; Salminen 2007; Pfleiderer et al., 2012; Simon et al., 2012). To verify this assumption, concentrations of total dissolved metals in digested samples will be measured with conventional ICP-MS and will get confronted with present data of heavy metal concentrations in Vienna's upper crust and urban sediments and soils. Road runoff waters exposed sediment samples were collected at Vienna's west exit which is a one-way road along the river Wien that has an accessible road runoff system. In addition, one indirectly traffic exposed sediment sample from the river retention basin sediment was collected which will be expected to contain lower trace metal concentrations than direct road runoff exposed sediment.

In the frame of this analysis, a protocol has been developed to digest road runoff water and road runoff exposed sediment samples containing INMs such as TRPs (tire rubband brake wear).

Hypotheses 2

For the quantification of TRPs, it is assumed that the addition of extractants may play a possible

role for enhanced dispersion of TRPs in waters and sediments, as extraction reagents are often used to favorize a release of particles as primary particles and small aggregates by breaking up heteroaggregates between NMs (Hartman et al., 2013; Loosli et al., 2019). Samples will be treated with different extraction protocols in addition of various extraction reagents (SPP, SOx, FL-70 and SDS) and compared on enhanced detection of TRPs.

Hypotheses 3

Sampling spots were chosen by following the assumption of TRPs' spatial distribution as different driving maneuvers may lead to emissions of particles with different physicochemical properties (Boulter, 2006). So, in this study it is expected that before traffic lights it comes more often to braking events, as driving vehicles are forced to stop during red light phases which may lead to higher amounts of non-exhaust TRPs (in the form of brake and tire particles) in runoffs located in front of traffic lights. Thus, one runoff before and one after a traffic light situation has been selected as sampling spot for runoff waters and runoff exposed sediments, where it is expected to finally detect higher mass concentrations of at least Sb, Ba and Pb (Boulter, 2006; Thorpe and Harrison, 2008; Puisney et al., 2018) before than after the traffic lights. To investigate this assumption, ME-spICP-MS will be applied to determine the presence of particles with target metal composition. ME-spICP-MS will be performed on an inductively coupled plasma-time of flight mass spectrometer (ICP-TOF-MS), a method that offers the opportunity to analyze multiple isotopes at the same time (Hendriks et al., 2018). To distinguish between natural and incidental particulates, mass ratios between two trace metals ocurring in potential TRPs with chemical compositions similar to natural nano materials (NNM), are getting calculated and compared with reported constant natural ratios (Kreiner, 2004; Salminen 2007; Pfleiderer et al., 2012; Simon et al., 2012). Within the scope of this single particle analysis, the presence and amount of exhaust TRPs (particulate PGEs and CeO_2) in road runoffs will also be observed.

2.4. Terms and definitions

Colloid

After Everett (2009) a colloid or also colloidal system is defined as "a state of subdivision such that the molecular and polymolecular particles dispersed in a medium have at least one direction

or dimension roughly between 1nm an 1µm, or that in a system, discontinuities are found at distances of that order".

Nanomaterial

The definition of nanomaterial is explained by the European Comission (EC) as "a natural, incidental or manufactured material containing particles, in an unbound state or as aggregate or agglomerate and where 50% or more of the particles in the number size distribution, one or more external dimensions is in the size range 1nm-100nm", since "(..) in specific cases where warranted by concerns of the environment, health, safety or competitiveness the number size distribution threshold of 50% may be replaced by a treshhold between 1 and 50%." (Gottardo et al., 2017¸European Commission, 2013, 2011). However, since this definition is only concerning on the size as the only defining property, mainly for regulatory purpose, there is still an ongoing scientific and regulatory debate to also involve novel properties especially by materials in nano size range (1nm-1µm) (Gottardo et al., 2017; Kah and Hofmann, 2014; Kah et al., 2013).

3. Materials and Methods

3.1. Sampling site

Road runoff exposed sediment samples S1, S2 and S3 were taken in January 2019 at various spots from road runoffs along the Hadikgasse which is a one-way road at Vienna's west exit along the river Wien. S1 was exposed by a runoff that can be found in an area with average city traffic flow while S2 was exposed by a road runoff in front and S3 was exposed by a road runoff after a traffic light. In September 2019 after a dry weather period of three weeks one sediment sample was taken at the retention basin of the river Wien and runoff water samples (W2 and W3) were taken during a heavy rain event (around 5mm/h) at the same runoffs which exposed S2 and S3.

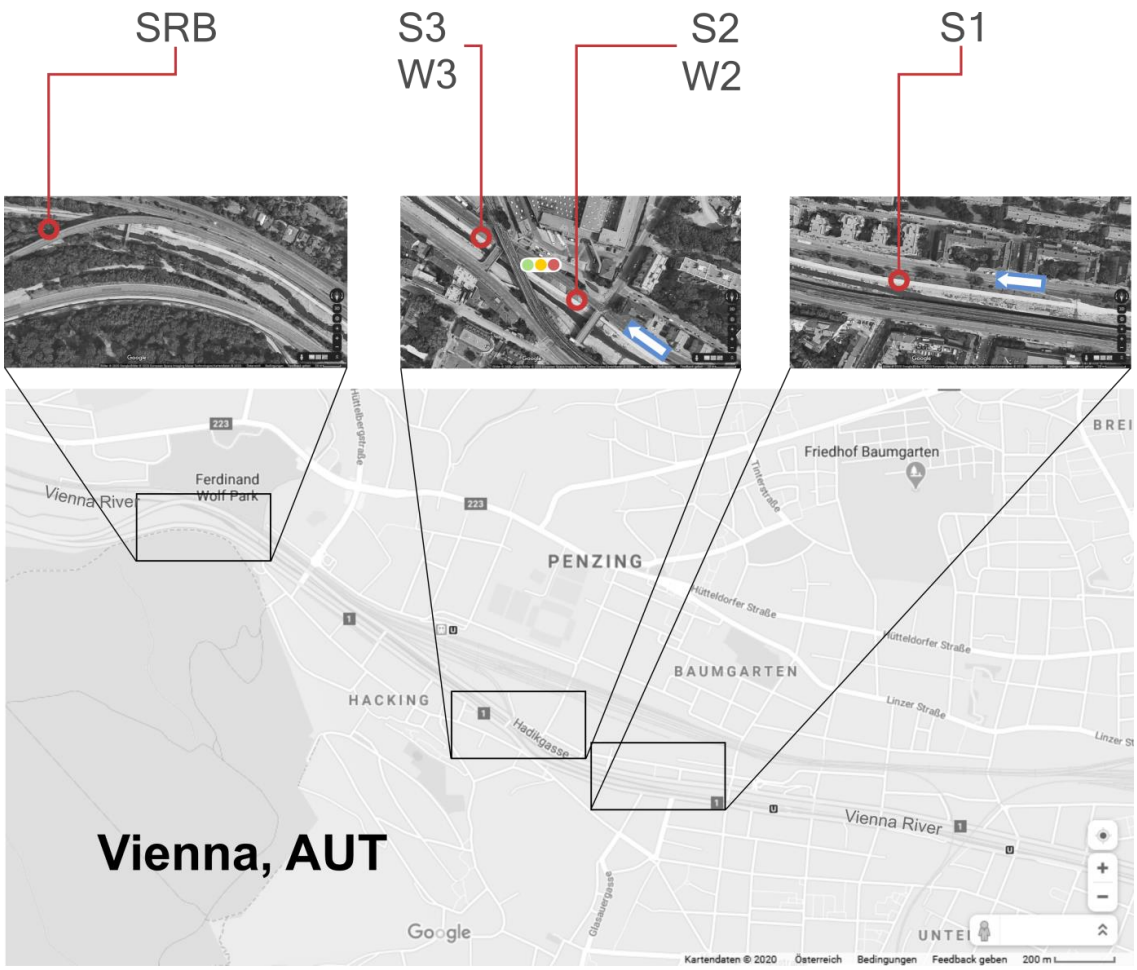

Fig.1. Vienna's west exit along the river Wien. Samples S(1,2,3) represent road runoff sediment samples, SRB represents retention basin sediment sample and samples W(2,3) represent road runoff water samples.

3.2. Extraction of sediment and water suspensions

3.2.1 Preparation of Sediment Stock Dispersions (<125µm)

The matrix of the significant dark sediment gets expected to mainly consist of tire rubber mixed with NOM, gravel and clay and other solid materials. To prepare the 125µm stock fraction it is necessary to get rid of the coarse size fraction of the sediment. The wet sediment got diluted (1:2) with ultra pure water (UPW) and homogenized in 1000mL polyethylene (PE) bottles (Thermo Scientific, USA) to lower the dispersion viscosity for wet sieving step and got sonicated for 1h. Serial sieving (2mm, 1mm, 500µm, 250µm, 125 µm) was applied through a tower of stacked nylon sieves with lowest mesh size of 125µm while UPW was used for flushing during the sieving process. The 125µm size-cutoff got collected with UPW in pre acid cleaned 50ml polypropylene (PP) tubes (Roth, USA). The dispersions were centrifuged (Jouan Mod. CR 4-22, FRA) for 80 minutes at 4000g to separate the sediment from the supernatant by using the sedimentation method (Tang et al., 2009). For the following treatments, a 125µm stock fraction needs to be prepared by carefully removing the supernatant. This happens by carefully soaking off the supernatant with a 5mL pipette without getting in contact or to resuspend the centrifuged sediment which is concentrated on the tube bottom. The supernatant got collected in clean 1000ml PE bottles for further analysis and stored at 4°C in a dark place. Finally, the respective sediment of each tube gets collected in 50ml PP tubes to obtain the 125µm stock fraction.

3.2.2 10µm and 1µm size-cutoff Sediment Suspensions

To prepare the 10µm and the 1µm cut off fraction out of the 125µm stock dispersions. The five extractants for this step are ultra pure water (UPW) and four reagents such as SPP (Acrōs, USA), SOx (Merck, Germany), SDS (Acrōs, Japan) and FL70 (Fisher Scientific, USA). These reagents may favour the release of engineered particles as primary particles and small aggregates by breaking heteroaggregates of engineered- and natural particles (Loosli et al., 2019). So respectively 4g of the 125µm stock got diluted with 36ml of UPW, SPP (1mM), SOx (1mM), SDS (1wt.%) and FL70 (1wt.%) into 50ml PP Tubes and mixed for 12h at 150rpm on an orbital shaker (IKA Mod. KS 260 conrol, Germany). The 125µm dispersions need to become homogenized and sonicated in an ultrasonic bath (Bandelin Sonorex Super Mod. RK 106, GER)

for 1h without heating up the dispersions due to increasing temperature of the bath water. To prevent a temperature increase it is necessary to release the bathing water every 10min and refill it with fresh (T=10°C) UPW. To obtain the 10µm size-cutoff the sedimentation method was again applied. Hence the 125µm fraction got centrifuged for 3min at 200rpm (Jouan Mod. CR 4-22, FRA) assuming a particle density of 2.5g cm^{-3} and spherical particle shape for using the Stokes' Law calculation (Tang et al., 2009). Supernatant in the 50mL PP tube containing the 10µm size-cutoff gets soaked with a pipette and collected in a clean 50mL PP tube (Roth, USA). To obtain the 1µm cutoff fraction the dispersions get homogenized and follow the same treatment than the 10µm cutoff fraction but were centrifuged for 12.5min at. The supernatant was collected in 50mL tubes contains and stored in the dark at 4°C. Additionally suspensions of 1µm fraction got ultra filtrated in filtration tubes (10.000MWCO Sartorious Vivaspin) with a pore size of 30kDa while centrifuging for 20min at 800rpm to extract the dissolved metal fraction of the suspensions.

Eq.2. Calculation of centrifugation time

t... time [sec]
r_{out}... sampling point [cm]
r_{in}... sample fill-up point [cm]
η... medium viscosity [mPs] (25°C)
ρ... particle density [g /cm^3]
d... size cutoff diameter [µm]

$$t_s = ln\left(\frac{r_{out}}{r_{in}}\right)\frac{18\eta}{4\pi^2\Delta\rho d^2\left(\frac{rpm}{60}\right)^2}$$

3.2.3 Preparation of Runoff Water Stock Dispersions

Runoff samples have been collected on September 28th, 2019, during a rain event (around 5mm) after a dry period of three weeks. 500ml PP bottles (Thermo Scientific, USA) have been fixed at the lower end of the rain drainages to collect the rainwater flow containing traffic wear particles that may have been accumulated on the road asphalt surfaces. The rainwater that has been collected on two different spots showing a around 1cm thick layer of white foam at the water/air interface seems to get already in contact with any reagent such as surfactant before reaching the bottle. However, this reagent is assumed to be cleaning agent from road sweepers. Since there is also vegetation next to the road, the rainwater not only contains traffic related particles but also large particles (>2mm) that must get filtered out before the proper sample treatment starts. Therefore, a clean nalgene Filter and Filter holding system (Thermo Scientific, USA) with a size-cutoff of 2mm has been used for a coarse pre-filtration, before the sonicated

(10min) rainwater gets filled into 50mL PP tubes. One part of the respective sample got diluted to 1:99 dispersion with UPW and 100mM SPP (Acrōs, USA). For the extraction process, all dispersions (pure and SPP) have been shaken overnight and afterwards sonicated for 1h by controlling the water temperature of the sonication bath to prevent overheating which could cause a destabilization of the particles.

3.2.4 10µm and 1µm size-cutoff Runoff Water Suspensions

To extract particles in the size range smaller than 10µm, the samples got centrifuged in 50mL PP Tubes for 3min at 200rpm (Jouan Mod. CR 4-22, FRA) assuming spherical shapes and a particle density of 2.5g/cm^3. Finally, the supernatant containing the 10µm size cutoff fraction gets carefully collected out of each tube, filled into 50mL PP tubes and stored in a dark place at 4°C. For the extraction the 1µm size-cutoff the samples got centrifuged for 12.5min at 1000rpm before the supernatant got collected. For the 1µm size cutoff has beside the sedimentation method also been generated through vacuum filtration, to see how it affects particle-loss do loss of high-density material (e.g., PGE) during centrifugationg process. Therefore, Cellulose nitrate membrane filters (GE Whatman, USA) with a pass-through of 1.0µm and a diameter of 47mm and a Nalgene Filter holding System (Thermo Scientific, USA) have been used. Additionally, suspensions of 1µm fraction got ultra filtrated in filtration tubes (10.000MWCO Sartorious Vivaspin) with a pore size of 30kDa while centrifuging for 20min at 800rpm to extract the dissolved metal fraction of the suspensions.

3.3. Zeta potential and hydrodynamic diameter measurements

The z-average hydrodynamic diameter as well as zeta potential known as the electrophoretic mobility of NMs have been determined by dynamic light scattering (DLS) (Malvern Instruments, Zetasizer Nano ZS instrument, UK). Suspensions from both size-cut offs of each sediment sample have been diluted 1:99 with the respecting reagent while all rainwater samples have been diluted 1:4 with UPW or SPP because of lower particle concentrations. The values have been generated through three independent runs during each measurement so as final output a z-average hydrodynamic diameter mean ± standard deviations is reported. All measurements are performed at 22°C. For the calculation of the zeta (ζ) potential the calculation according to Henry's function using Smoluchowski approximation was applied (Baalousha, 2009), while the

z-average hydrodynamic diameter has been calculated by using the cumulant analysis (International Organization for Standardization ISO 22412:2017). PDI values from the z-average measurements indicate the dispersity of the NM matrices with values between ≥0 and ≤1. By that, a PDI value above 0.7 indicates a polydispersed sample (International Organization for Standardization ISO 22412:2017).

3.4. Additional analysis on road runoff suspensions

In addition to the DLS measurements, laser obscuration particle size analysis has also been performed with Eyetech (Ankersmid, NED) to see if there is a different in suspension's PSDs as during DLS analysis smaller particulates will get overshadowed by bigger particulates In polydispersed suspensions. Furthermore UV-Vis absorbance (Perkin Elmer Lambda 35, USA) at a wavelength of 254nm (A_{254}) was recorded for soil organic matter (SOM) concentration measurements in sediment suspensions as measurements were normalized at 600nm. In road runoff water samples anion concentrations have been determined through ionchromatography (IC) (Dionex) while cation concentrations were determined by measuring optical emission wavelength of corresponding element with ICP-OES (Agilent 5110).

3.5. Total Digestion of Sediment containing Tire Particles

During the digestion 10mL perfluoralkoxy (PFA) vials (Savillex, USA), a hotplate (HPX-100 Savillex, USA) and vessel racks (Savillex, USA) with a special carbon coating for a steady heat transfer have been used. To get the weight from the dry matter that is around 20mg for 2mL of dispersion, all vials have been filled up with 2mL of 10µm sediment dispersion before heating them up to 140°C for 90 minutes. After the vessels have been weighed the dry matter is ready to get treated with inverse aqua regia HNO_3 : HCl (3:1). First the vials get filled with 3mL of HNO_3 65% (Merck, GER) two times subboiled (Savillex, USA) before adding 1 mL of concentrated HCl suprapur (Merck, GER) producing NOCl and chloride ions (Cl^-) that aggressively attack the sediment with their high oxidization behavior. The reason why preventing a too high HCl concentration is to take care about the chlorine concentration inside the solutions that could have a negative impact on the ICP-MS instrument during the analysis, as it is known that chlorine forms $^{35}Cl^{16}O^+$ interfering with vanadium and $^{40}Ar^{35}Cl^+$ that

interferes with arsenic (Fitz-James, 2003). After adding the acids, the solutions are getting heated up to 140°C overnight with closed caps and finally reopened until the liquid phase has totally evaporated. As next step 1mL od HNO_3 was added followed by carefully adding dropwise 2mL H_2O_2 suprapur (Merck, GER) at 70°C to oxidize the NOM of the sediment. While adding H_2O_2 it is very important to consider foam formation caused by CO_2 developement. After the CO_2 development starts to decrease and the reaction is finished the solutions can be heated up to 140°C to evaporate the liquid phase again for around 90min. To prepare the digestion part, the samples are getting dosed with ammonium biflouride NH_4HF_2 (99.999% trace element basis) as digestion salt. The atvantage of NH_4HF_2 is that it has a higher boiling point (239.5 °C) than conventional acids such as HF which allows for an elevated digestion temperature (Zhang et al., 2012). The dose is 5 times the mass of the sample as in this case 5 times 20mg (100mg per solution) (Zhang et al., 2012). After the digestion salt is added, the vials are getting closed with their caps and heated up to 240°C so the digestion salt melts and gets in contact with the whole sample while HF and HNO3 get formed. This step takes 4 hours before the vial caps are getting opened again. Then 1ml of HNO_3 gets added to all samples before the vials are getting closed again and heated up to 170°C to dissolve the dry "cake" that contains the digested material into a homogenous solution. After the temperature gets reached the solutions need to react for one hour. Due to vaporization during this process, drops of the solution accumulate on the caps that carefully need to get flushed back into the vial by using one or two drops (around 200µL) of UPW. Before starting the next step, the samples need to get dried down again at 140°C for around 90min. Then to make sure that the organic carbon is totally oxidized it is necessary to add once again 1mL HNO_3 and 1ml H_2O_2 while being prepared for a severe foam development when CO_2 gets produced during the reaction. The solutions should be clear and colorless. Finally, the solutions dry down at 120°C for around 100min before they get dissolved and stabilized in 1ml HNO_3 and 0.1mL concentrated HCl. Finally, the digested samples of the 10µm size cutoff fraction get diluted with ultra pure water to a 40mL solution in already acid pre-cleaned PP sample tubes. Digested sediment of the 1µm size cutoff fraction gets less diluted to 4.5mL with UPW as mass of digested dry matter is lower. Digested water samples get diluted to 5mL with UPW.

3.6. Total Digestion of Tire rubber

As reference material for this study also recycled crumb tire rubber (KIAS recycling Austria) with a grain size between 1 and 3mm has been digested. The approach of digesting tire rubber followed the same procedure as the total digestion process as mentioned for sediment containing tire particles and the result turned out as successful by getting a clear solution in the end. Before the digestion process started, the tire particles have been crushed into smaller fractions by freezing them with liquid nitrogen before they got grinded in an agate mortar.

3.7. ICP-MS elemantal analysis

The elemental concentrations of the digested and the ultra filtrated water and sediment samples have been analyzed through inductively coupled plasma-mass spectrometry (ICP-MS). As measuring instrument, the Agilent 7900 ICP-MS (USA) was used by operating with the ISIS 3 (Integrated Sample Introduction System) containing a piston pump that delivers the samples at 10µL min^{-1} to the glass concentric nebulizer (~0.4ml min^{-1} actual uptake) that finally introduces the samples into the UHMI (Ultra High Matrix Introduction) spray chamber. The Agilent 7900 ICP-MS operates with a hyperbolic quadropole as mass analyzer and detects the signals through a ODS (Orthogonal Detector System) with a measurement range from 0.1cps to 10Gcps. During the measurement Ni sample- and skimmer cones have been used. Measured isotopes are ^{107}Ag,^{75}As, ^{137}Ba, ^{111}Cd, ^{140}Ce, ^{59}Co, ^{53}Cr, ^{133}Cs, ^{63}Cu, ^{163}Dy, ^{167}Er, ^{151}Eu, ^{57}Fe, ^{157}Gd, ^{72}Ge, ^{178}Hf, ^{165}Ho, ^{115}In, ^{139}La, ^{175}Lu, ^{55}Mn, ^{95}Mo, ^{93}Nb, ^{146}Nd, ^{60}Ni, ^{208}Pb, ^{105}Pd, ^{141}Pr, ^{195}Pt, ^{85}Rb, ^{103}Rh, ^{121}Sb, ^{45}Sc, ^{149}Sm, ^{118}Sn, ^{88}Sr, ^{181}Ta, ^{159}Tb, ^{232}Th, ^{47}Ti, ^{169}Tm, ^{238}U, ^{51}V, ^{182}W, ^{89}Y, ^{173}Yb, ^{66}Zn and ^{90}Zr. All isotopes have been measured at low resolution for maximum sensitivity ($m/\Delta m$=100) while the concentrations have been calculated against a freshly prepared multi-element standard mixture made by adding every single element solution (1000mg/l). Standart concentrations of each element in the solution were 50ppb, 25ppb, 5ppb, 2.5ppb, 0.5ppb, 0.25ppb, 0.05ppb, 0.025ppb, 0.005ppb and blank 0ppb.

3.8. Multi element-single particle-ICP-MS

Before the analysis, the extracted sediment and runoff water have been sonicated for 1min at 437Ws in 1.5ml PP tubes (Eppendorf, MEX) with a Hielscher UP200St ultrasonic lab before the sediment (1:10 000) and rainwater dispersions (1: 100) got diluted with UPW into clean 15mL PP tubes (Roth, USA). The multi element-single particle ICP-MS has been performed on an inductively coupled plasma-time of flight mass spectrometer (ICP-TOFMS, TOFWERK, CHE). The signal of the instrument gets determined through the detecting ion velocity depending on its mass to charge ratio while the ion gets accelerated by an electric field with a known strength, meaning that ions with a high mass and same charge will reach lower speeds than higher charged ions (Hendriks et al., 2017). So, the instrument measures the flight time the ion takes to reach the detector at a known distance through its velocity (Hendriks et al., 2017). The measurement has been performed with an Apex Ω high sensitivity desolvation system (Elemental Scientific, GER) coupled with a two-way syringe pump (Elemental Scientific, GER) that furthermore injects the sample into the spray chamber. As carrier gas Ar^{38} without additional make-up gas has been used. The transport efficiency of the instrument was calculated following the instructions of the known size method after *Pace et al* by using Au nanoparticles with a certified particle size of 100nm (NIST, USA) prepared in UPW (1:250 000) and an Au standard solution prepared with UPW and 1% HCl (Merck, Suprapur, GER).To process the raw particle signal a python script was used that calculates a quantitative result by indentifying particle signals of the respective isotope through filtering out the background noise of the ICP-TOFMS spectra. As data processing output the python script delivers a calibration curve of each selected isotope calculated through the concentration sequence of the standard solution to obtain information about the measurement quality and two csv files per sample where one file shows the number of counts per time and the other gives an overall information about calculated particle size, mass and volume of each isotope along the measured time sequence. For the measurement, a dwelltime of 3.00ms was used. For the characterization of relevant particles, the isotopes ^{27}Al, ^{46}Ti, ^{48}Ti, ^{52}Cr, ^{53}Cr, ^{55}Mn, ^{56}Fe, ^{57}Fe, ^{58}Ni, ^{59}Co, ^{60}Ni, ^{63}Cu, ^{64}Zn, ^{65}Cu, ^{66}Zn, ^{68}Zn, ^{75}As, ^{90}Zr, ^{91}Zr, ^{92}Mo, ^{92}Zr, ^{93}Nb, ^{94}Zr, ^{95}Mo, ^{96}Mo, ^{98}Mo, ^{100}Mo, ^{103}Rh, ^{104}Pd, ^{105}Pd, ^{107}Ag, ^{108}Cd, ^{108}Pd, ^{109}Ag, ^{110}Cd, ^{110}Pd, ^{111}Cd, ^{112}Cd, ^{113}Cd, ^{114}Cd, ^{116}Sn, ^{118}Sn, ^{120}Sn, ^{121}Sb, ^{122}Sn, ^{122}Te, ^{123}Sb, ^{124}Sn, ^{124}Te, ^{125}Te, ^{126}Te, ^{128}Te, ^{130}Te, ^{137}Ba, ^{138}Ba, ^{139}La, ^{140}Ce, ^{142}Ce, ^{181}Ta, ^{182}W, ^{183}W, ^{184}W, ^{186}W, ^{191}Ir, ^{193}Ir, ^{194}Pt, ^{195}Pt, ^{196}Pt, ^{197}Au, ^{198}Pt, ^{204}Pb, ^{206}Pb, ^{207}Pb, ^{208}Pb are used as trace elements. So, after the peak/background correction one peak gets counted as relevant peak if both isotopes of the respective element occur at the same time before the ratio

between the two isotopes gets calculated as verification if they are in an acceptable range or need to get excluded as outliers. Therefore, the csv files of each sample got treated with Microsoft excel using “if true or false” commands, meaning one peak out of 20.000 measurements in one sample gets counted as relevant or true if the mass of one isotope from one element is higher than zero.

3.9. Scanning electron microscopy

Scanning electron microscopey (SEM) has been performed after researching the morphological properties of non-exhaust TRPs (Kukutschová et al., 2011; Adachi et al., 2004). Therefore, two different dispersions of each size cutoff from one sample (S2: UPW-10µm, SPP-10µm, UPW-1µm, SPP-1µm) have been analysed. The SEM samples have been prepared through vacuum filtration by rinsing the dispersions through a glass vacuum filter holder (Sartorius) while using a 0.02µm passthrough alumina-based membrane cap Anodisc Filter with a diameter of 25mm (Whatman). The dilutions of each sample have been calculated to get a well analyzable 1 and 5% membrane surface coverage of each SEM sample, assuming spherical particle shape with an average particle diameter of 100nm, a dispersion concentration of 500mg/l, and a particle mass of 35fg and density of 2.5g/cm^3. After the filtration procedure, the filter membranes carrying the filtered sediment get covered on top to prevent a contamination through dust particles while drying in a clean oven at 120°C. While the membranes get dry it is necessary to cover them in a way the water vapor can vent to avoid an increase of humidity underneath the cover (e.g., stored on a rack with holes on the bottom). Each dry filter membrane gets taped on a SEM pin stub with the same diameter as the filter membrane (25mm) before they are ready to get coated with an ultrafine layer (around 10nm) of carbon by a high-resolution sputter coater, to prevent sample charging caused by the accumulation of static electric fields that produces a low image resolution and decreases the signal to noise ratio (Höflinger., 2013). SEM samples have been analyzed on a FEI Nova200 dual focused ion beam scanning electron microscope operating with HV at 3 to 20kV produced by a tungsten hairpin electron gun while observations have been made at 3 kV and 10 kV. Micrographs have been recorded at magnifications up to 50.000x to detect nanoparticles at the expected average size of 100nm to significantly determine the morphology of the NMs on the filter membrane. Energy-dispersive X-ray microanalysis (EDX) pattern performed on an EDAX Apollo 40 Silicon Drift Detector.

4. Results and discussion

4.1. General sample characteristics

All values of zeta (ζ) potential, z-average hydrodynamic diameter as well as pH of extracted road runoff water, road runoff exposed sediment and retention basin sediment suspensions are represented in Table.S1. Additional determined hydrodynamic diameters with Eyetech laser particle size analysis, are represented in Table.S2. Furthermore, ζ potentials as a function of hydrodynamic diameter of road runoff sediments (S1, S2 and S3) retention basin sediment (SRB) and road runoff waters (W2, W3) suspensions are represented in Fig.2.

To study reagents on affecting colodial stability, it will be necessary to have a look on the suspensions' measured ζ potentials. As illustrated (Fig.2.) ζ potentials of road runoff sediment suspensions S1, S2 and S3 as well as retention basin sediment SRB suspensions extracted with UPW indicate values between -20 and -35 mV in both 1µm and 10µm size fractions which means after Bhattacharjee (2016) colloid stability in UPW suspensions will be defined as moderately stable. Probably the reason for moderate colloid stability may be high concentrations of NOM in the suspensions that promote colloidal stability by enhancing NM surface charge whereas high concentrations of NOM on the other hand promote NM aggregation via bridging mechanisms (Chen et al., 2006; 2007). Nevertheless, suspensions extracted with SPP, SOx, SDS, FL-70 in both size fractions from runoff sediment samples S1, S2 and S3 are delivering even higher ζ potential magnitudes than UPW suspensions with more negative values significantly above -30 mV and thus colloid stability may be defined as highly stable (Bhattacharjee, 2016). This can be explained through selective sorption of phosphate or oxalate anions on NNM surfaces while these anions replace NOM such as SOM on NNM surfaces as previously assumed (Jolivet, 2000).

SDS extracted suspensions are indicating highest ζ potential magnitudes in all road runoff exposed sediments S1, S2 and S3 of both 1µm and 10µm size cut off fractions whereas SOx extracted suspensions are indicating lowest ζ potential magnitudes after UPW. Furthermore, SPP and FL-70 extracted suspensions in both size cutoff fractions of S1, S2 and S3 having ζ potential magnitude values

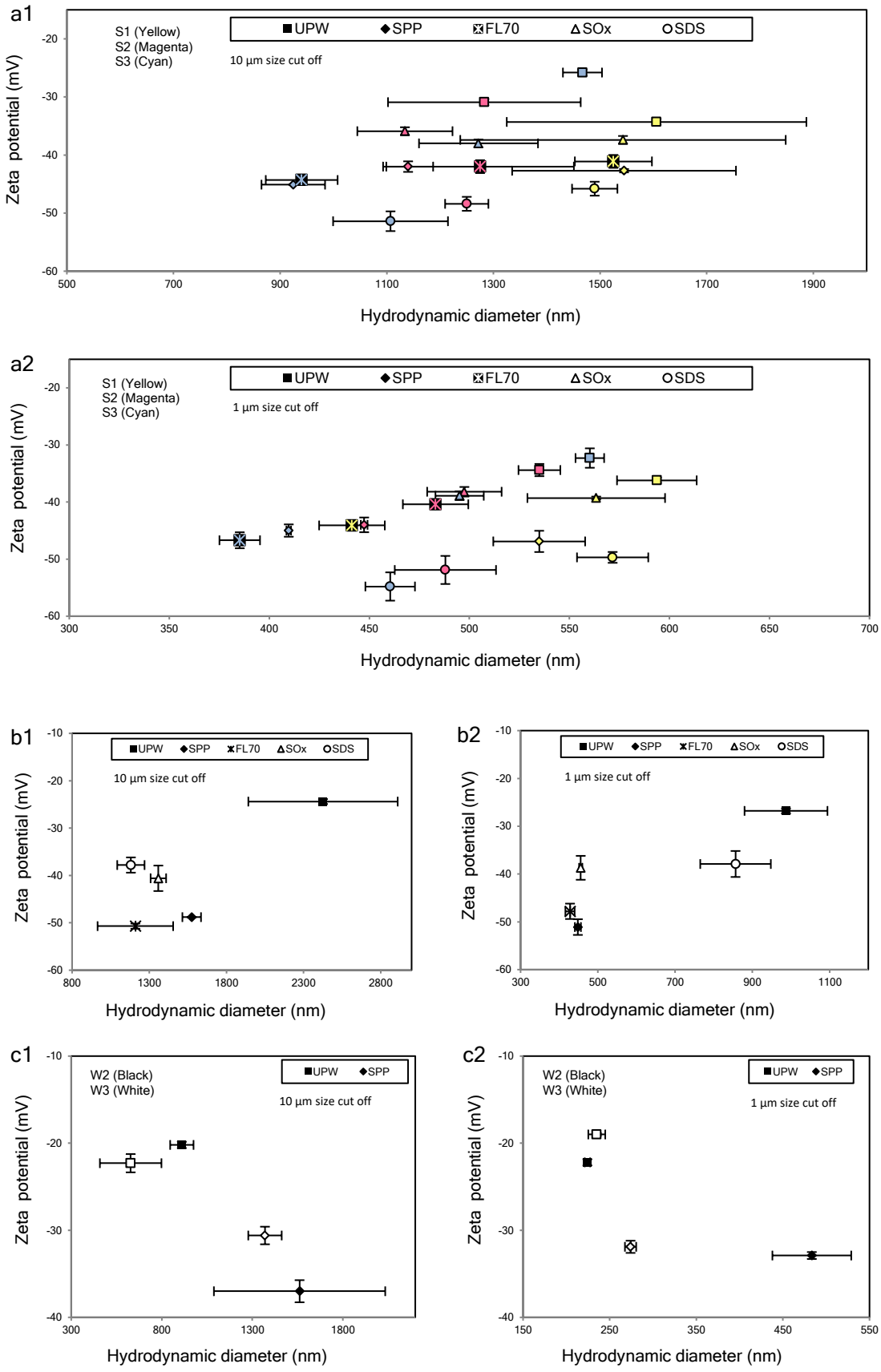

Fig.2. Zeta Potential as a function of hydrodynamic diameter determined with DLS of 10µm (1) and 1µm size-cutoff (2) from (a) road runoff sediments S1 (yellow), S2 (magenta) and S3 (cyan), SRB (b) and road runoff waters suspensions (c) W2 (black) and W3 (white). The error bars represent the standard deviation of the results from several independent measurements (n=3).

that switch their order in between S1, S2 and S3 and lay between ζ potential values of SOx and SDS.

Hydrodynamic diameters in suspensions of S1, S2 and S3 are decreasing with increasing ζ potential magnitude which can be observed in the 1µm (Fig.2.a2.) cutoff fraction and will be explained through the break-up of heteroaggregates between NMs (Hartman et al., 2013; Loosli et al., 2019). In detail this means that in S1, S2 and S3 UPW suspensions with lowest ζ potential magnitude indicate highest hydrodynamic diameters followed by SOx suspensions while FL-70 and SPP have lowest hydrodynamic diameters. Nevertheless, SDS suspensions in 1µm (Fig.2.a2.) cutoff fraction indicate highest ζ potential magnitude while hydrodynamic diameters did not decrease much compared to UPW suspensions. This may be explained that during SDS extraction eventually more NOM has been extracted, leading to enhanced surfaces charges (Chen et al., 2006; 2007) wheras bridging mechanisms between NOM and NM may not have been released during sonication. However, DLS observations of polydispersed suspensions may lead to inaccurate hydrodynamic diameter measurements as smaller particulates will get overshadowed by bigger particulates (Xing et al., 2016) which may be the case while analyzing 10µm (Fig.2.a1.) cutoff fractions. Hence as comparison hydrodynamic diameter measurements were also determined with laser particle size analysis performed with Eyetech as results are represented in Table.S2. Nonetheless, there is no significant trend concerning hydrodynamic diameters between the several extraction protocols in 10µm cutoff fraction of S1, S2 and S3 as results from Eyetech and DLS measurements show different values due to highly polydispersed suspensions (Table.S2, Table.S2.).

Furthermore, between different sediments S1, S2 and S3 it can be observed that FL-70 extraction in the 1µm (Fig.2.a2.) cutoff fraction had the most significant effect in S1 and S3 by indicating lowest hydrodynamic diameters while in the same size fraction of S2 result of SPP extraction shows lowest hydrodynamic diameters. This may conclude that SPP and FL-70 suspensions in comparison to SDS and SOx suspensions favour the release of heteroaggregation.

Additionaly, Retention basin sediment sample SRB also indicates lowest ζ potential magnitudes in UPW extracted suspensions from both size cutoff fractions (Fig.2.b1.2.) followed by SOx and SDS extracted suspensions while significantly highest ζ potential magnitudes (above -40 mV) can be observed in FL-70 and SPP extracted suspensions. Hydrodynamic diameter measurements in 1µm (Fig.2.b2.) cutoff fraction of SRB also show a certain trend of decreasing hydrodynamic diameters with increasing ζ potential magnitudes. The 10µm (Fig.2.b1.) cutoff fraction of SRB also seems to have highly polydispersed suspensions which makes it difficult

to give statements about comparisons of hydrodynamic diameters in between the different extraction protocols of the 10µm size cutoff fraction. Nevertheless, DLS measurement results (Table.S1.) in comparison with Eyetech measurement results (Table.S2.) show similar large hydrodynamic diameter values for UPW extracted suspensions of SRB in the 10µm (Fig.2.b1.) cutoff fraction with a mean value that is around 500nm larger than in suspensions extracted with extractants. This may conclude that extractants could have a similar effect on SRB as it has on S1, S2 and S3 which means that SOx, SDS, SPP and FL-70 may have caused a release of heteroaggregation NMs (Hartman et al., 2013; Loosli et al., 2019).

When having a look on road runoff water suspensions W2 and W3, it can be observed that UPW extraction delivers ζ potential values in the range around -20 mV in both size cutoff fractions (Fig.2.c1.2) indicating moderate colloid stability (Bhattacharjee, 2016) while ζ potential magnitudes by applying SPP extraction increase into the negative range above -30 mV indicating high colloid stability (Bhattacharjee, 2016) in both size cutoff fractions. However, hydrodynamic diameter values of both size cutoff fractions from W2 and W3 are significantly smaller in UPW than in SPP extracted suspensions of road runoff water samples (Fig.2.c1.2) so a trend of increasing ζ potential magnitude and decreasing hydrodynamic diameter in the suspensions cannot be observed. This may be either due to unreleased heteroaggregation or reaggregation of NMs in the suspensions due to too long or too short sonication time (Cohen et al., 2018).

UV-VIS absorbance at λ_{254} (A_{254}) has been measured to investigate the amount of released SOM during the extraction performance (Albrektienė et al., 2012; Buchanan et al., 2005) in both size cutoff fractions of road runoff sediment (S1, S2 and S3) as well as retention basin sediment (SRB) suspensions. The desorption of SOM from colloid surfaces through higher A_{254} values as investigated in Loosli et al. (2019) will be observed with this method. It is illustrated in Fig.4.a. that SPP extraction shows highest A_{254} signal compared to UPW extraction in almost all sediment suspensions of both size cutoff fractions except in 1µm size fraction of S1. This is in good agreement with the observations of Loosli et al. (2019) reporting enhanced SOM desorption through the presence of SPP.

TOC analysis by measuring CO_2 development initiated during sediment combustion by constant heating up (1°C per 10sec at atmospheric pressure) the 125µm stock fraction of sediment samples S1, S2 and S3 was performed and is illustrated in Fig.4.b. Results from sediment combustion show that all sediment samples have a significant peak in CO_2 development between 210 and 320°C which is likely to represent the combustion of SOM as Thomaz (2016) suggests, whereas this peak is most significant in S1 as it is up to one order of

magnitude higher than S2 and S3 which could eventually mean most SOM is present in S1. Which is in good agreement with values of total carbon and water showing highest values in S1 [Carbon = 21.12 %, Water = 23.58 %] followed by S2 [Carbon = 18.38 %, Water = 13.45 %] and S3 [Carbon = 14.51 %, Water = 8.38 %]. However, between 600 and 800°C all sediment samples show a secondary significant but flatter peak in CO_2 development that probably could represent the combustion of tire wear particles as it is suggested that tire particles incinerate at around this temperature at atmospheric pressure (Juma et al., 2006).

Furthermore, SEM analysis was preformed to get an overview about the particle morphologies in the road runoff sediment samples. For the observations, road runoff sediment S2 has been used as it is assumed to detect most TRPs especially due to potentially high brake wear particle concentration as this sample was exposed to road traffic in front of traffic lights. Results show that the suspension matrices from S2 seems to mostly consist of clay minerals according to the shape of visualized particulates as particle morphologies look like potential layer silicates such as clay minerals of the kaolin-serpentine and pyrophylitic talc group as well as elongated tubular clay mineral structures, similarly, as described in SEM observations of Christidis (2010). NMs that are suspiciously looking like from anthropogenic origin around 300nm have been visually detected as demonstrated in Fig. 3. Spherical particles with a diameter around 8µm were also detected which could be of anthropogenic origin as these particles look similar to micrographs of silica gel from Nakamura et al (2015) observations. However, SEM images of previous studies (Kukutschová et al., 2011; Adachi et al., 2004) have been used as orientation to visually identify TRPs. According to the morphologies various detected particles and aggregates in SEM images (Fig.3) that appear to have low contrast also show undefined near-spherical surfaces and thus look like detected tire particles that have been analyzed via SEM in Adachi et al. (2004). Due to the particle concentration of NNMs as mainly clay minerals in the matrix of road runoff sediment S2 it was challenging to certainly identify TRPs. Especially the visual identification of brake wear particles in natural matrices is problematic due to their morphologies that may be like multiangular morphology of various clay minerals (Adachi et al., 2004; Kukutschová et al., 2011; Christidis, 2010). Nevertheless, during EDX analysis detection errors occurred due to too small particulates showing diameters below the size of the EDX window which means various particles with different elemental compositions were detected at the same time.

4.2. Applied methods to detect TRPs in road runoff water and sediment

Concentrations of trace metals that are reported to be found in TRPs are analyzed in total digested road runoff sediment and retention basin sediment dispersions by conventional ICP-MS. Measured metal concentrations get normalized with 1g of respecting size cutoff fraction to determine what is the predominant trace metal in the suspensions of each extraction protocol. Also, measured metal concentrations normalized with 1g of corresponding dry 125µm stock are getting compared to observe differences in metal concentrations between sampling sides. Finally, measured metal concentrations get confronted with natural background data from top soil and upper crust in Vienna determined in previous studies (Kreiner, 2004; Salminen 2007; Pfleiderer et al., 2012; Simon et al., 2012) to observe elevated trace metal concentrations and changes in chemical compositions.

Furthermore ICP-TOFMS was applied for ME-spICP-MS to determine particle amounts in road runoff water (W2, W3), road runoff exposed sediment (S1, S2, S3) and retention basin sediment (SRB) suspensions as well as the mass of each detected particle of corresponding element as calculated through the python script during data treatment. As criterion to identify specified particle events representing TRPs during ME-spICP-MS, tarce metals such as titanium (Ti), iron (Fe), copper (Cu), zinc (Zn), rhodium (Rh), palladium (Pd), antimony (Sb), barium (Ba), platinum (Pt) and lead (Pb) were primarily selected whereas aluminum (Al) for the identification of NNMs like aluminum rich clay minerals has been used. Concentrations of chromium (Cr), manganese (Mn), cobalt (Co), nickel (Ni), arsenic (As), zirconium (Zr), molybdenum (Mo), cadmium (Cd) and tellurium (Te) have also been measured as these elements are expected to appear in brake and tire wear paricles (Boulter, 2006; Thorpe and Harrison, 2008; Puisney et al., 2018; Kukutschová et al., 2011). Cerium (Ce) was measured as trace metal for exhaust and non-exhaust TRPs by determining La/Ce ratios below the natural range of each detected Ce and lanthanum (La) particulate by following the ENM / NNM distinction method of Montaño et al. (2014). Also, mass ratios between associated elements of detected particulates have been determined to distinguish between TRPs and NNMs that have interferences in elemental compositions as it will be assumed that NNMs may have constant ratios between two selected elements. Calculated mass ratios in such detected particles are La/Ce, Ba/Pb, Sb/Pb and Cr/Mn. La/Ce and Cr/Mn mass ratios of detected particulates containing these element associations have also been compared with measured concentration ratios of digested tire particles analyzed with

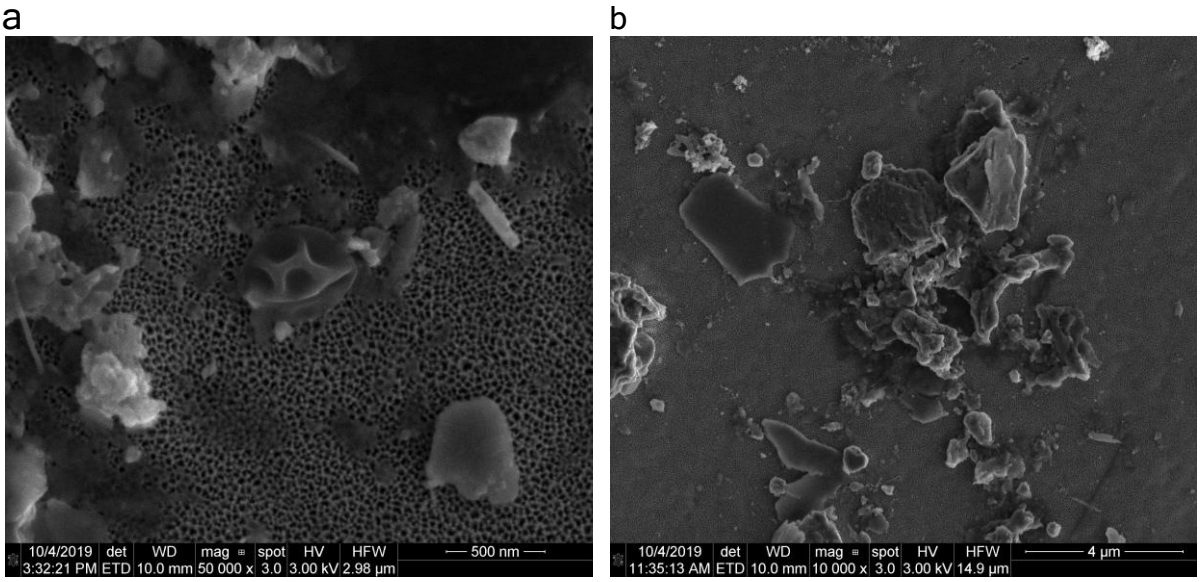

Fig.3. SEM images of road runoff sediment. Picture (a) represents a 50.000x magnification of the 1µm size cutoff and picture (b) demonstrates a 10.000x magnification of the 10µm size cutoff. For the SEM observation sediment S2 was used.

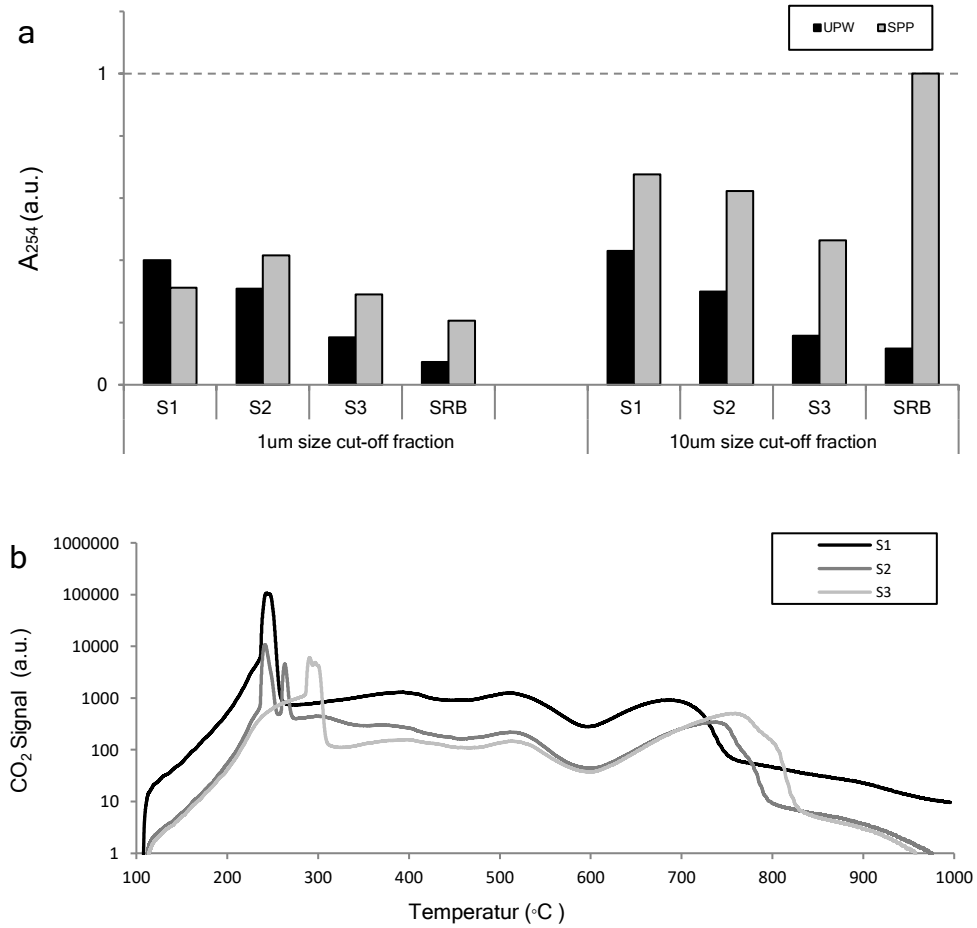

Fig.4. (a) UV-Vis absorbance at 254nm (A254) normalized at 600nm of UPW and SPP extracted sediment suspensions of 1µm and 10µm size cutoff fractions further normalized by 1g of corresponding dry 125µm sediment stock fraction. (b) Represents TOC pattern from combustion of 125µm stock fraction of road runoff sediment samples S1, S2 and S3. The UV-Vis signal (a) and the CO_2 signal are reported in arbitrary units (a.u.).

conventional ICP-MS to identify potential tire wear particles that could correlate with the La/Ce and Cr/Mn ratio of digested tire particles. For ME-spICP-MS UPW, SPP and FL-70 extracted suspensions of the 1µm size cutoff have been used as lowest hydrodynamic diameters were measured in SPP and FL-70 suspensions thus less heteroaggregation and more released TRPs will be assumed.

4.3. Total metal content in suspensions extracted with different extraction protocols

Digested suspensions were analyzed by conventional ICP-MS and normalized by 1g of dry sediment from the corresponding size cutoff fraction to determine the concentrations of trace metals in total digested road runoff and retention basin sediment and thus to observe the extraction effect between applied extraction protocols in 1µm and 10µm size cutoff fractions. In Fig.5. and Fig.6. as well as Table.S3. it is illustrated, values from 10µm S1, S2 and S3 fractions show no significant differences in composition between extraction protocols as overall concentrations of trace metals appear to be almost in the same range. Whereas values from 10µm fraction of SRB significantly show that between extraction protocols (UPW, SPP, FL-70, SOx and SDS) a higher number of Ti, Zn and Ba was extracted with SPP and UPW while highest number of Mn, Cu and Pb may have been extracted with FL-70 (Table.S3). Also, in 10µm SRB fraction Ti is after Fe the predominant metal in UPW, SPP, SOx and SDS extraction protocols while Mn after Fe is predominant by applying FL-70 extraction. Same can be observed in 1µm fraction of SRB but anyway, statements concerning the composition in 1µm cutoff fractions should only be made while considering that dry mass of digestion material was very low due to low particle concentrations in the suspensions of all sediments (S1, S2, S3 and SRB). So, measured concentrations may be very sensible on variations that could occure through tiny weight errors or even conatminations.

During digestion of runoff water suspensions (W2 and W3) mass of digested dry material was even lower. So, undigested water suspensions additionally have been observed on ICP-OES on their metal concentrations. It is shown (Table.S7.) that Zn after Ca > Na > K > Si is the most predominant trace metal with even higher concentrations than Al and Fe in both runoff water suspensions W2 and W3 which can be explained trough presence of tire particles. In previous studies Zn is reported to be the most abundant element in road runoffs and thus will be defined as significant tracer for possible elevated abundances of tire particles (Klöckner et al., 2019; Hwang et al., 2016, Helmreich et al., 2010).

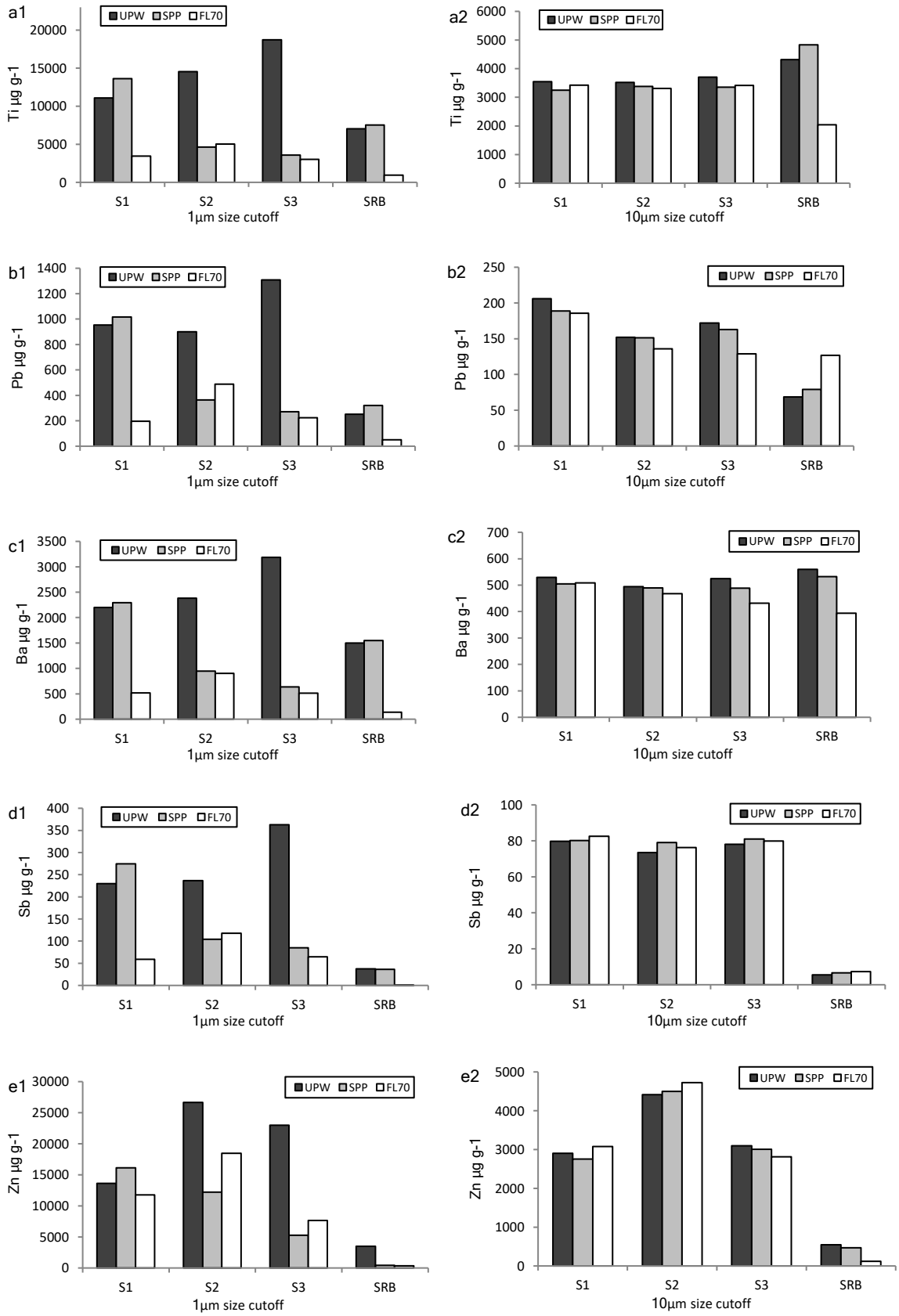

Fig.5.a.b.c.d.e. Element contents of total digested sediment suspensions normalized by 1g of corresponding dry sediment size fraction from road runoff and retention basin sediment samples extracted with UPW, SPP and FL70, determined via conventional ICP-MS. (1) represents 1µm size cutoff fraction suspensions while (2) represents each 10µm size cutoff fraction. Furthermore each element is indicated as follows: (a.) Ti, (b.) Pb, (c.) Ba, (d.) Sb, (e.) Zn,.

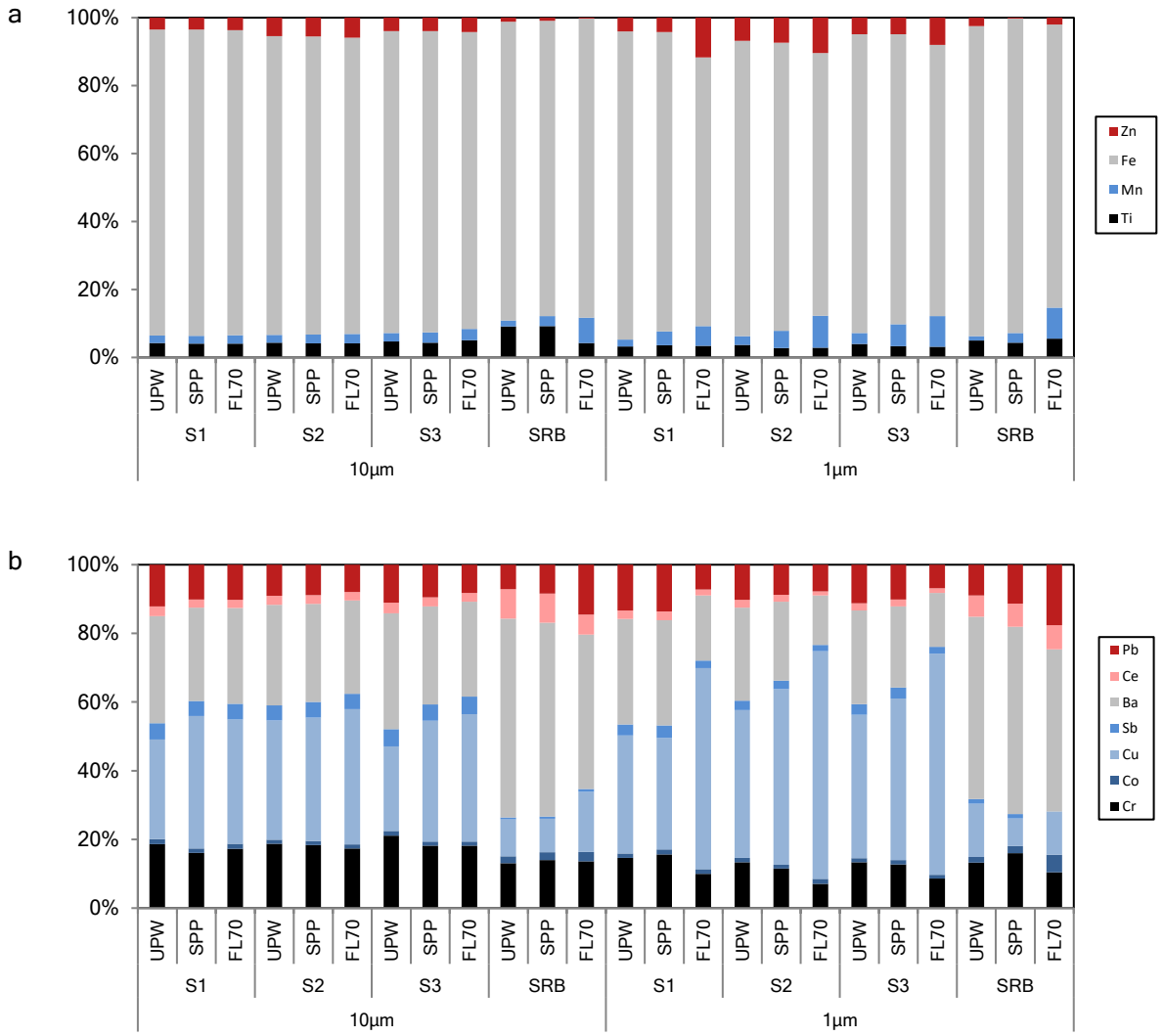

Fig.6. Metal composition extracted with UPW, SPP and FL-70 in total digested road runoff sediment (S1,S2,S3) and retention basin sediment (SRB) in 10µm and 1µm size cutoff fractions. Percentage has been calculated through concentrations of total digested suspensions which were analyzed by conventional ICP-MS and normalized by 1g of dry sediment from the corresponding size cutoff fraction. (a) represents metals that have concentrations significantly above 1 mg g-1 while (b) represents metals whose concentrations lay significantly below 1 mg g-1 and thus are below 1% of compositions from (a).

4.4. Total metal content in digested sediment

To compare metal concentrations between sediment dispersions and thus to make comparisons between extraction protocols and sediment dispersions, metal concentration measured by conventional ICP-MS in 1µm and 10µm size cut off sediment fractions got normalized by 1g of the corresponding dry 125µm stock fraction as listed in Table.S4 and illustrated in Fig.7. Road runoff sediment samples S1, S2 and S3 have Zn concentrations that are at least one order of magnitude higher than Zn concentration in retention basin sediment SRB which was less

exposed to traffic emissions. Furthermore, it is shown in Fig.7 that S1 is indicating highest TRP trace metal concentrations followed by S2 and S3. This may conclude that according to the sampling site most non exhaust TRPs were emitted during continuos traffic flow while in front of the traffic light (S2) more brake particles have been emitted than after the traffic light (S3). Through the investigation of digested sediment samples, it can be assumed that in road runoff sediment elevated Zn concentrations have been detected primarily caused by non-exhaust TRPs as it is known from previous studies that Zn is one of the most abundant components in brake and tire wear particles (Boulter, 2006; Thorpe and Harrison, 2008). Compared to SRB elevated concentrations of Ti, Cr, Mn, Fe, Co, Ni, Cu, Zn, As, Zr, Mo, Sb, Ba, Ce and Pb can also be found in both size cutoff fractions of road runoff sediments S1, S2 and S3 (Fig.7) and may as well have been caused through higher traffic exposure.

Table.1. Concentrations of trace metals detected in various soils in Vienna during various studies.

		Vienna Area Natural Background		Upper Crust		Top Soil Vienna				Sewage Sludge
		Sub Soil	Top Soil	Flysh	Alluvium	Urban Soils	Urban Soils (Dynamic)	Urban Soils (Stable)	West Exit Area	
		(1)	(1)	(2)	(2)	(3)	(4)	(4)	(3)	(5)
Cr	[mg/kg]	53	68	38	36	35	80	31	44	46.48
Mn	[mg/kg]	415	460	n.a.	n.a.	n.a.	346	501	n.a.	n.a.
Fe	[g/kg]	n.a.	n.a.	n.a.	n.a.	n.a.	13	12	n.a.	71.12
Co	[mg/kg]	7.8	9.5	9.5	7.9	8	8.8	6.5	7.4	3.12
Ni	[mg/kg]	25.65	22	30	28	28	n.a.	n.a.	31	26.98
Cu	[mg/kg]	12	15.2	34	39.5	56	18	11	77	188.48
Zn	[mg/kg]	40.5	60.5	127	141	164	97	75	233	585.8
As	[mg/kg]	4.83	5.7	7.9	8.1	8.6	8	4.8	7.4	2.85
Zr	[mg/kg]	200	215	n.a.	n.a.	n.a.	n.a.	n.a.	n.a.	n.a.
Mo	[mg/kg]	0.46	0.9	0.8	0.8	0.9	n.a.	n.a.	2.3	4.65
Cd	[mg/kg]	0.08	0.12	0.5	0.5	0.6	0.2	0.3	0.9	1.58
Sb	[mg/kg]	0.57	0.71	n.a.	n.a.	n.a.	n.a.	n.a.	n.a.	n.a.
Ba	[mg/kg]	350	310	n.a.	n.a.	n.a.	69	75	n.a.	231.33
La	[mg/kg]	23	20.8	n.a.	n.a.	n.a.	n.a.	n.a.	n.a.	n.a.
Ce	[mg/kg]	48	42.5	n.a.	n.a.	n.a.	n.a.	n.a.	n.a.	n.a.
Pt	[µg/kg]	n.a.	n.a.	n.a.	n.a.	<30	n.a.	n.a.	80	16
Pb	[mg/kg]	11	20.5	54	64	79	65	54	118	43.05

(1) Salminen, 2007
(2) Pfleiderer et al., 2012
(3) Kreiner, 2004
(4) Simon et al., 2012
(5) Hohenblum et al., 2000

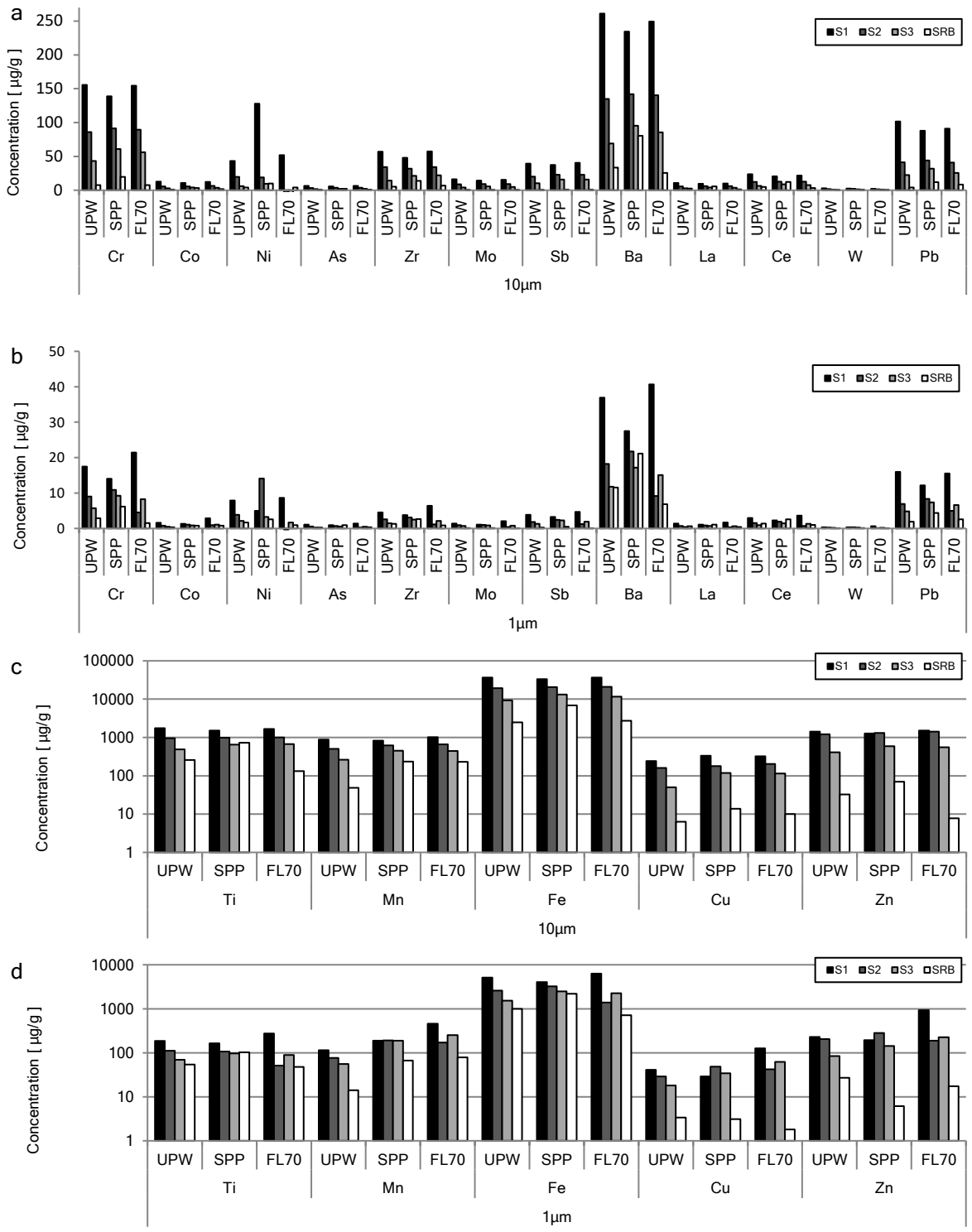

Fig.7.a.b.c.d. Trace metal concentrations in total digested 1µm and 10µm fractions of road runoff and retention basin sediment extracted with UPW, SPP, FL-70, detected with conventional ICP-MS and normalized by 1g of corresponding dry sediment from 125µm stock fraction. (a) and (b) represent elements having concentrations below 500 µg g^{-1} while (c) and (d) represent elements having concentrations above 500 µg g^{-1}. Y-axis in (c) and (d) is logarithmic due to concentration differences up to 4 orders of magnitude in between various elements.

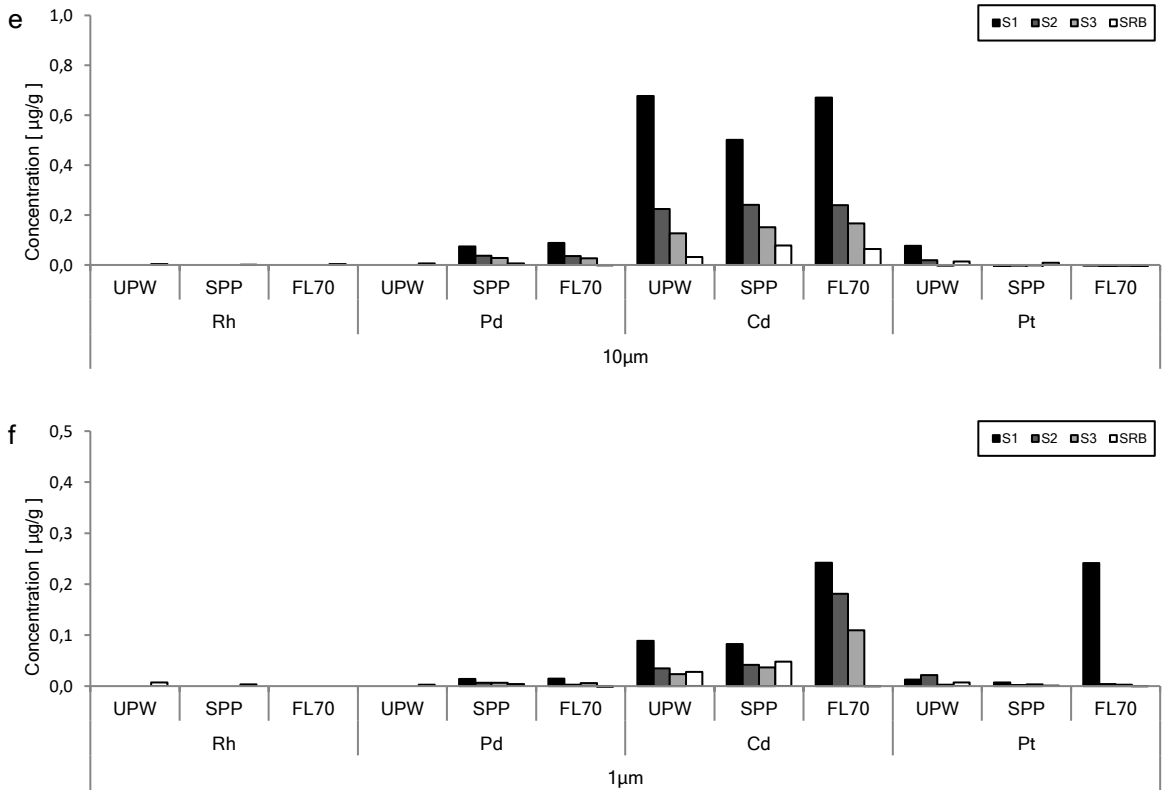

Fig.7.e.f. Trace metal concentrations in total digested 1µm and 10µm fractions of road runoff and retention basin sediment extracted with UPW, SPP, FL-70, detected with conventional ICP-MS and normalized by 1g of corresponding dry sediment from 125µm stock fraction. (e) and (f) represent elements having concentrations below 1 µg g^{-1} .

Table.2. Ratios and cocentrations of trace metals to be found in TRPs.

		Ba/Pb	Sb/Pb	Co/Zn	Mn/Cr	La/Ce	Pt [g/L]	Pd [g/L]	Rh [g/L]
Brake Dust	Pusiney et al., 2018	2.00	7.00	n.a.	0.15	n.a.	n.a.	n.a.	n.a.
	Thorpe and Harrison, 2008	62.00	13.00	0.00	4.30	n.a.	n.a.	n.a.	n.a.
	Adachi et al., 2004	5.00	3.00	n.a.	n.a.	n.a.	n.a.	n.a.	n.a.
Tire Wear	Adachi et al., 2004	1.00	0.70	n.a.	1.00	n.a.	n.a.	n.a.	n.a.
Digested Tire Wear		n.a.	n.a.	0.01	0.93	0.56	n.a.	n.a.	n.a.
Conventional TWC	Domesle, 1997	n.a.	n.a.	n.a.	n.a.	n.a.	0.30	1.5 - 5	0.1 - 0.4

UPW extraction amounts from 1µm out of 10µm size cutoff fractions in S1 and S2 ranging from 7.5% (Zr) to 19.5% (Ni) (this means that 7.5% of Zr and 19.5% of Ni concentrations in 10µm size cutoff fraction are caused through digested particulates with a hydrodynamic diameter below 1µm). In S3 UPW extraction amounts from 1µm out of 10µm size cutoff fractions are higher with a range up to 36.24% (Ni).

Furthermore, 20.8% of Zn was extracted from 1µm out of 10µm size cutoff fraction with UPW in road runoff sediment S3 which is around 5% more than in S1 and S2. FL-70 extraction is showing even higher Zn extraction amounts from 1µm out of 10µm size cutoff fraction in sediment S3 with 40.5% which concludes that more than one third of the Zn concentration in the 10µm size cutoff fraction of road runoff sediment S3 is caused through the digestion of Zn particulates with a hydrodynamic diameter below 1µm. It is reported that tire particles that contain Zn either have a size below 1µm (Panko et al., 2009) so it is likely that emitted tire particles during acceleration could have led to elevated Zn concentrations in S3. Nevertheless, Zn extraction shows different values for the extraction of the 10µm size cutoff from the 125µm stock fraction where it can be observed that in S1 and S2 FL-70 while in S3 SPP extracted the highest amont of Zn. So, it seems that every extraction protocol has a different response to each trace element in each sediment thus it is challenginf to give a statement on what extraction protocol is the most efficient for the extraction of TRPs.

In comparison to the natural backgrounds (Kreiner, 2004; Salminen 2007; Pfleiderer et al., 2012; Simon et al., 2012) to be found in Table.1 it is significant that all trace metal concentrations except Zr are elevated in the 125µm stock fraction of S1, S2 and S3 (Table.S4). It can be observed that Zn concentrations in S1, S2 and S3 are around two orders of magnitude higher than Zn concentrations in average topsoil of Vienna and even one order of magnitude higher than reference soil from a public park at Vienna's west exit area (Kreiner, 2004).

Sb concentrations in S1, S2 and S3 are even up to three orders of magnitude higher while Ba and Pb concentrations are around double as high as concentrations measured in average topsoil of Vienna. This may conclude that these elevated trace metal concentrations may be explained through traffic exposure of S1, S2 and S3.

This is also in good agreement concerning the composition of trace metals (Fig.8.) where it can be observed that S1, S2 and S3 show significant difference compared to composition of Vienna average soil. From natural compositon Mn > Zr > Ba > Zn > Pb > Cr > Ce > Cu > Ni > La > Co > As > Sb > Mo > Cd the composition of trace metals is changing in S1, S2 and S3 to Zn > Mn > Cu > Ba > Cr > Pb > Zr > Ni > Sb > Ce > La > Mo > As > Cd likely caused due to the exposure to individual traffic emissions and the resulting presence of TRPs in sediments.

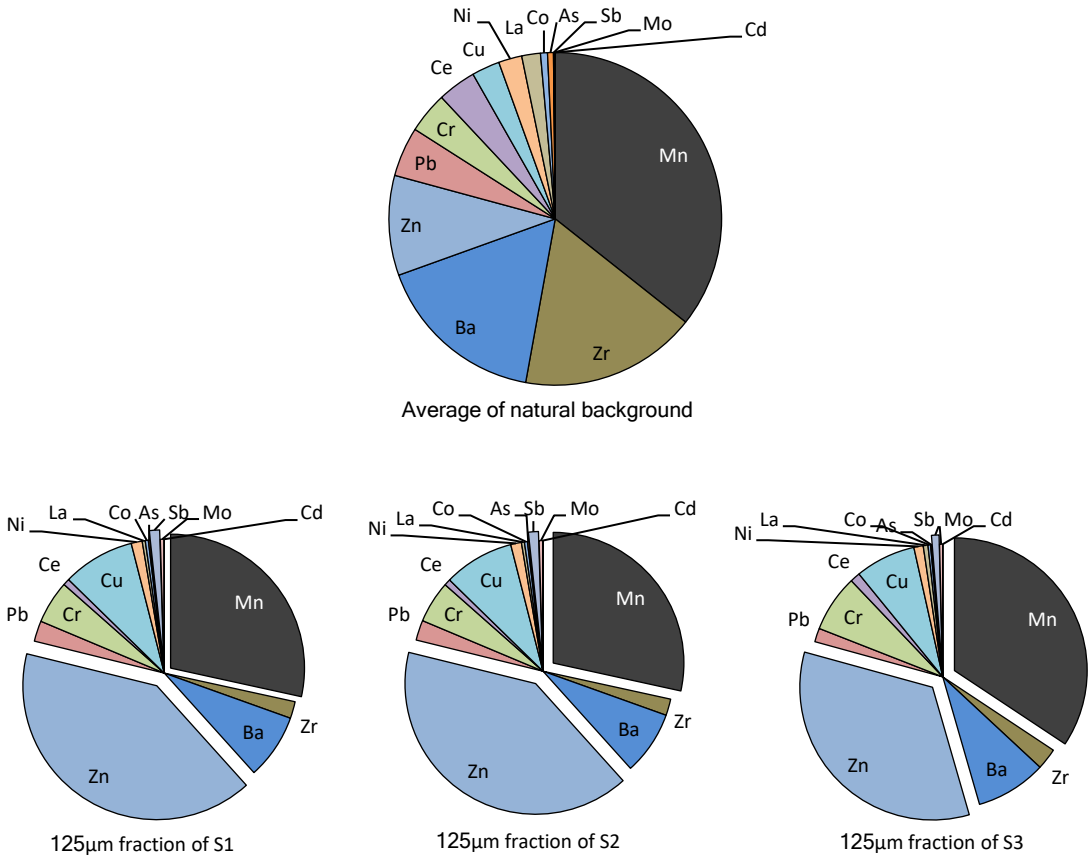

Fig.8. Trace metal composition in total digested 125µm fraction in road runoff sediment compared with average trace metal composition in soil of Vienna.

4.5. Trace metal concentration ratios in total digested sediment

Elemental ratios have been determined to analyze differences of trace metal amounts between the different sediment samples and furthermore for comparisons with natural ratios that would indicate elevated abundances of a certain trace element. It is reported that the natural system contains an assortment of natural mineral particles that have a certain amount of two associated elements e.g., La and Ce whose element concentrations may closely co-vary with the variation of particle concentrations (Montaño et al., 2014). La and Ce is also present in ENMs while La appears to have a significant lower abundance in ENMs than in NNMs which means that a ratio shift to Ce compared to the natural background could indicate increased engineered CeO_2 abundance (Montaño et al., 2014). Ce is also used as additive in diesel as it is suggested that Ce addition can increase the number of Ce containing particles (Skillas et al, 2000) which means that elevated Ce values could be a hint for the presence of exhaust and non-exhaust TRPs.
Furthermore, elevated Sb (up to 16900µg/g) concentrations compared to Pb (1290 µg/g) in emitted brake dust is reported (Thorpe and Harrison, 2008). This means that a shift towards Sb

compared to the natural Sb/Pb background ratio could indicate increased TRP abundance in form of brake wear. Thorpe and Harrsion, 2008 also report that brake dust contains up to 74400µg/g Ba. As a result, Ba/Pb ratios are also used to observe brake wear particle abundances.

Metal concentration measurements from conventional ICP-MS in total digested reference tire particles (Table.2) show a Co/Zn ratio of 0.011 and a Mn/Cr ratio of 0.93. This advises to compare Co/Zn and Cr/Mn ratios of total digested road runoff and retention basin sediment samples with ratios of total digested reference tire particles, to determine elevated abundance of tire particles.

In Fig.9 in can be observed that La/Ce ratios (Fig.9.a) of total digested sediment as shown in are exactly in the natural range of 0.45 (Salminen, 2007) which means that the natural background of Ce containing particles in both runoff and retention basin sediment is high in an order the presence of engineered CeO_2 particles cannot get observed without ME-spICP-MS.

La/Ba, La/Pb, La/Sb, La/Zn and La/Cu (Fig.9.b.,c.,d.,e.,f.) ratios in S1, S2 and S3 are significantly below the natural background wheras ratios in SRB are higher than in S1, S2 and S3 so it is assumable that road runoff and retention basin sediment have an elevated amount of engineered Cu, Zn, Sb, Ba and Pb particles likely to be caused due to the contamination of non-exhaust TRPs. Nontheless Sb, Ba and Pb are also present in other INMs and will be used as tracer for e.g., gunshot residue (GSR) that can elevate the abundance of Sb, Ba and Pb in soils (d. Heringer et al., 2018). Emitted brake dust as previously discussed contains more Sb and Ba than Pb compared to GSR which has a higher Pb than Sb and Ba content (d. Heringer et al., 2018). Anyway in Fig.9.g. it is shown that S1, S2 and S3 which indicates Pb/Ba ratios at least in the range of emitted brake dust.

Furthermore Fig.9.i.,j. shows Mn/Cr and Zn/Co ratios in total digested road runoff and retention basin sediment suspensions compared to natural background and total digested tire material. Mn/Cr ratios in total digested sediments are more ore less in the range of the natural background except FL-70 extracted suspensions which lay significantly above the Mn/Cr ratio of digested reference tire material (Table.2). Zn/Co ratios indicate that S1, S2 and S3 have ratios that even lay significantly above the natural background and above the ratios of digested reference tire material (Table.2). This could mean that metal contamination is primarily not happening through tire particles but also through other INMs e.g., TRPs

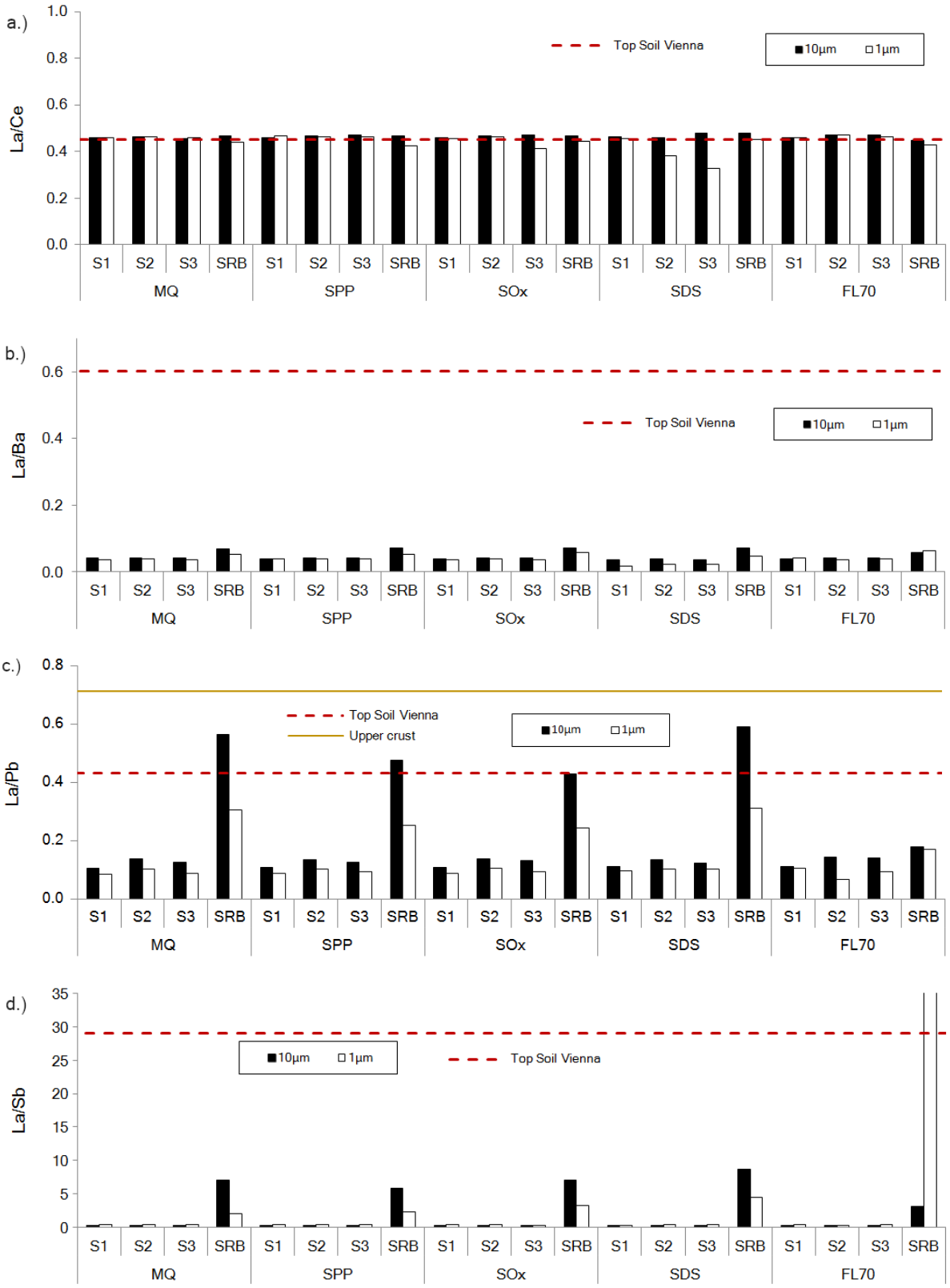

Fig.9.a.b.c.d. Element concentration ratios of total digested road runoff and retention basin sediment determined by respecting element mass concentrations in all suspensions of 1µm and 10µm size cutoff fractions analyzed via conventional ICP-MS. Reference ratios are the mean from values listed in Table.1 and Table.2.

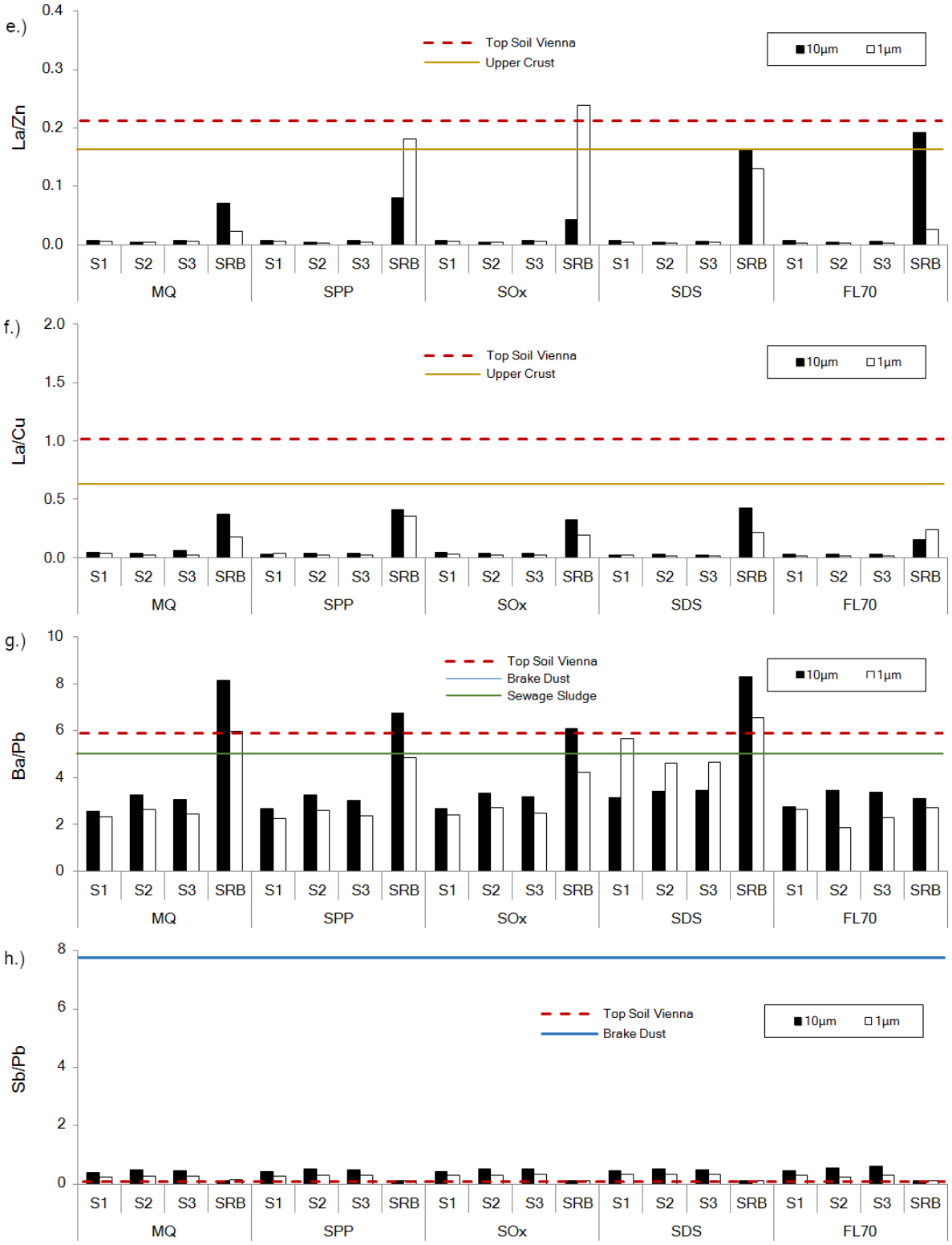

Fig.9.e.f.g.h. Element concentration ratios of total digested road runoff and retention basin sediment determined by respecting element mass concentrations in all suspensions of 1µm and 10µm size cutoff fractions analyzed via conventional ICP-MS. Reference ratios are the mean from values listed in Table.1 and Table.2.

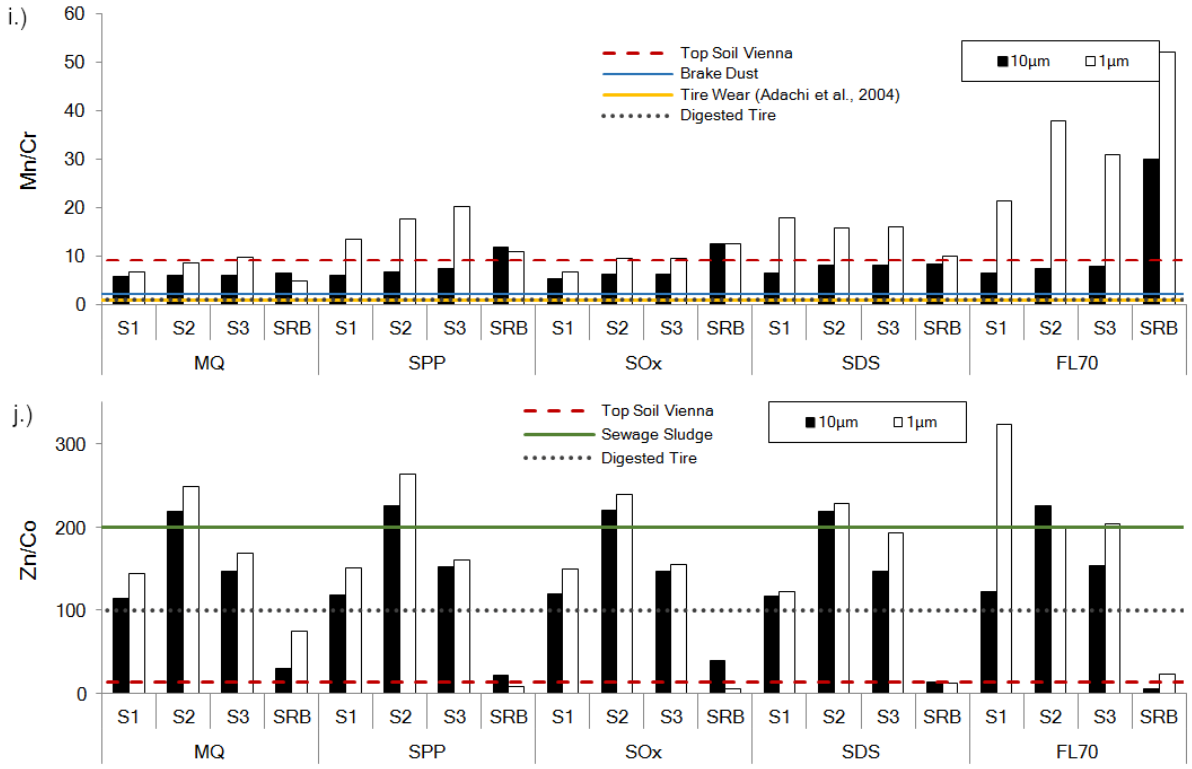

Fig.9.i.j. Element concentration ratios of total digested road runoff and retention basin sediment determined by respecting element mass concentrations in all suspensions of 1µm and 10µm size cutoff fractions analyzed via conventional ICP-MS. Reference ratios are the mean from values listed in Table 1 and Table 2

containing Cr, Mn, Co and Zn such brake wear. Nevertheless, it must be considered that several tires from numerous brands could contain different Cr/Mn and Zn/Co ratios.

Ratios from total digested retention basin sediment are almost in all graphs closer to the natural background than total digested road runoff sediment which means that concentration of TRPs are overall lower in retention basin sediment than in road runoff exposed sediments. This was expected resulting the higher traffic exposure through road runoff which is also in good agreement with normalized to 125µm stock fraction heavy metal concentrations in Table.1.

4.6. Element association with Aluminum

Metal concentrations analyzed via ME-spICP-MS by ICP-TOFMS in the 1µm size cutoff fraction of road runoff sediment (S1,S2 and S3) retention basin sediment (SRB) (Table.S8) extracted and road runoff water (W2 and W3) (Table.S9.) samples got determined by observing particle events of tracemetals that appear together with or without Al as it is known that Al is one of the most abundant metals in natural clay minerals (Murray, 2006). This method was

chosen as approach to expose the potential source of metals in the samples by investigating if trace metal concentrations are either caused through natural Al rich clay minerals or through the contamination by TRPs. Especially, as it is suggested that the amount of Al by mass in emitted car brake dust is only 3% of the emitted mass from Ba and Sb together while Al in tire wear is also only reported as trace element below 1ppm (Boulter, 2006; Thorpe and Harrison, 2008). Therefore, measured metal concentrations in road runoff and retention basin sediment suspensions are normalized per gram of corresponding dry 125µm sediment stock fraction to observe metal concentration differences between the several sediment samples as shown in Fig.10. Also, road runoff water suspensions W2 and W3 were normalized by 1 liter of corresponding road runoff water Fig.11.

Now in Fig.10 it is illustrated that especially in road runoff sediment S1 and S2, FL-70 compared to UPW extraction has a significant effect on concentrations of some trace metals such as Ti, Mn, Zn, Sb, Ba Ce and Pb by indicating lower ratios from metals associated to Al to metals not associated to Al (e.g., in S1 the ratio *Ti with Al* to *Ti without Al* from UPW extraction is 0.85 while this ratio with FL-70 extraction reaches only 0.20). Maybe this could mean that the FL-70 extraction protocol could have released more INMs such as TRPs by braking up heteroaggregates with Al rich NNMs. Furthermore, it is also significant that trace metal concentrations especially Cr, Mn, Cu, Sb, Ba and Pb are around one order of magnitude lower in retention basin sediment SRB than in road runoff sediment samples which is probably due to the higher traffic exposure of road runoff sediment samples and that result is also in good agreement with conventional ICP-MS analysis from total digested sediment samples. Nevertheless, to give a statement about which one of all three road runoff sediment samples has the highest concentration of a certain element is problematic due to different concentrations in between the extraction protocols.

Therefore, in road runoff water samples W2 and W3 it is again significant (Fig.11) that all trace metals in W2 are showing higher concentrations than in W3, so it can be assumed that runoff water sample W2 is more contaminated with metals due to higher emissions of TRPs before than after the traffic lights likely caused by braking events. Anyway, improved extraction efficiency through 1mM SPP in runoff water by indicating higher metal concentrations can not be observed in the 1µm size cutoff fractions.

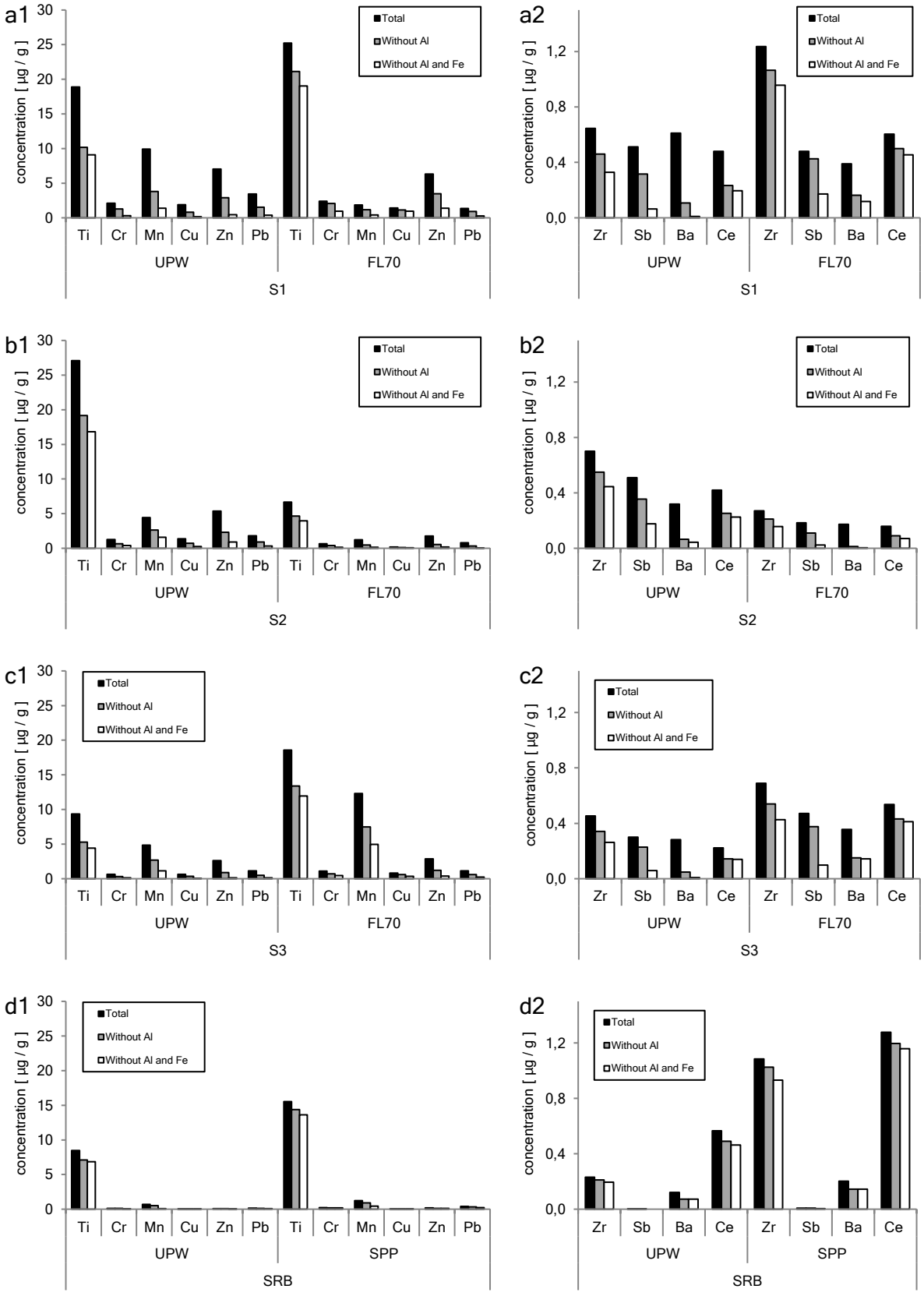

Fig.10. Metal concentrations determined via multi element-spICP-MS by ICP-TOFMS from 1µm size cutoff fraction in road runoff sediment S1 (a), S2 (b), S3 (c) extracted with UPW and FL-70 as well as retention basin sediment SRB (d) extracted with UPW and SPP that got normalized by 1g of corresponding dry 125µm sediment stock fraction.

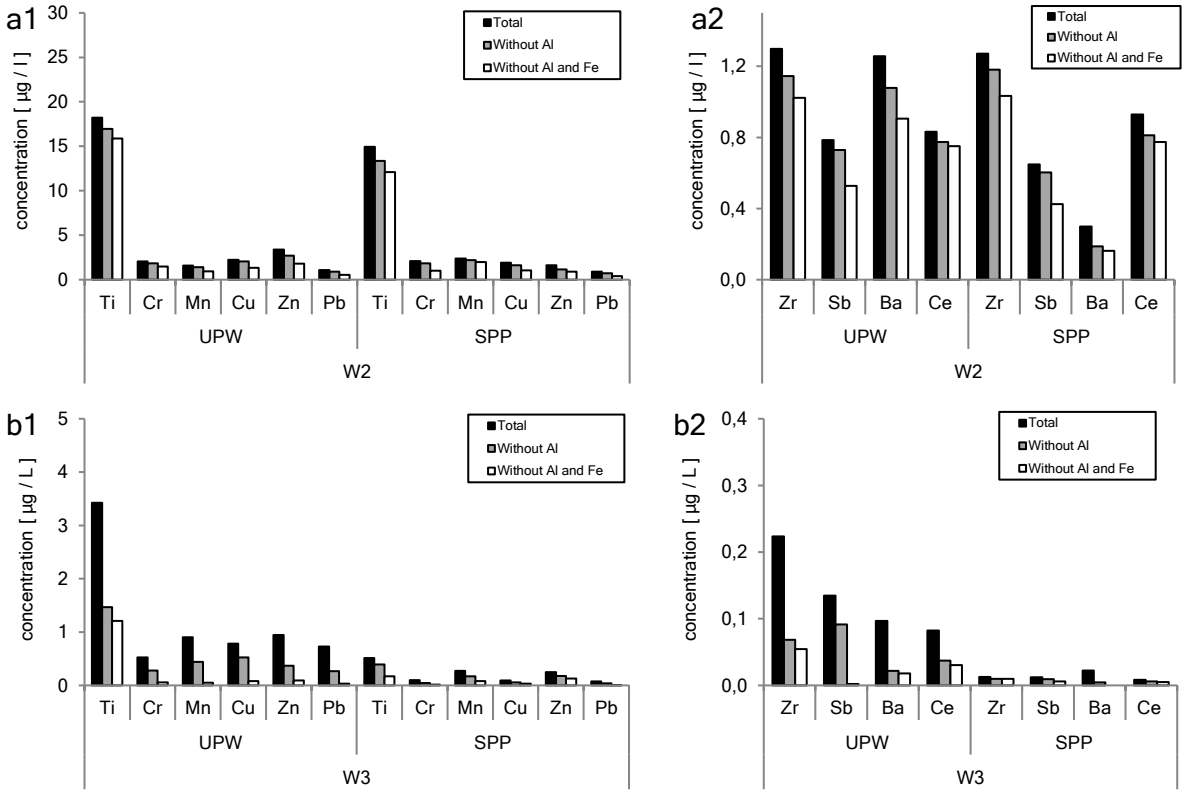

Fig.11. Metal concentrations determined via multi element-spICP-MS by ICP-TOFMS from 1µm size cutoff fraction in road runoff water suspensions W2 (a) and W3 (b) UPW and SPP that got normalized by 1L of corresponding road runoff water sample.

4.7. Detection of traffic related particles

For the detection of non-exhaust and exhaust traffic related particles the road runoff sediment and water suspensions were analyzed by ICP-TOFMS during multi element-spICP-MS. Since through this method it is possible to detected particles of more than one isotope at the same time, NMs can be classified by their elemental fingerprint. Hence selective criteria can be applied to classify TRPs according to their respecting sources. During this study, a method was developed to distinguish between potential brake wear and tire wear particles by using frequently reported metal as identification criterion. To identify one brake wear particle, the occurrence of Ba, Sb and Pb (Boulter, 2006; Thorpe and Harrison, 2008) has been observed which means that if two of the three or all three elements appear together in one particle event, this particle gets counted as one brake wear particle. For a certain characterization of tire particles, Zn was used as main trace metal by saying that if Zn appears together with Ti, Co, Te or W the peak gets counted as tire wear particle.

Results in Fig.12.d show a comparison of brake and tire particle concentrations (particle L^{-1}) in the respecting 1µm fraction suspensions. S1, S2 and S3 are indicating more or less the same number of particles so that way it is not possible to say if the particle emission is higher on one site than on the other. Theoretically it is assumed that on site S2 which is located in front of the traffic light on the one-way road the emission of brake particles by mass is higher than on site S3 located after the traffic light. To determine differences between local particle emission amounts by mass it is necessary to analyze road runoff water samples that are particle composition snapshots taken during the same time. So, a significant difference of brake to tire particle ratio in the 1µm fraction suspensions of rainwater road runoff samples W2 and W3 is shown in Fig.12.a proving the assumption that according to the sampling location more brake particles by mass were emitted in front of the traffic light in W2.

Problems show up when it comes to the identification of Pb particles together with Ba and Sb, as mineral data base from the Hudson Institute of Mineralogy (Mindat.org) reports that 276 minerals of natural minerals have Pb and Sb associations while also 1.17% 19 natural minerals indicate associations between Pb and Ba. So, it is likely that particles that have been detected as brake wear particles containing Pb and Sb or Pb and Ba could be clay minerals with the same chemical fingerprint.

A certain distinction between engineered from natural Pb particles is only possible with mass ratio comparison. However, associations between Ba and Sb are reported to not occur naturally, so it is obvious to use particles containing Ba and Sb as certain tracer to identify INMs or potential TRPs as shown in Fig.12. Nevertheless, if the identification of brake wear particles gets minimized to only Ba and Sb, ratios of emission amounts between different sites will not change much according to the detection results. Percentages of particle associations from total number of particles of one trace metal are represented in Table.3. It may be observed that in most cases Ba and Sb associations often appear together with Pb than alone together.

Automotive catalyst particles have been identified by observing particles containing PGEs such as Rh, Pd and Pt that get emitted as exhaust TRPs in metallic and metal oxide form with an estimated solubility of 10% (Inacker and Malessa, 1992, Hill and Mayer, 1977), so it is likely that PGE particles after they go airborne

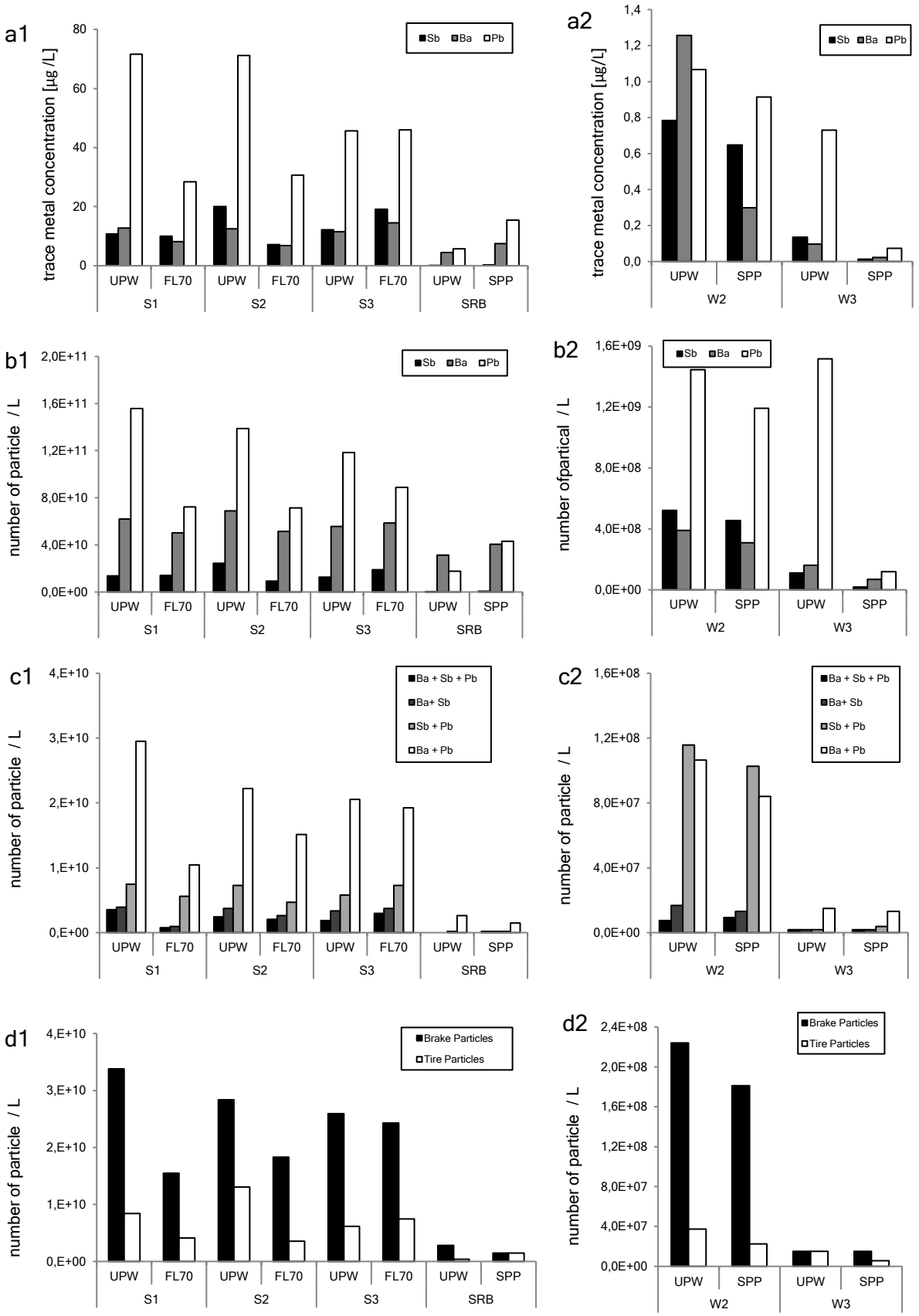

Fig.12. (a) Total concentration of Sb, Ba and Pb in 1L of respective suspension. (b) Number of detected Sb, Ba and Pb particles in 1L of corresponding suspension. (c) Number of particulates with certain element associations and (d) number of non-exhaust TRPs in 1L of respective suspension. (1) represents sediment and (2) rainwater samples. ME-spICP-MS was performed with ICP-TOFMS of 1µm size cutoff fractions.

Table.3. Percentage of particle amount with element associations from total particle amount of certain tarce metal.

		Sb			Ba			Pb		
[%]		Sb + Ba + Pb	Sb + Ba	Sb + Pb	Sb + Ba + Pb	Sb + Ba	Ba + Pb	Sb + Ba + Pb	Sb + Pb	Ba + Pb
S1	UPW	26	29	55	6	6	48	2	5	19
	FL70	5	7	40	1	2	21	1	8	14
S2	UPW	10	15	30	4	5	32	2	5	16
	FL70	22	28	50	4	5	29	3	7	21
S3	UPW	15	27	46	3	6	37	2	5	17
	FL70	16	20	39	5	6	33	3	8	22
SRB	UPW	0	0	100	0	0	8	0	1	15
	SPP	33	33	33	0	0	4	0	0	3
W2	UPW	1	3	22	2	4	27	1	8	7
	SPP	2	3	23	3	4	27	1	9	7
W3	UPW	2	2	2	1	1	9	0	0	1
	SPP	10	10	20	3	3	19	2	3	11

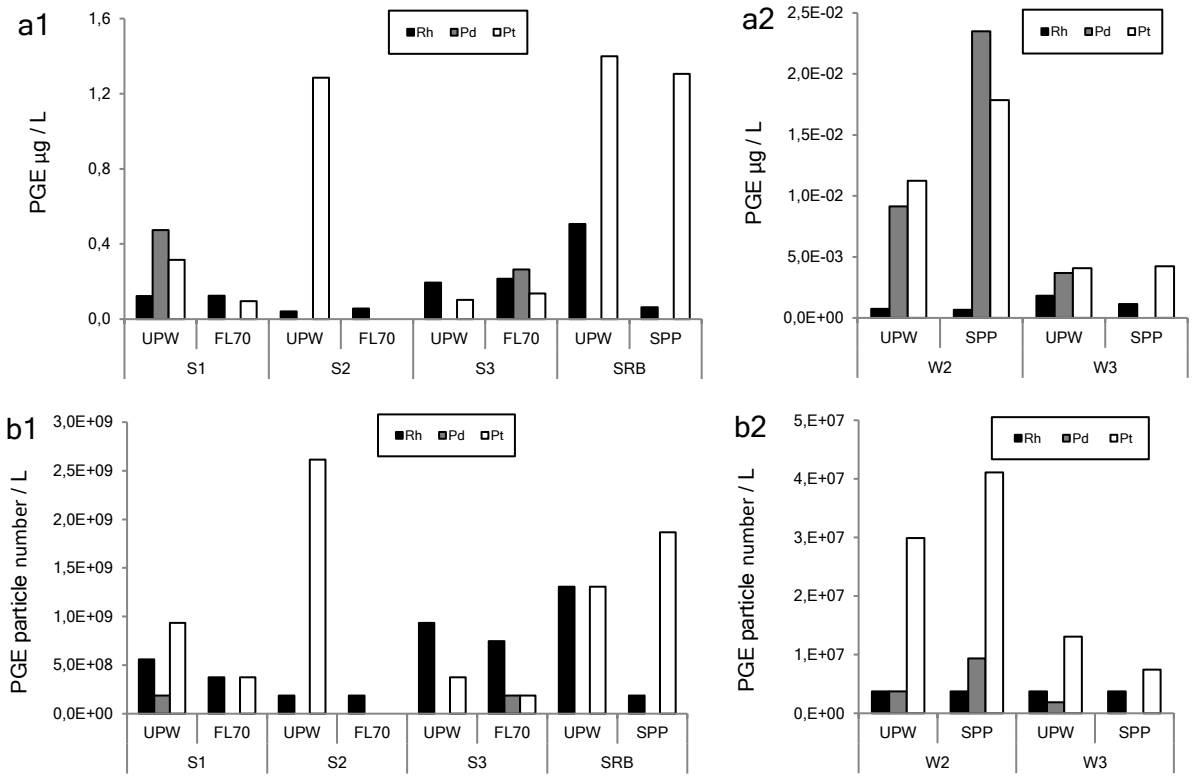

Fig.13. (a) Concentratiosn and (b) number of PGEs in 1µm size fraction normalized by 1L of corresponding. (1) represents sediment and (2) rainwater samples. ME-spICP-MS was performed with ICP-TOFMS of 1µm size cutoff fractions.

accumulate on road surfaces and furthermore cause elevated Rh, Pd and Pt abundance in road runoff. As natural background PGEs mean values of measured earth crust concentration such 0.06ppb for Rh and 0.4ppb for Pd and Pt are commonly used (Wedepohl, 1995). During

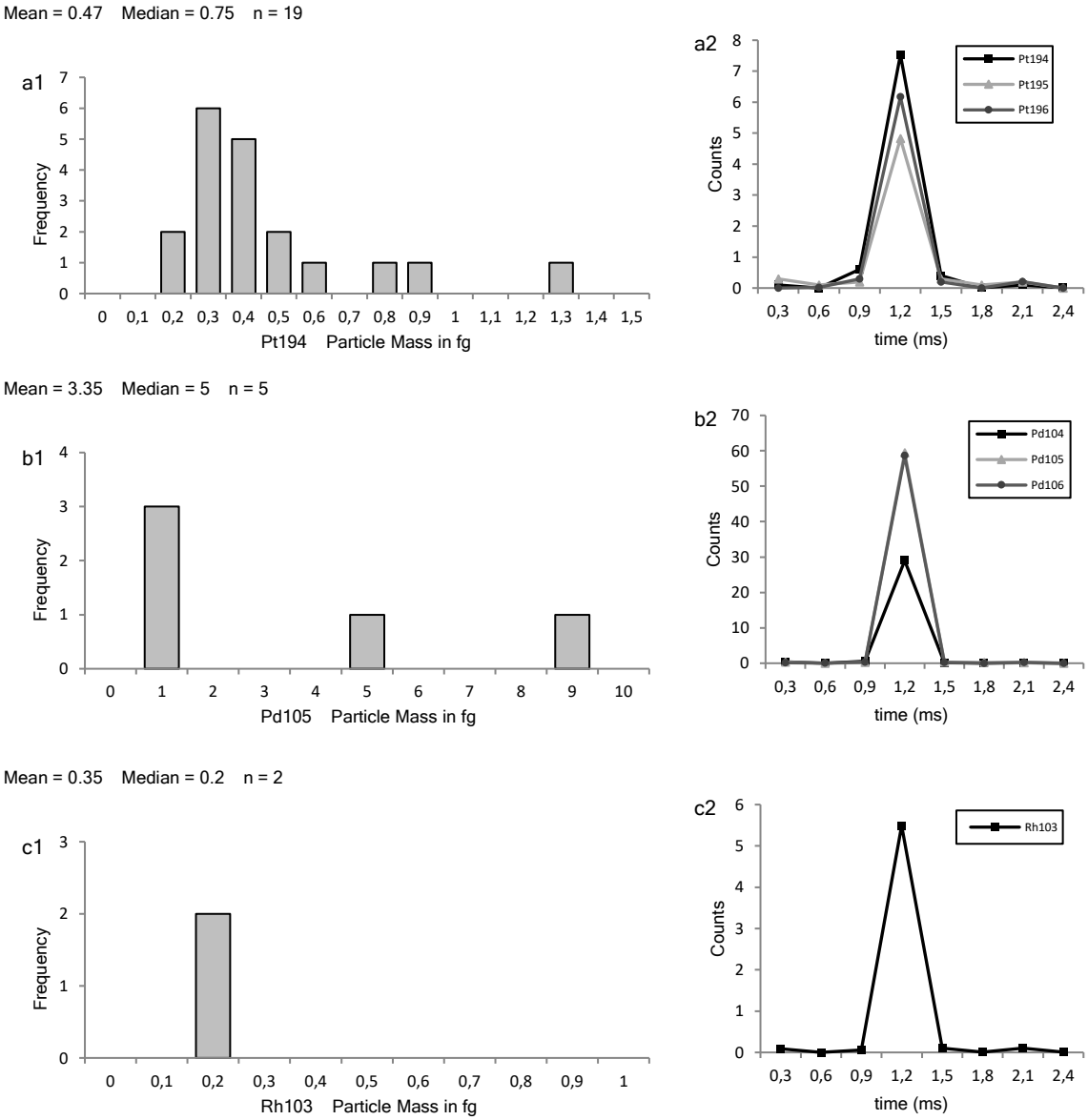

Fig.14. (1) Particle Mass distribution of PGE particles in W2 extracted with SPP and detected with ICP-TOFMS. Sample was diluted 1:99. (2) Peak of detected PGE particle from raw signal of ICP-TOFMS.

ME-spICP-MS multiple particles containing Rh, Pd and Pt have been detected in 1µm size fraction dispersions as seen in Fig.13. It is shown that sediment suspensions do not have a constant seequence of Rh, Pd and Pt concentrations but it can be observed that Pt and Rh are present in all road runoff sediments (S1, S2 and S3) and SRB while Pd only occures in S1 and S2. Nevertheless, according to the resulting variation of PGE concentrations it is not possible to make a statement about PGE extraction efficiency in between several extraction protocols applied on sediments.

Anyway, road runoff water samples W2 and W3 appear to have a constant concentration seequences in between extraction protocols. It can be observed that SPP had a positive effect

on PGE extraction in W2 while W3 has almost no difference between the two extraction protocols.

Furthermore, it is significant that W2 (30 to 40 particles μL^{-1}) contains up to four times more Pt particles than W3 (around 10 particles μL^{-1}) whereas both runoffs are indicating the same number of Rh particles (<10 particles μL^{-1}).

Pd particles are as previously discussed rarely detected in sediments but therefore around 10 Pd particles μL^{-1} have been detected in W2 with SPP extraction. It is reported that 1L of conventional TWC contained 0.3-2.0g Pt and 0.1-0.4g Rh with 1.5-5g Pd (Domesle, 1997). Although less Pd than Pt and Rh particles are detected it is shown in Fig.14, that the mean of Pd particle mass is about 10 times higher than mean of Pt and Rh particle mass. Also, raw ICP-TOFMS signal (Fig.14.) of Pd particles shows a peak that is about 10 times of counts higher than peaks of Pt and Rh particles which concludes that Pd particles may have a significant higher mass (around 10 times) than Pt and Rh particles. This explains why although less Pd particles are detected in road runoff water but Pd particle emission by mass (Fig.13.a2) is higher than Pt and Rh. Which means PGE observations in W2 are in good agreement with the PGE mass content in conventional TWCs reported in Domesle (1997).

4.8. Mass ratios of associated elements in detected particles

As previously mentioned, natural clay minerals could have similar elemental composition as TRPs and thus it is necessary to distinguish between NNMs and TRPs which will be done through mass ratios in comparison with natural background. Results of total digested sediment already showed that the natural background of trace elements especially Ce is relatively high This means, that the number of NNMs prevails the number of TRPs having a similar elemental composition which makes it necessary to observe the mass ratio of every detected single particulate.

In theory engineered CeO_2 nanoparticles appear as a single Ce peak in an ICP-TOFMS signal without the presence of La if engineered CeO_2 nanoparticles are not associated to NNMs. Nevertheless, it is suggested that average elemental composition of NNMs is around 60ppm Ce^{4+} and 30ppm La^{3+} which means a detected particulate containing associated CeO_2 with NNM would indicate a La/Ce mass ratio shift toward Ce (Montaño et al., 2014). Furthermore, results of previously mentioned total digested tire particles show that tire wear has a La/Ce ratio of 0.56 (Table.2.) that is above the natural background of 0.45 (Salminen, 2007). So, tire wear particles could appear to have a higher La content as NNMs. According to these assumptions a

particle event detected by ICP-TOFMS containing La and Ce that has a La/Ce mass ratio below the natural background is assumed to be engineered CeO_2 related to NNM while a detected particle with a La/Ce mass ratio above the natural background has the potential to be a tire wear particle.

However, it is illustrated in Fig.15. that according to sampling site La/Ce mass ratios in detected NMs could either significantly vary or follow the natural trend. In all suspensions around half the number of particles containing La and Ce are in natural range while the other half of particles is indicating either La/Ce mass ratios above or below natural trend. It is significant that primarily small particles (<0.5fg) are indicating La/Ce ratios that are close to 1, meaning that La content is equal or even above the Ce content in one particle. In W2 (Fig.15.c.) from 251 detected particles containing La and Ce, 100 particles appear to be above natural background (>0.45) while 26 particles are showing La/Ce ratios below 0.29 and having a Ce particle mass up to 14fg. So, the 26 particles below the natural background could be CeO_2 particles related to NNM as von der Kammer et al (2012) suggests while particles above the natural background could appear to be tire particles as they are related to La/Ce slope of digested tire particles. Similar observations can be seen in S3 (Fig.15.a.) where 57 La/Ce particles have been detected from which 38 particles (34 above and 4 below the natural ratio) do not follow the natural La/Ce trend. In SRB (Fig.15.b.) 211 La/Ce particles have been detected including 109 outliers from whom only 2 are significantly below the natural La/Ce background.

Anyway, particles containing La and Ce do not follow the natural La/Ce mass ratio around 0.45 and mostly seem to have mass ratios above 0.69 which indicates elevated La content in detected particles, that could be a hint for tire wear. Particles with La/Ce mass ratios significantly below the natural background (<0.45) that are likely to be CeO_2 related to NNM are less present (<10% of total La/Ce particles) but have a striking higher mass. As comparison the occurrences of detected Ce particles appearing without the presence of La assumed to be engineered CeO_2 are demonstrated in Fig.16.

All measurements show that detected Ce particles have an average mass between 0.3fg and 0.5fg (Ce particle with a mass of 0.93fg has a spherical shape diameter of 100nm) while in W2 Ce particles appear with an average mass up to 4fg and thus are smaller than Ce particles appearing together with La (up to 14fg Ce mass). The amount of Ce particles without La in W2, W3 and S3 is also around 50% higher than the amount of Ce particles occurring together with La (e.g., 365 counts of Ce particles without La and 251 Ce particles together with La in W2) while in SRB the amount of Ce particles without La and the amount of Ce particles with La is almost equal (217:211).

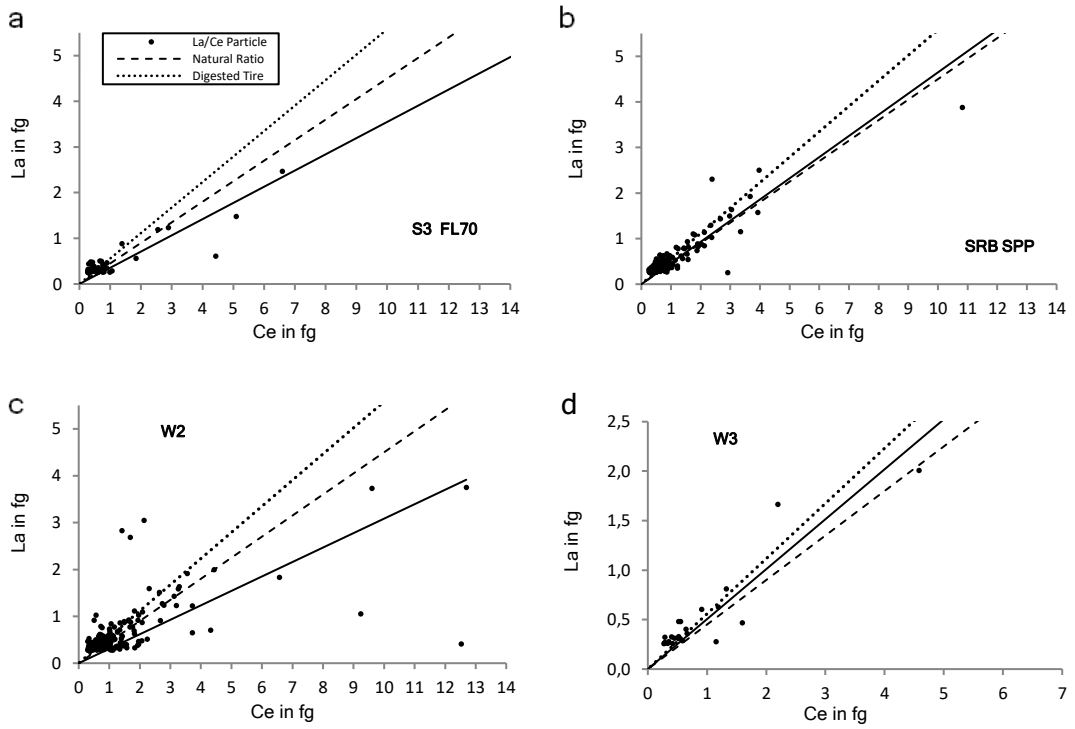

Fig.15. Detected La/Ce particles in 1µm size cutoff dispersion (sediment diluted 1:9999, water diluted 1:99). Multi element-spICP-MS signal detected by ICP-TOFMS. Dashed line represents the natural background (FOREGS), continuous line represents the linear of all detected La/Ce particle mass ratios and dotted lines representing digested tire ratio. Graph (a)illustrates particles in dispersion S3 FL70, (b) SRB SPP, (c) W2 pristine and (d) W3 pristine.

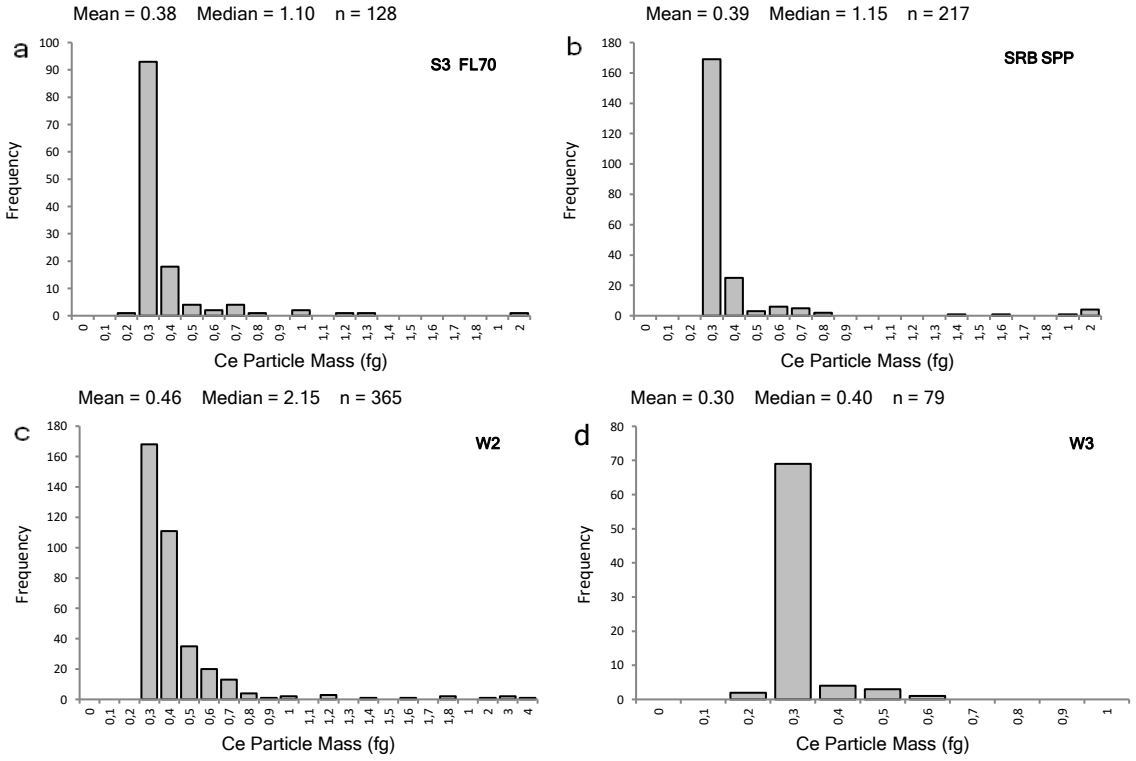

Fig.16. Detected Ce particles not associated to La in 1µm size cutoff dispersion (sediment diluted 1:9999, water diluted 1:99). Multi element-spICP-MS signal detected by ICP-TOFMS. Graph (a)illustrates particles in dispersion S3 FL70, (b) SRB SPP, (c) W2 pristine and (d) W3 pristine.

As previously mentioned, 276 minerals containing Pb and Sb and 19 minerals containing Pb and Ba occur naturally (Mindat.org) which means that brake particles having the same elemental composition could also get detected as NNM. Therefore, it is necessary to have a look onto the mass ratio between Ba/Pb and Sb/Pb as natural minerals contain more Pb by mass than Ba or Sb. So, theoretically a detected colloid whose particle mass of Ba or Sb is higher than the particle mass of Pb is assumed to be INM and thus in that case very likely to be brake wear as it is known that brake dust contains more Ba or Sb than Pb by mass (Boulter, 2006; Thorpe and Harrison, 2008; Puisney et al., 2018). While in SRB no particles containing Ba and Pb or Sb and Pb have been detected, most of such particles were found in W2 and as seen in Fig.17. most of them have lower Pb content than Ba and Sb. In W2 20 particles containing Ba and Pb were detected where all have a higher Ba than Pb mass while 57 particles containing Sb and Pb have been indicated where 47 have a higher Sb than Pb mass. W3 counts 10 particles Ba and Pb particles where all have Ba/Pb mass ratios above 1 and 22 Sb and Pb particles where 17 have Sb/Pb mass ratios above 1. In S3 all 17 Ba and Pb particles also have Ba/Pb mass ratios above 1 while 36 Sb and Pb particles have been counted from which only the half (18) has Sb/Pb mass ratios above 1. So overall all detected Ba and Pb particles that were detected in all samples show higher Ba than Pb content. In rainwater road runoff samples around 80% of Sb and Pb particles have a higher Sb than Pb content and thus are assumed to be TRPs while in road runoff sediment only 50% of all detected Sb and Pb particles have a higher Sb than Pb content. This is also in good agreement with the assumption that theoretically the amount of natural minerals in sediment samples should be higher than in road runoff rainwater.

As total results of digested reference tire particles study already showed (Table.2), Cr/Mn ratio of tire particles is around 1.08 and thus tires would appear to have a significantly higher Cr content than the natural Cr/Mn background of 0.13, Cr/Mn ratios would be useful to characterize potential detected tire particles. Overall, 17 known natural minerals are reported (Mindat.org) to contain Cr and Mn which means that a detected particulate only showing associations between Mn and Cr is not a certain tracer to define INMs, so it is important to investigate Cr/Mn mass ratios in every detected particulate showing assocuiations between Cr and Mn. Fig.18. illustrates detected Cr/Mn particulates where in all samples a distribution can be observed that on one hand shows particles that either follow the natural Cr/Mn ratio trend while on the other hand particles with higher Cr content follow either the Cr/Mn ratio of digested tire particles. It can be observed that suspensions extracted with FL-70 indicate compared to UPW extraction more Cr/Mn particulates from total measured Cr and Mn

concentrations in all road runoff sediment suspensions (Table.5). In S3 extracetd with FL-70 (Fig.18.a) 46 Cr/Mn particulates have been detected from which 38 have Cr/Mn mass ratios

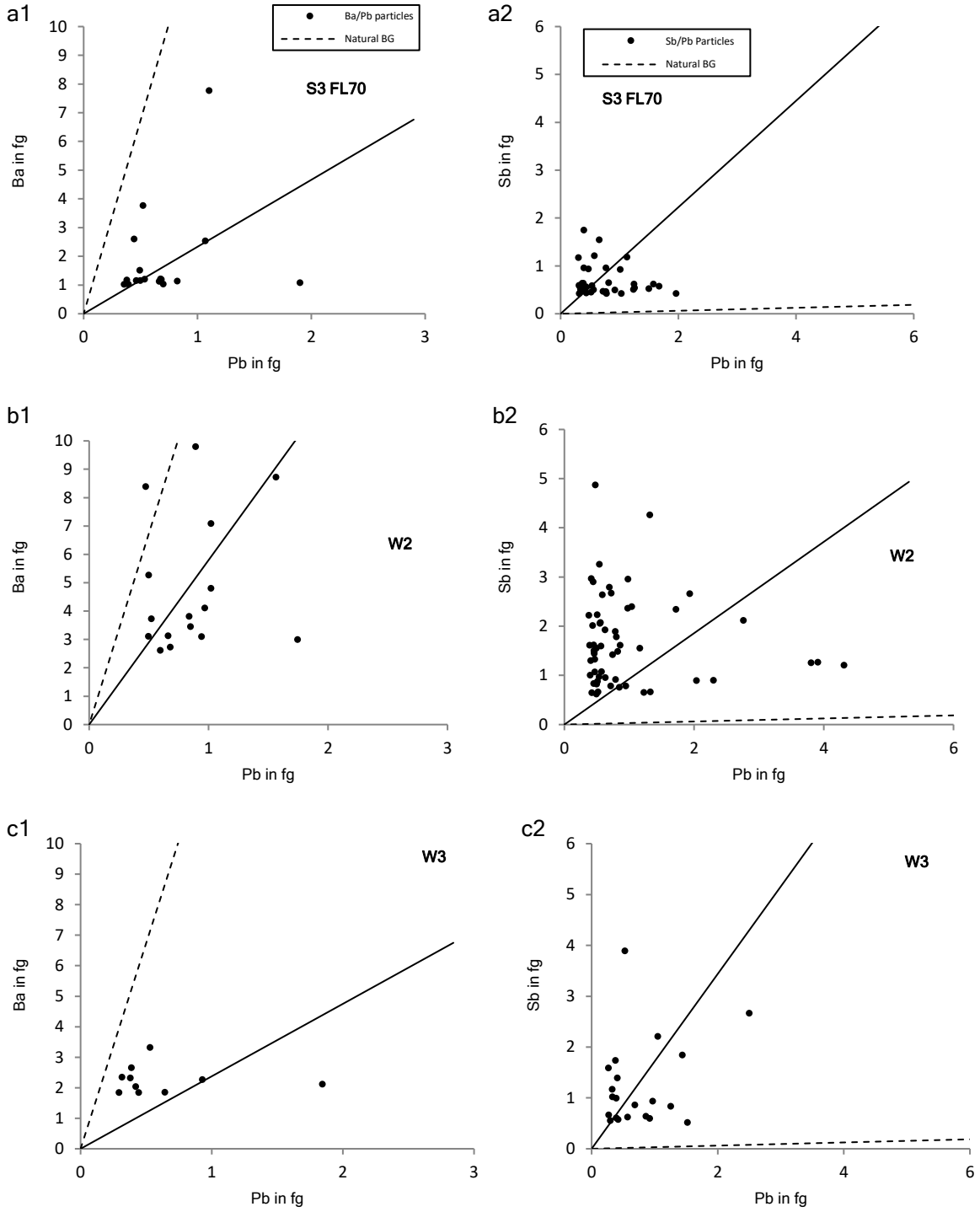

Fig.17. Detected (1) Ba/Pb and (2) Sb/Pb particles in 1µm size cutoff dispersion (sediment diluted 1:9999, water diluted 1:99). Multi element-spICP-MS signal detected by ICP-TOFMS. Dashed line represents the natural background (FOREGS), continuous line represents the linear of all detected La/Ce particle mass ratios and dotted lines representing digested tire ratio. Graph (a)illustrates particles in dispersion S3 FL70, (b) W2 pristine and (c) W3 pristine.

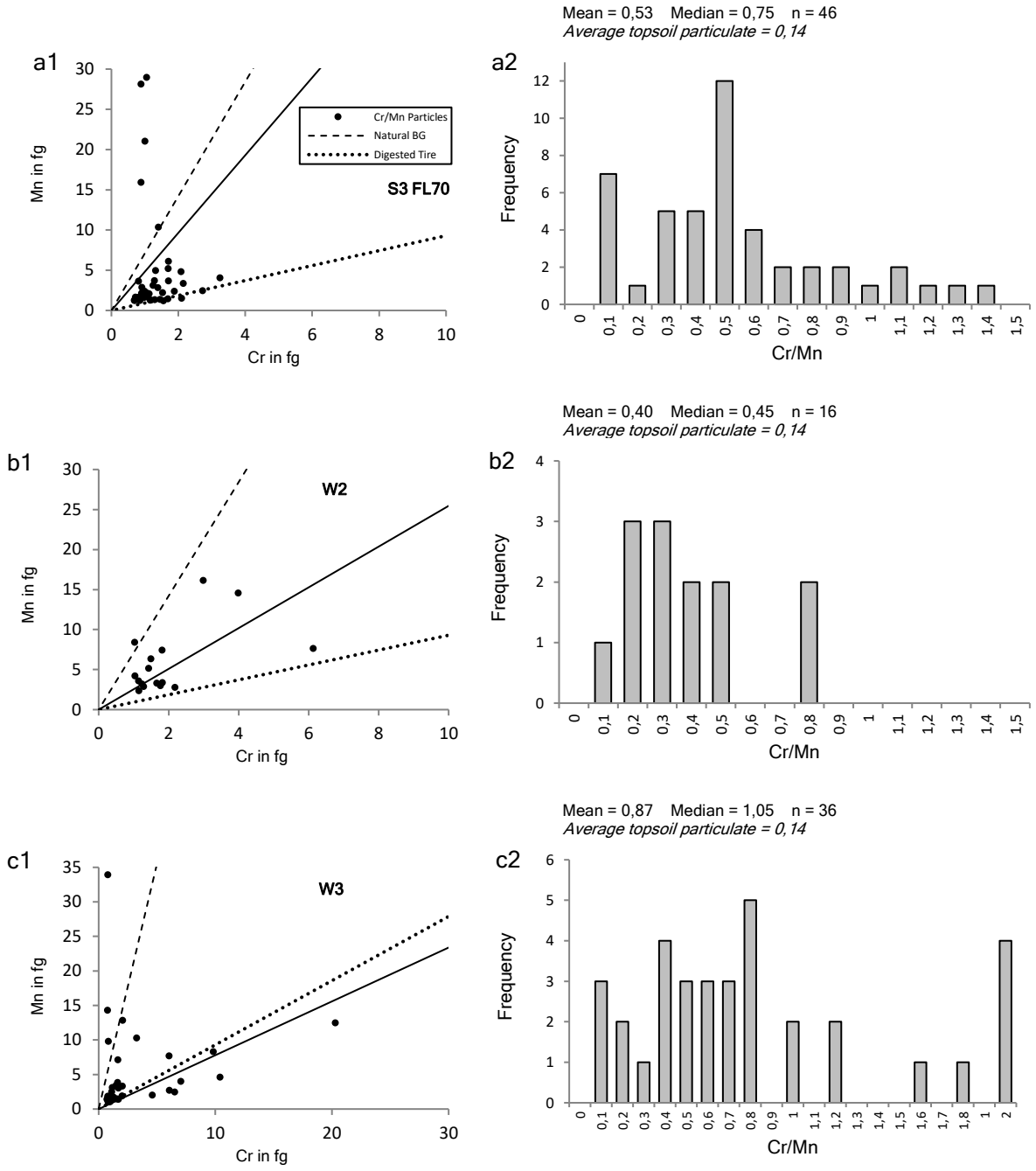

Fig.18. Detected Cr/Mn particles in 1µm size cutoff dispersion (sediment diluted 1:9999, water diluted 1:99). ME-spICP-MS signal detected by ICP-TOFMS. Dashed line represents the natural background (FOREGS), continuous line represents the linear of all detected Cr/Mn particle mass ratios and dotted lines representing digested tire ratio. Graph (a) illustrates particles in dispersion S3 FL70, (b) W2 pristine and (c) W3 pristine.

above 0.25 and thus are significantly higher than the natural background of 0.14 while 6 particulates appear to have Cr/Mn mass ratios in the range (1.06±0.2) of total digested tire particles. Interestingly in W3 more than twice as much (36) Cr/Mn particulates have been detected as in W2 (16) which is the opposite from the detection of Pb/Ba and Pb/Sb particulates

where more particulates have been detected in W2 than W3. This can maybe be explained (while taking the location of sampling spots into account) that during acceleration events a higher number of fine tire particles with a hydrodynamic diameter below 1µm may have been emitted after the traffic light while overall more brake particles have been emitted in front of the traffic light. This would also be in good agreement with the assumption of spatial distribution. From 36 detected Cr/Mn particulates, 31 have mass ratios above 0.25 from which 6 are in the range (1.06±0.2) of digested tire particles while in W2 only 1 particle has been detected in the range of digested tire particles.

Nevertheless, Puisney et al (2018) reports that brake wear powder also contains Cr and Mn but with Cr/Mn mass ratio of 6.5. However, particulates with such high Cr content have not been detected in any road runoff sample, so detected Cr/Mn particulates are very likely not emitted as brake wear.

According to these observations it is assumable that more brake particles (particulates containing Sb, Ba and Pb) have been detected before the traffic light where the brake event frequency of vehicles is higher than after the traffic light. On the other hand more potential tire particles (particulates containing Cr and Mn) have been detected after the traffic light event probably due to tire abrasion and the resulting emission of fine (<1µm) tire particulates caused during accelerations of vehicles.

Table.4. Percentage of particle amount having Pb associations with Sb and Ba as well as percentage of potential brake particles charcaterized by mass ratios between corresponding trace metal associations. Percentages are related to total particle concentrataions of each trace metal (Sb, Ba and Pb).

trace metal		Sb		Ba		Pb			
		Sb + Pb		Ba + Pb		Ba + Pb		Sb + Pb	
[%] from total trace metal concentration		Total Associations	Brake Particles	Total Associations	Brake Particles	Total Associations	Brake Particles	Total Associations	Brake Particles
S1	UPW	54.8	1.8	47.6	4.5	18.9	1.8	4.8	0.7
	FL70	40.0	0.0	20.8	0.0	14.5	0.0	7.8	0.0
S2	UPW	30.0	1.4	32.2	3.0	16.0	1.5	5.2	0.7
	FL70	50.0	1.4	29.3	0.4	21.2	0.3	6.5	1.0
S3	UPW	46.3	1.7	36.9	4.0	17.4	1.9	4.9	0.8
	FL70	38.6	0.6	32.8	3.5	21.6	2.3	8.2	0.4
SRB	UPW	100.0	0.0	8.4	1.8	14.7	3.2	1.1	0.0
	SPP	33.3	0.0	3.7	0.0	3.5	0.0	0.4	0.0
W2	UPW	22.2	11.5	27.3	4.3	7.4	1.2	8.0	3.1
	SPP	22.5	9.1	27.3	4.8	7.1	1.3	8.6	2.4
W3	UPW	1.7	0.0	9.3	4.7	1.0	0.5	0.1	0.0
	SPP	20.0	0.0	18.9	2.7	10.9	1.6	3.1	0.0

Table.5. Percentage of particle amount having Cr and Mn associations as well as percentage of potential tire particles charcaterized by mass ratios between corresponding trace metal associations. Percentages are related to total particle concentrataions of each trace metal (Cr and Mn).

trace metal		Cr		Mn	
		Mn + Cr		Mn + Cr	
[%] from total trace metal concentration		Total Associations	Tire Particles	Total Associations	Tire Particles
S1	UPW	6.8	0.7	1.8	0.2
	FL70	11.9	4.6	10.0	3.8
S2	UPW	5.6	0.0	2.3	0.0
	FL70	23.2	3.2	18.8	2.6
S3	UPW	3.8	0.0	0.6	0.0
	FL70	29.3	3.8	8.1	1.1
SRB	UPW	0.0	0.0	0.0	0.0
	SPP	6.5	3.2	1.7	0.8
W2	UPW	4.8	0.3	10.7	0.7
	SPP	1.0	0.3	1.8	0.6
W3	UPW	25.0	4.2	21.3	3.6
	SPP	0.0	0.0	0.0	0.0

5. Conclusion

The aim of this study was to detect and quantify the amount of emitted TRPs in Vienna's road runoff waters and road runoff exposed sediments. Two independent analytical approaches were performed to observe assumed changes in chemical composition on roadside soils and sediments caused through exposure to individual traffic emissions.

Results of investigated sediment suspensions showed elevated concentrations of metals reported to be present in brake- and tire wear particles. This was verified in comparison to present average soil data of Vienna and samples of the river's retention basin. The resulting change of chemical composition in road runoff exposed sediments is very likely to be caused through local enrichments of adsorbing metal containing TRPs, which were determined in road runoff waters during this research. Considering that during heavy rain events, higher amounts of TRPs in road runoffs will not get adsorbed by soils or sediments but directly be flushed into the river Wien. This study pointed out, that especially in this case, focus on fate and environmental impact of TRPs should get enhanced in respect to potential damages concerning at least human health. Results of this study also suggest, as mentioned earlier, that road runoff systems should be modified in the future so that runoff water contaminated with TRPs will be filtered out before it comes back into contact with surface waters, sediments, or soils.

Moreover, it was assumed that TRP emission by mass will be higher in front of traffic lights due to an increased density of braking vehicles. While analyzing road runoff water samples, it

was observed that the number of TRPs is significantly higher in road runoff in front than after the traffic light which clearly verifies the assumption of TRP spatial distribution. This reveals that TRP emissions, and their following environmental impact can be expected to be even higher at areas around traffic light.

It was supposed that extraction reagents may play a possible role for enhanced dispersion of TRPs in waters and sediments. Results collected during this research reveal, that different extraction protocols show at least recognizable differences in particle concentrations of various detected metals. So far, applied protocols do not indicate a constant result for only one specific reagent delivering enhanced concentrations for all observed metals. It was also figured out, that by applying UPW extraction, TRP analysis delivers already sufficient, in some cases even enhanced metal concentration results as observed during this study. Anyway, results of ME-spICP-MS, 1% FL-70 extraction showed that trace metals are less associated to aluminum in road runoff sediment suspensions which seems to be successful in braking up heteroaggregation between NNMs and TRPs. This concludes that FL-70 may be a promising extraction reagent for future studies that will investigate on extraction behavior of certain TRPs from natural matrices. These future studies will also focus on optimizing reagent concentrations that fit best for enhanced TRP characterizations.

Furthermore, analysis of total digested tire material showed that tire particles may have La/Ce, Cr/Mn and Co/Zn mass ratios above the natural background which may be helpful information for future studies that focus on the characterization of tire wear particles in natural matrices. Through mass ratios of two associated trace metals, potential brake-, tire wear and automotive catalyst particles were detected via ME-spICP-MS and have been distinguished from NNMs in road runoff sediments and waters.

In conclusion, the findings of this study will contribute to expose the contamination potential through particulate emissions by individual traffic. This may be another suggestion for road departments to improve monitoring of TRP emission and fate and to include this aspect in future road construction concepts. Overall, this research may be a supportive orientation to upcoming projects that will focus on the modeling of TRP concentrations in complex natural matrices and apply total digestion on sediments that contain tire particles or use multi element-fingerprinting for the distinction between NNMs and TRPs.

6. References

Adachi, K. and Tainosho, A., 2004. Characterization of heavy metal particles embedded in tire dust. Environ. Int. 30 (8), 1009e1017

Albrektienė, R., Rimeika, M., Zalieckienė, E., Šaulys, V. and Zagorskis, A. 2012. Determination of organic matter by UV absorption in the ground water. J. Environ. Eng. Landsc. Manag. 20 (2) 163-167

Apeagyei, E., Bank, M.S. and Spengler, J.D. 2011. Distribution of heavy metals in road dust along an urban-rural gradient in Massachusetts. Atmospheric Environment 45:2310-2323

Baalousha, M., 2009. Aggregation and disaggregation of iron oxide nanoparticles: influence of particle concentration, pH and natural organic matter. Sci. Tot Environ. 407 (6), 2093-2101

Baalousha, M., Sikder, M., Prasad, A. and Lead, J. 2016. The concentration-dependent behavior of nanoparticles. Environ. Chem. 13:1-3

Bhattacharjee, S. 2016. DLS and zeta potential–What they are and what they are not? Journal of Controlled Release. 235:337-351

Bakshi, S., He, Z.L. and Harris, W.G. 2014. A new method for separation, characterization, and quantification of natural nanoparticles from soils. J. Nanopart. Res. 16(2)

Baur, S., Reemtsma, T., Stärk, H.J. and Wagner, S. 2019. Surfactant assisted extraction of incidental nanoparticles from road runoff sediment and their characterization by single particle ICP-MS. Chemosphere 246:125765

Boulter, P.G., 2006. A review of emission factors and models for road vehicle non-exhaust particulate matter: final report on emission modelling – Published project report PPR110, TRL limited, Wokingham.

Buchanan, W., Roddick, F., Porter, N. and Drikas, M. 2005. Fraction of UV and VUV pretreated natural organic matter from drinking water. Environ. Sci. Technol. 39 (12), 4647-4654

Buffle, J., Wilkinson, K.J., Stoll, S., Filella, M and Zhang, J.W. 1998. A generalized description of aquatic colloidal interactions: the three-colloidal component approach. Environ. Sci. Technol. 32(19):2887-2899

Charters, F.J., Cochrane, T.A. and O'Sullivan, A.D. 2015. Particle size distribution variance in untreated urban runoff and its implication on treatment selection. Water Res. 85:337-345

Chen, K.L., Mylon, S.E. and Elimelech, M. 2006. Aggregation kinetics of alginate-coated hematite nanoparticles in monovalent and divalent electrolytes. Environ. Sci. Technol. 40(5):1516-1523

Chen, K.L., Mylon, S.E. and Elimelech, M. 2007.Enhanced aggregation of alginate-coated Iron oxide (hematite) nanoparticles in the presence of calcium, strontium and barium cations. Langumir 23(11):5920-5928

Christidis, G.E. 2010. Industrial Clays. European Mineralogical Union Notes in Mineralogy. 9:341-414

Cohen, J.M., Beltran-Huarac, J.,Pyrgiotakis, G. and Demokritou, P. 2018. Effective delivery of sonication energy to fast settling and agglomerating nanomaterial suspensions for cellular studies: Implications for stability, particle kinetics, dosimetry and toxicity. Nanoimpact. 10:81-86

Colvin, V.L. 2003. The potential environmental impact of engineered nanomaterials. Nature Biotrchnology 21:1166-1170

Cornelis, G., Hund-Rinke, K., Kuhlbusch, T., van den Brink, N. and Nickel, C. 2014. Fate and bioavailability of engineered nanoparticles in soils: a review. Crit. Rev. Environ. Sci. Technol. 44(24):2720-2764

Dahl, A., Gharibi, A., Swietlicki, E., Gudmundsson, A., Bohgard, M., Ljungman, A., Blomqvist, G. and Gustafsson, M. 2006. Traffic-generated emissions of ultrafine particles from pavement-tire interface. Atmospheric Environment 40:1314-1323

Derjaguin, B. 1939. A Theory of Interaction of Particles in Presence of Electric Double-Layers and the Stability of Lyophobe Colloids and Disperse Systems. Acta Physicochimica U.R.S.S. 10:333-346.

Derjaguin, B. and Landau, L.D. 1941. Theory of the Stability of Strongly Charged Lyophobic Sols and of the Adhesion of Strongly Charged Particles in Solutions of Electrolytes. Acta Physicochimica U.R.S.S. 14:633-662

Domesle. 1997. Katalysatortechnik in Edelmetall-Emissionen. GSF-Forschungszentrum für Umwelt und Gesundheit GmbH. 8–17

Everett, D. 2009. Manual of symbols and terminology for physiochemical quantities and units, appendix II: Definitions, terminology and symols in colloid and surface chemistry. Pure and Applied Chemistry. 31(4)

European Commission (EC). 2011. Comission Recommendation on the definition nanomaterial. (4):2010-2012

European Comission (EC). 2013. Second regulatory review on nanomaterials. Communication from the Commission of the European Parliament, the Council and the European Economic and Social Committee. Brussels: 3.10.2012, COM(2012) 572 final

Falciani, R., Novaro, Z, Gucciardi, M. and Marchesini M. 2000. Multi-element analysis of soil and sediment by ICP-MS after a microwave assisted digestion method. J. Anal. At. Spectrom. 15(5):561-565

Folens, K., Van Acker, T., Bolea-Fernandez, E., Cornelis, G., Vanhaecke, F., Du Laing, G. and Rauch, S. 2018. Identification of platinum nanoparticles in road dust leachate by single particle inductively coupled plasma-mass spectrometry. Sci. Total Environ. 615:894-856

Fitz-James, S. 2003. Use of Hydrochloric Acid (HCl) in digests for ICP-MS analysis. EPA.Washington D.C. 20460

Fujitake, N., Kusumoto, A., Tuskamoto, M., Kawahigashi, M., Suzuki, T. and Otsuka, H. 1998. Properties of soil humic substances inn fractions obtained by sequential extraction with pyrophosphate solutions at different pHs 1. Yield and particle size distribution. Soil Sci. Plant Nutr. 44 (2), 253-260

Gaillardet, J., Viers, J. and Dupré, B. 2004. Trace Elements in River Waters. Treatise on Geochemistry. 5:225-272

Garg, B.D., Cadle, S.H., Mulawa, P.A. and Groblicki, P.J. 2000. Brake wear particulate matter emissions. Environmental Science and Technology 34:4463-4469

Grigoratos, T. and Martini, G. Non-exhaust traffic related emissions. Brake and tyre wear PM; European Comission, Joint Research Centre, Institute of Energy and Transport: Ispra, Italy, 2014.

Gottardo, S., Alessandrelli, M., Atluri, R., Barberio, G., Bergonzo, P., Bleeker, E., Andy, M., Borges, T., Buttol, P., Castelli, S., Chevillard, S., Dekkers, S., Delpivo, C., Fanghella, D. P., Dusinska, M., Einola, J., Ekokoski, E., Fito, C., Gouveia, H., Hoehener, K., Jantunen, P., Laux, P., Lehmann, H. C., Leinonen, R., Mech, A., Micheletti, C., Pesudo, L. Q., Polci, M. L., Walser, T., Wijnhoven, S. and Crutzen, H. 2017.NANoREG framework for the safety assessment of nanomaterials

Gustafsson, M., Blomqvist, G., Gudmundsson, A., Dahl, A., Swietlicki, E., Bohgard, M., Lindbom, J. and Ljungman, A. 2008. Properties and toxicological effects of particles from the interaction between tyres, road pavement and winter traction material. Science of the Total Environment 393:226-240

Häder, D-P., Banaszak, A.T., Villafañe, V.E., Narvarte, M.A., González, R.A. and E.W. 2020. Anthropogenic pollution of aquatic ecosystems: Emerging problems withglobal implications. Sci. Total. Environ. 713:136586

Hall, G.E.M., Vaive, J.E. and McLaurin, A.I. 1996. Analytical aspects of the application of sodium pyrophosphate reagent in the specific extraction of the labile organic component of humus and soils. J. Geochem. Explor. 56 (1), 23-26

Harrison, R.M., Jones, A.M., Gietl, J., Yin, J. and Green, D.C. 2012. Estimation of the contributions of brake dust, tire wear, and resuspension to non-exhaust traffic particles derived from atmospheric measurements. Environmental Science and Technology 46:6523-6529

Hartman, G., Hutterer, C. and Schuster, M. 2013. Ultra-trace determination of silver nanoparticles in water samples using cloud point extraction and ETAAS. J. Anal. At. Spectrom. 28:567-572

Helmreich, B., Hilliges, R., Schriewer, A. and Horn, H., 2010. Runoff pollutants of a highly trafficked urban road – correlation analysis and seasonal influences. Chemosphere 80:991-997

Hendriks, L., A. Gundlach-Graham, A., and Günther. D., 2018. Analysis of Inorganic Nanoparticles by Single-Particle Inductively Coupled Plasma Time-of-Flight Mass Spectrometry, CHIMIA International Journal for Chemistry, 72 :221 —226

Hendriks, L., A. Gundlach-Graham, A., Hattendorf, B., and Günther. D., 2017. Characterization of a new ICP-TOFMS instrument with continuous and discrete introduction of solutions, J. Anal. At. Spectrom., 32:548-561

Helmenstine, A.M. 2019. Definition of Zeta Potential. ThoughtCo

d. Heringer, R., Ranville, J., F. and Borovinskaya, O. 2018. Análise de Nanopartículas de GSR por spICP-ToFMS

Hill, R.F. and Mayer, W.J. 1977. Radiometric determination of platinum and palladium attrition from automotive catalysts, TEEE Transactions on Nuclear Science NS 24 (6):2549-2554

Hilliges, R., Endres, M., Tiffert, A., Brenner, E. and Marks, T. 2017. Characterization of road runoff with regard to seasonal variations, particle size distribution and the correlation of fine particles and pollutants. Water Sci. Technol. 75:1169-1176

Höflinger, G., 2013. Brief Introduction to Coating Technology for Electron Microscopy.

Hohenblum, P., Sattelberger, R. and Scharf, S. 2000. Abwasser- und Klärschlamm-Untersuchungen in der Pilotkläranlage Entsorgungsbetriebe Simmering (EbS). Federal Environment Agency – Austria. M-121

Hwang, H.M., Fiala, M.J., Park, D. and Wade, T.L. 2016. Review of pollutants in urban road dust and stormwater runoff: Part 1, Heavy metals released from vehicles. Int. J. Urban Sci. 20:334-360

Inacker, O and Malessa, R. 1992. Abschlußbericht zum Forschungsvorhaben "Experimentalstudie zum Austrag von Platin aus Automobilabgaskatalysatoren und dessen Auswirkungen auf Mensch und Umwelt", Naturwissenschaftliches und Medizinisches Institut der Universität Tübingen

International Organization for Standardization (ISO 2241:2017) Particle size analysis. Dynamic light scattering, ISO 2241:2017.

IARC 1989. Some organic solvents, resin monomers and related compounds, pigments and occupational exposures in paint manufracture and painting. International Agency for Research on Cancer Manograph, Volume 47, Lyon, France, pp. 291-305

Jolivet, J.P. 2000. Metal Oxide Chemistry and Synthesis: From Solution to Solid State. Wiley.

Juma, M., Koreňová, Z., Markoš, J., Annus, J. and Jelemenský, L'., 2006. Pyrolysis and combustion of scrap tire. Petroleum & Coal 48 (1): 15-26.

Ju-Nam Y and Lead JR. 2008. Manufactured nanoparticles: an overview of their chemistry, interactions and potential environmental implications. Sci Total Environ. 400 (1-3):396-414.

Kah, M., Beulke, S., Tiede, K. and Hofmann, T. 2013. Nanoparticles: State of knowldege, environmental fate, and exposure modeling. Critical Reviews in Environmental Science and Technology. 43(16):1823-1867

Kah, M. and Hofman, T. 2014. Nanopesticide research: Current trends and future priorities. Environment International. 63:224-235

von der Kammer, F., Ferguson, P.I., Holden, P.A., Masion, A., Rogers, K.R., Klaine, S.J., Koelmans, A.A., Horne, N. and Unrine, J.M. 2012. Analysis of engineered nanomaterials in complex matrices (environment and biota): general considerations and conceptual case studies. Environ. Toxicol. Chem. 31:32-49

Klaine, S. J., Alvarez, P. J. J., Batley, G. E., Fernandes, T. F., Handy, R. D., Lyon, D. Y. Mahendra, S., McLaughlin, M. J., and Lead, J. R. 2008. Nanomaterials in the environment: Behavior, fate, bioavailability, and effects. Environmental Toxicology and Chemistry, 27:1825–1851

Klöckner, P., Reemtsma, T., Eisentraut, P., Braun, U., Ruhl, A.S. and Wagner, S. 2019. Tire and road wear particles in road environment – Quantification and assessment of particle dynamics by Zn determination after density speration. Chemosphere 222:714-721

Kreiner, P. 2004. Untersuchung des Wiener Bodens auf Schwermetalle und Polyaromatische Kohlenwasserstoffe. Natur und Naturschutz - Studien der Wiener Umweltschutzabteilung (MA 22). 81:1-27

Kukutschová, J., Moravec, P., Tomášek, V., Matějka, V., Smolík, j., Schwarz, J., Seidlerová, J., Šafářová, K. and Filip, P., 2011. On airborne nano/micro-sized wear particles released from low-metallic automotive brakes. Environmental Pollution 159:998-1006

Kumar, P., Pirjola, L., Ketzel, M. and Harrison, R.M. 2013. Nanoparticle emissions from 11 non-vehicle exhaust sources – A review. Atmospheric Environment 67:252-277

Labille, J., Harns, C., Bottero, J.Y. and Brant J. 2015. Heteroaggregation of Titanium Dioxide Nanoparticles with Natural Clay Colloids. Environmental Science & Technology. 49:6608–6616.

Lanzerstorfer, C. 2018. Heavy metals in the finest size fractions of road-deposited sediments. Environ. Pollut. 239:522-531

Lee, S., Bi, X.Y., Reed, R. B., Ranville, J. F., Herckes, P. and Westerhoff, P. 2014. Nanoparticle Size Detection Limits by Single Particle ICP-MS for 40 Elements. Environ. Sci. Technol. 48:10291−10300

Loosli, F., Le Coustumer, P. and Stoll, S. 2015. Effect of electrolyte valency, alginate concentration and pH on engineered TiO2 nanoparticle stability in aqueous solution. Sci. Total. Environ. 535, 28-34

Loosli, F., Wang, J., Rothenberg, S., Bizimis, M., Winkler, C., Borovinskaya, O., Flamigni, L. and Baalousha, M. 2019. Seewage spills are a major source of titanium dioxide engineered (nano)-particle release into the environment. Environ. Sci. Nano. 6:763-777

Loosli, F., Yi, Z., Berti, D. and Baalousha, M. 2018. Toward a better extraction of titanium dioxide engineered nanomaterials from complex environmental matrices. NanoImpact 11:119-127

Loosli, F., Yi, Z., Wang, J. and Baalousha, M. 2019. Improved extraction efficiency of natural nanomaterials in soils to facilitate their characterization using a multimethod approach. Science of the Total Environment. 667:34-46

Li, W., He, Y., Wu, J. and Xu, J. 2012. Extraction and characterization of natural soil nanoparticles from Chinese soils. Eur. J. Sci. 63(5):754-761

Li, Y., Lau, S., Kayhanian, M., Asce, M., Stenstrom, M.K. and Asce, F. 2005. Particle size distribution in highway runoff. J. Environ. Eng. 131,1267-1276

Mohammed A.S., Kapri A. and Goel R. 2011. Heavy Metal Pollution: Source, Impact, and Remedies. Environ. Pollut. 20:1-28

Montaño, M.D., Lowry, G.V., von der Kammer, F., Blue, J. and Ranville, J.F. 2014. Current status and future direction for examining engineered nanoparticles in natural systems. Environ. Chem. 11:351-366

Mosleh, M., Blau, P.J. and Dumitrescu, D. 2004. Characteristics and morphology of wear particles from laboratory testing of disc brake materials. Wear 256:1128-1134

Murray, H. H. 2006. Chapter 2 Structure and Composition of the Clay Minerals and their Physical and Chemical Properties. Developments in Clay Science. 2:7-31

Nakamura, Y., Hasebe, A., Johno, T. and Murakami, T.N. 2015. Effect of Tween 20 Concentration on Macropore Formation in Spherical Diopside Particles. J. Jpn. Soc. Colour Mater. 88(1):2-7

Nowack, B. and Bucheli, T.D. 2007. Occurrence, behavior and effects of nanoparticles in the environment. Environ. Pollut. 150: 5–22.

Pace, H. E., Rogers, N. J., Jarolimek, C., Coleman, V. A., Higgins, C. P., and Ranville, J. F., 2011. Determining Transport Efficiency for the Purpose od Counting and Sizing Nanoparticles via Single Particle Inductively Coupled Plasma Mass Spectrometry, Anal. Chem. 83(24):9361-9369

Panko, J., McAtee, B.L., Kreider, M., Gustafsson, M., Blomqvist, G., Gudmundsson, A., Sweet, L. and Finley, B. 2009. Physio-Chemical Analysis of Airborne Tire Wear Particles. 46th Congress of the European Societies of Toxicology, Eurotox, 13-16 September 2009, Dresden, Germany

Pfleiderer, S., Englisch, M. and Reiter. R. 2012. Current state of heavy metal contents in Vienna soils. Environ Geochem Health. 34:665–675

Philippe, A and Schaumann, G.E. 2014. Interactions of dissolved organic matter with natural and engineered inorganic colloids: a review. Environ. Sci. Technol. 48(16):8946-8962

Pope, C.A., Burnett, R.T., Thun, M.J., Calle, E.E., Krewski, D., Ito, K. and Thurston, G.D. 2002. Lung cancer, cardiopulmonary mortality, and long-term exposure to fine particulate air pollution. The Journal of American Medical Association 287:1132-1141

Praetorius, A., Grundlach-Graham, A., Goldberg, E., Fabienke, W., Navratilova, J., Gondikas, A., Kaegi, R., Gunther, D., Hofmann, T. and von der Kammer, F. 2017. Single-particle multi-element fingerprinting (spMEF) using inductively-coupled plasma time-of-flight mass spectrometry (ICP-TOFMS) to identify engineered nanoparticles against the elevated natural background in soils. Environ. Sci.: Nano 4 (2):307-314

Praetorius, A., Labille, J., Scheringer, M., Thill, A., Hungerbühler, K. and Bottero J.Y. 2014. Heteroaggregation of titanium dioxide nanoparticles with model natural colloids under environmentally relevant conditions, Environmental Science & Technology. 48: 10690–10698

Pronk, G.J., Heister, K. and Kogel-Knabner, J.R. 2011. Iron oxides as major available Interface component in loamy arable topsoils. Soil, Sci. Soc. Am. J. 75 (6):2158-2168

Puisney, C., Oikonomou, E.K., Nowak, S., Chevillot, A., Casale,S., Baeza-Squiban, A. and Berret, J.F. 2018. Brake wear (nano)particle characterization and toxicity on airway epithelial cells in vitro. Environ. Sci. Nano. 14:30-39

Reemstma, T., Gnirss, R. and Hekel, M. 2006. Infiltration of combined sewer overflow and tertiary treated municipal wastewater: an integrated laboratory and field study on various metals. Water. Environ. Res. 72:466-650

Regelink, I.C. 2014. Natural Nanoparticles in Soilsand their role in organic-mineral interacions and colloid-facilitated transport. PhD thesis, Wageningen University, Wageningen, NL

Salminen R. 2007. The geochemical atlas of Europe continent-wide distribution patterns of elements. Geochim Cosmochim Acta 71: A869– A869

Sanders, P.G., Xu, N., Dalka, T.M. and Maricq, M.M. 2003. Airborne brake wear debris: size distributions, composition, and a comparison of dynamometer and vehicle tests. Environ. Sci. Technol. 37:4060-4069

Simon, E., Braun, M. and Fábián I. 2012. Trace element concentrations in soils along urbanization gradients in the city of Wien, Austria. Environ Sci Pollut Res. 20(2)917-24

Skillas, G., Qian, Z., Baltensperger, U., Matter, U. and Burtscher, H. 2000. The influence of additives on size distribution and composition of particles produced by diesel engines. Combust. Sci. Technol. 154:259-27

Sutherland, R.A., Tack, F.M.G. and Ziegler, A.D. 2012. Road-deposited sediments in an urban environment: a first look sequentially extracted element loads in grain size fractions. J. Hazard Mater 225-226, 54-62

Tang, Z.Y., Wu, L.H., Luo, Y.M., Christie, P. 2009. Size fractionation and characterization of nanocolloidal particles in soils. Environ. Geochem. Health 31 (1): 1-10.

Tatzber, M., Stemmer, M. and Spiegel, H. 2007. An alternative method to measure carbonate in soils by FT-IR spectroscopy. Environ Chem Lett. 5:9–12

Therezien, M., Thill, A. and Wiesner, M.R. 2014. Importance of heterogeneous aggregation for NP fate in natural and engineered systems. Sci. Total Environ. 485–486, 309–318

Thomaz, E.L. 2016. Realistic soil-heating gradient temperature linearly changes most of the soil chemical properties. Soil Science and Plant Nutrition. 63:84-91

Thorpe, A. and Harrison, R.M. 2008. Sources and properties of non-exhaust particulate matter from road traffic: A review. Sci. Total Environ. 400:270-282

Tuoriniemi, J., Johnsson, A.C.J.H., Holmberg, J.P., Gustafsson, S., Gallego-Urrea, J.A., Olsson, E., Pettersson, J.B.C. and Hassellöv, M. 2014. Intermethod comparison of the particle size distributions of colloidal silica nanoparticles. Sci. Technol. Adv. Mater. 15: 035009

Varrica, D., Bardelli, F., Dongarrà, D. and Tamburo, E. 2013. Speciation of Sb in airborne particulate matter, vehicle brake linings, and brake pad wear residues. Atmospheric Environment 64:18-24

Verwey, E.J.W. and Overbeek, J.Th.G. 1948. Theory of the Stability of Lyophobic Colloids: The Interaction of Sol Particles Having an Electric Double Layer. Elsevier, Amsterdam

Wagner, S., Gondikas, A., Neubauer, E., Hofmann, T., and von der Kammer, F. 2014. Spot the difference: engineered and natural nanoparticles in the environment—release, behavior, and fate. Angewa. Chem. Intern. Edn. 53 :12398–12419

Wang, H., Adeleye, A.S., Huang, Y., Li, F. and Keller, A.A. 2015. Heteroaggregation of nanoparticles with biocolloids and geocolloids. Adv Colloid Interface Sci. 226(A):24-36.

Wang, J., Nabi, M.M., Mohanty, S.K., Afrooz, ARM., Cantando, E., Aich, N. and Baalousha, M. 2019. Detection and quantification of engineered particles in urban runoff. Chemosphere. 248:126070

Wedepohl, K. H. 1995. The composition of the continental crust, Geochemica at Cosmochemica Acta. 95 (7): 1217-1232

Wiesner, M.R., Lowry, G.V., Alvarez, P.J.J., 2006. Assessing the risks of manufactured nanomaterials. Environmental Science and Technology 40 (14): 4337–4345

Wik, A. and Dave, G. 2009. Occurrence and effects of tire wear particles in the environment – A critical review and an initial risk assessment. Environmental Pollution 157:1-11

Xing, B., Vecitis, C. and Senesi, N. 2016. Engineered Nanoparticles in the Environment. Wiley-IUPAC Series in Biophysico-Chemical Processes in Environmental Systems.

Supplementary data

Table.S1. Z. Average hydrodynamic diameter and Zeta Potential determined by DLS as well as measured pH of 10µm (a) and 1µm size-cutoff (b) from all road runoff sediment (S1, S2, S3), retention basin sediment (SRB) and road runoff water (W2, W3) suspension. Standard deviation represents the results from several independent measurements (n=3).

a

	Suspension	Z. Average [nm]		Z. Average PdI		Zeta Potential [mV]		Zeta Potential Dev. [mV]		pH
		Mean	stdev	Mean	stdev	Mean	stdev	Mean	stdev	
S1	UPW	1606	281.0	0.65	0.19	-34.3	0.7	5.8	0.2	7.3
	SPP	1545	209.9	0.81	0.21	-42.7	0.3	10.2	4.4	7.0
	SOx	1543	305.2	0.88	0.06	-37.4	0.7	6.4	0.6	7.2
	SDS	1490	42.6	0.77	0.19	-45.8	1.2	8.4	0.4	4.1
	FL - 70	1525	72.3	0.80	0.17	-41.1	1.1	19.0	19.7	7.8
S2	UPW	1283	180.7	0.87	0.10	-30.9	0.6	5.1	0.6	7.3
	SPP	1140	46.9	0.61	0.06	-42.0	0.9	7.4	1.0	7.2
	SOx	1134	89.3	0.79	0.05	-35.9	0.7	6.1	0.3	7.3
	SDS	1250	40.6	0.90	0.08	-48.4	1.2	9.2	0.1	5.9
	FL - 70	1275	175.9	0.81	0.18	-42.0	1.1	9.3	3.9	7.6
S3	UPW	1467	36.6	0.67	0.30	-25.8	0.5	4.9	0.3	7.4
	SPP	924.6	59.6	0.66	0.09	-45.1	0.1	7.5	0.3	7.1
	SOx	1272	111.6	0.78	0.05	-38.0	0.7	5.7	0.8	7.5
	SDS	1107	107.7	0.75	0.08	-51.4	1.7	8.8	1.3	5.9
	FL - 70	940.4	67.4	0.69	0.08	-44.3	0.6	8.1	0.7	7.5
SRB	UPW	2426	484.0	1.00	0.00	-24.4	0.6	4.7	0.6	7.2
	SPP	1575	60.3	0.88	0.03	-48.8	0.3	10.6	1.5	7.0
	SOx	1359	50.2	0.51	0.05	-40.6	2.7	7.1	0.2	7.2
	SDS	1181	88.5	0.71	0.05	-37.8	1.6	7.2	0.7	7.2
	FL - 70	1210	244.8	0.82	0.16	-50.7	0.4	9.4	0.7	6.9
W2	UPW	910.9	64.4	0.82	0.13	-20.2	0.4	4.7	0.2	7.4
	SPP	1370	92.3	0.82	0.18	-30.6	1.0	4.5	0.4	7.4
W3	UPW	628.2	170.0	0.65	0.09	-22.3	1.1	6.1	1.1	7.1
	SPP	1561	473.1	0.88	0.17	-37.0	1.3	7.1	0.9	7.3

b

	Suspension	Z. Average [nm]		Z. Average PdI		Zeta Potential [mV]		Zeta Potential Dev. [mV]		pH
		Mean	stdev	Mean	stdev	Mean	stdev	Mean	stdev	
S1	UPW	593.7	19.9	0.41	0.06	-36.2	0.5	6.1	0.6	7.4
	SPP	534.9	23.0	0.43	0.05	-46.9	1.9	7.6	0.6	7.2
	SOx	563.4	34.4	0.43	0.04	-39.3	0.3	7.5	0.9	7.5
	SDS	571.6	17.8	0.52	0.06	-49.7	1.0	8.3	1.2	4.0
	FL - 70	441.3	16.4	0.41	0.06	-44.1	0.9	7.3	0.7	7.1
S2	UPW	535	10.5	0.40	0.04	-34.4	1.1	5.8	0.3	7.3
	SPP	447.4	1.7	0.38	0.03	-44.0	1.3	7.2	0.4	7.2
	SOx	497.5	18.6	0.45	0.07	-38.2	0.8	5.8	0.3	7.7
	SDS	488	25.3	0.41	0.04	-51.9	2.5	8.6	1.1	4.4
	FL - 70	483.1	16.4	0.42	0.06	-40.4	0.6	6.7	0.5	7.6
S3	UPW	560.2	7.1	0.37	0.00	-32.3	1.7	5.7	0.5	7.1
	SPP	409.7	1.2	0.37	0.04	-45.0	1.1	6.9	0.2	7.1
	SOx	495.1	12.1	0.36	0.02	-38.9	0.8	7.2	1.3	7.3
	SDS	460.4	12.4	0.46	0.09	-54.8	2.5	9.1	0.5	5.1
	FL - 70	385.2	10.1	0.36	0.01	-46.7	1.4	7.9	1.0	7.2
SRB	UPW	987	107.3	0.57	0.07	-26.8	0.5	4.8	0.2	7.4
	SPP	448.4	7.9	0.45	0.02	-51.1	1.6	7.6	0.7	7.0
	SOx	455.7	4.2	0.42	0.07	-38.7	2.5	6.1	0.6	7.5
	SDS	856.4	91.3	0.64	102.30	-37.9	2.7	12.4	0.2	7.4
	FL - 70	428	12.0	0.40	0.92	-47.8	1.6	7.1	0.5	7.3
W2	UPW	224.3	3.1	0.24	0.02	-22.2	0.4	5.6	0.3	7.4
	SPP	483.4	45.5	0.76	0.07	-32.9	0.4	4.6	0.1	7.4
W3	UPW	235.1	9.8	0.28	0.04	-19.0	0.2	7.4	0.4	7.1
	SPP	274.1	6.5	0.42	0.02	-31.9	0.7	10.4	0.6	7.5

Table .S2. Eyetech laser particle size analysis results of both size cutoff fractions from sediment suspernsions.

		Hydrodynamic Diameter [nm]			
		10μm size cutoff fraction		1μm size cutoff fraction	
	Suspension	Mean	stdev	Mean	stdev
S1	UPW	1540	1480	1130	700
	SPP	1460	1340	1080	630
	SOx	1550	1430	1250	690
	FL - 70	1360	1200	1400	570
	SDS	1400	1160	1130	650
S2	UPW	1290	1090	1270	590
	SPP	1300	1070	1290	560
	SOx	1290	1060	1430	590
	FL - 70	1320	1160	1420	580
	SDS	1390	1160	1080	630
S3	UPW	1460	1190	1530	610
	SPP	1300	1030	1410	600
	SOx	1400	1150	1580	630
	FL - 70	1400	1120	1500	580
	SDS	1340	1020	1280	700
SRB	UPW	2150	1610	2927	2502
	SPP	1670	770	1668	774
	SOx	1570	1390	1565	1385
	FL - 70	1510	1150	1506	1152
	SDS	1620	1220	1615	1216

Table.S3.a.b. Trace metal concentration in total digested 1µm and 10µm fractions of road runoff and retention basin sediment samples extracted with UPW, SPP and FL-70. Normalized by 1g of dry sediment from corresponding size cutoff fraction. S3 (c) and SRB (d).

a

Sample		S1									
Size fraction		10µm					1µm				
Extractant		UPW	SPP	FL70	SOx	SDS	UPW	SPP	FL70	SOx	SDS
Ti	[mg/g]	3.54	3.25	3.42	3.58	2.13	11.10	13.62	3.46	17.87	0.59
Cr	[µg/g]	316.13	299.00	315.30	328.27	184.20	1044.36	1169.08	271.82	1381.47	44.60
Mn	[mg/g]	1.78	1.78	2.06	1.74	1.19	6.87	15.81	5.82	9.12	0.80
Fe	[mg/g]	74.79	71.54	74.83	75.75	43.87	307.20	336.89	79.68	406.91	12.47
Co	[µg/g]	25.48	23.27	25.27	24.41	14.62	94.63	106.79	36.47	126.34	5.46
Ni	[µg/g]	87.46	275.18	105.97	201.84	156.10	469.29	412.81	109.41	1175.13	10.68
Cu	[µg/g]	491.70	717.66	660.22	517.63	557.94	2462.22	2432.41	1590.04	3383.81	160.20
Zn	[mg/g]	2.90	2.75	3.08	2.91	1.71	13.63	16.12	11.76	18.93	0.67
As	[µg/g]	13.38	12.06	12.86	12.43	7.45	64.59	75.28	17.14	82.04	2.60
Zr	[µg/g]	115.47	102.89	116.80	108.78	64.13	268.66	312.44	81.22	399.64	13.88
Mo	[µg/g]	33.26	30.93	31.57	32.15	17.83	82.01	89.65	25.87	108.24	3.59
Rh	[µg/g]	n.a.	n.a.	n.a.	n.a.	<0.01	<0.01	n.a.	n.a.	n.a.	<0.01
Pd	[µg/g]	n.a.	0.16	0.18	0.12	0.13	n.a.	1.16	0.19	0.96	0.04
Cd	[µg/g]	1.37	1.08	1.37	1.21	0.83	5.31	6.89	3.06	7.71	0.29
Sb	[µg/g]	79.82	80.18	82.55	84.85	48.91	229.96	274.63	58.79	342.48	11.53
Ba	[µg/g]	529.64	504.93	508.21	533.48	340.17	2201.31	2294.47	515.01	2859.05	193.02
La	[µg/g]	21.87	20.31	20.51	21.59	12.27	81.10	89.41	21.07	104.26	3.29
Ce	[µg/g]	47.67	44.16	44.55	46.97	26.53	176.86	191.75	45.81	228.75	7.22
W	[µg/g]	5.78	5.16	4.40	5.86	3.33	20.66	26.81	7.79	31.51	0.91
Pt	[µg/g]	0.16	n.a.	n.a.	0.08	0.02	0.75	0.60	3.05	1.36	0.06
Pb	[µg/g]	206.10	188.97	185.70	198.95	108.68	953.38	1016.31	196.87	1192.96	34.13

b

Sample		S2									
Size fraction		10µm					1µm				
Extractant		UPW	SPP	FL70	SOx	SDS	UPW	SPP	FL70	SOx	SDS
Ti	[mg/g]	3.38	3.65	3.31	3.65	1.95	14.55	4.65	5.02	9.89	0.43
Cr	[µg/g]	314.66	308.91	297.90	308.91	167.50	1174.48	474.62	440.85	783.35	36.02
Mn	[mg/g]	2.13	1.95	2.20	1.95	1.37	10.07	8.37	16.73	7.38	0.57
Fe	[mg/g]	71.65	73.03	70.01	73.03	40.31	339.63	140.84	137.03	229.20	9.17
Co	[µg/g]	19.95	20.57	20.96	20.57	12.24	107.18	46.47	92.06	75.60	3.79
Ni	[µg/g]	65.38	8.21	n.a.	8.21	n.a.	502.78	616.47	n.a.	531.45	23.23
Cu	[µg/g]	615.81	604.06	675.96	604.06	407.26	3790.74	2110.90	4154.67	3350.63	270.09
Zn	[mg/g]	4.50	4.52	4.72	4.52	2.67	26.65	12.22	18.45	18.07	0.86
As	[µg/g]	12.48	12.40	11.86	12.40	6.26	73.11	32.26	27.89	54.70	1.81
Zr	[µg/g]	109.84	119.19	113.91	119.19	59.78	339.71	134.81	116.58	240.66	17.63
Mo	[µg/g]	31.40	32.06	30.45	32.06	16.77	121.85	44.84	39.51	76.09	3.45
Rh	[µg/g]	n.a.	n.a.	n.a.	n.a.	<0.01	<0.01	n.a.	n.a.	n.a.	<0.01
Pd	[µg/g]	0.13	0.14	0.12	0.14	0.08	n.a.	0.28	0.29	0.42	0.04
Cd	[µg/g]	0.83	0.78	0.80	0.78	0.49	4.54	1.83	17.77	3.13	1.16
Sb	[µg/g]	79.14	80.43	76.24	80.43	42.72	236.40	104.34	117.62	171.80	8.23
Ba	[µg/g]	489.40	507.69	467.77	507.69	275.58	2379.85	947.20	901.98	1567.60	118.53
La	[µg/g]	20.43	20.92	19.74	20.92	10.91	93.07	37.87	33.68	61.31	2.64
Ce	[µg/g]	43.58	44.72	42.01	44.72	23.76	201.56	81.70	71.42	132.03	6.96
W	[µg/g]	6.93	6.94	4.98	6.94	3.61	36.88	14.25	4.74	24.51	11.17
Pt	[µg/g]	n.a.	<0.01	n.a.	<0.01	n.a.	2.79	0.08	0.42	0.40	0.04
Pb	[µg/g]	151.41	151.77	136.00	151.77	80.93	900.71	363.07	487.90	575.92	25.60

Table.S3.c.d. Trace metal concentration in total digested 1µm and 10µm fractions of road runoff and retention basin sediment samples extracted with UPW, SPP and FL-70. Normalized by 1g of dry sediment from corresponding size cutoff fraction. S3 (c) and SRB (d).

c

Sample		S3									
Size fraction		10µm					1µm				
Extractant		UPW	SPP	FL70	SOx	SDS	UPW	SPP	FL70	SOx	SDS
Ti	[mg/g]	3.70	3.35	3.41	3.60	1.56	18.72	3.60	3.04	11.15	0.45
Cr	[µg/g]	327.52	310.78	284.14	331.39	131.98	1557.91	342.31	279.10	905.95	37.73
Mn	[mg/g]	1.98	2.29	2.22	2.02	1.08	15.04	6.94	8.60	8.58	0.60
Fe	[mg/g]	70.44	67.75	58.64	69.60	29.99	413.83	92.10	76.01	241.23	9.59
Co	[µg/g]	21.09	19.79	18.42	20.32	9.91	136.79	33.03	37.60	82.70	3.92
Ni	[µg/g]	44.48	49.36	n.a.	n.a.	n.a.	574.18	119.59	56.39	527.53	17.19
Cu	[µg/g]	382.93	602.31	580.44	547.48	358.22	4882.60	1265.50	2099.54	2728.05	279.87
Zn	[mg/g]	3.10	3.01	2.82	2.98	1.45	22.98	5.27	7.64	12.81	0.75
As	[µg/g]	12.45	11.22	10.32	11.37	5.30	78.95	20.24	16.98	54.69	1.96
Zr	[µg/g]	108.67	109.28	112.32	118.37	45.31	399.22	92.64	73.29	248.44	15.29
Mo	[µg/g]	30.58	28.14	24.92	29.41	11.73	198.30	31.93	26.20	105.41	3.66
Rh	[µg/g]	<0.01	n.a.	n.a.	n.a.	<0.01	<0.01	n.a.	n.a.	n.a.	<0.01
Pd	[µg/g]	n.a.	0.15	0.14	0.14	0.07	n.a.	0.23	0.20	0.73	0.05
Cd	[µg/g]	0.97	0.77	0.84	0.95	0.45	6.32	1.36	3.71	3.71	0.67
Sb	[µg/g]	78.05	81.02	79.96	83.90	34.23	362.73	85.22	64.66	231.08	8.66
Ba	[µg/g]	524.23	488.73	431.93	505.69	241.61	3185.71	635.81	512.14	1737.11	124.73
La	[µg/g]	21.74	20.65	18.26	21.14	8.72	117.05	25.39	20.69	65.37	2.77
Ce	[µg/g]	47.59	43.98	38.91	45.08	18.16	254.52	54.64	44.67	158.42	8.41
W	[µg/g]	6.21	5.88	3.43	6.80	2.49	40.27	8.70	5.39	25.69	19.84
Pt	[µg/g]	n.a.	n.a.	n.a.	0.02	n.a.	0.77	0.11	0.09	0.38	0.05
Pb	[µg/g]	171.94	162.95	128.99	159.10	70.07	1308.20	271.67	223.10	698.80	26.72

d

Sample		SRB									
Size fraction		10µm					1µm				
Extractant		UPW	SPP	FL70	SOx	SDS	UPW	SPP	FL70	SOx	SDS
Ti	[mg/g]	4.31	4.83	2.04	1.86	3.30	7.03	7.55	0.95	2.48	2.81
Cr	[µg/g]	126.79	131.65	118.75	55.44	96.28	372.80	453.31	29.89	147.11	148.26
Mn	[mg/g]	0.81	1.55	3.55	0.70	0.80	1.83	4.90	1.56	1.83	1.48
Fe	[mg/g]	41.42	45.62	41.96	18.88	30.89	128.53	159.82	14.21	52.13	51.49
Co	[µg/g]	18.60	21.73	24.01	9.34	14.59	46.83	58.98	14.95	22.17	20.15
Ni	[µg/g]	68.74	66.92	62.09	32.85	47.09	214.27	186.80	17.76	89.58	72.56
Cu	[µg/g]	104.62	91.77	153.24	48.31	74.18	437.18	228.30	35.85	153.62	147.58
Zn	[mg/g]	0.55	0.47	0.12	0.36	0.19	3.50	0.45	0.34	0.12	0.24
As	[µg/g]	12.05	13.67	13.98	5.59	12.99	33.41	68.27	7.21	15.83	26.93
Zr	[µg/g]	87.49	91.09	103.65	35.96	63.18	164.78	191.55	16.76	64.06	59.67
Mo	[µg/g]	2.51	1.72	2.64	1.11	0.39	11.42	8.01	1.21	3.10	n.a.
Rh	[µg/g]	0.07	0.01	0.05	0.01	<0.01	0.89	0.27	n.a.	0.05	n.a.
Pd	[µg/g]	0.10	0.04	<0.01	0.01	0.05	0.33	0.29	n.a.	0.02	0.00
Cd	[µg/g]	0.54	0.52	0.97	0.35	n.a.	3.65	3.51	0.00	1.30	0.33
Sb	[µg/g]	5.52	6.58	7.28	2.24	3.64	37.56	36.31	0.19	8.93	7.13
Ba	[µg/g]	559.35	532.26	393.38	222.09	442.05	1497.24	1546.95	136.22	504.96	659.73
La	[µg/g]	38.82	37.74	22.88	15.76	31.48	77.10	81.47	8.65	29.16	31.34
Ce	[µg/g]	83.29	80.53	51.28	33.83	65.76	175.09	191.52	20.14	65.94	69.35
W	[µg/g]	3.78	3.67	2.27	1.45	2.95	7.70	9.01	1.20	2.50	2.32
Pt	[µg/g]	0.22	0.06	n.a.	0.06	0.34	0.94	0.08	n.a.	<0.01	0.40
Pb	[µg/g]	68.69	79.09	126.88	36.56	53.17	251.46	320.65	50.66	119.19	100.54

Table.S4.a.b. Concentrations in digested sediment dispersions normalized per gram of 125um. Determined with conventional ICP-MS.

a

Sample		S1										
Size fraction		125µm	10µm					1µm				
Extractant		UPW	UPW	SPP	FL70	SOx	SDS	UPW	SPP	FL70	SOx	SDS
Ti	[mg/g]	5.30	1.75	1.51	1.68	1.47	1.36	0.19	0.16	0.27	0.17	0.21
Cr	[µg/g]	446.17	155.83	138.80	154.66	135.12	117.66	17.50	13.99	21.46	13.23	15.54
Mn	[mg/g]	2.44	0.88	0.83	1.01	0.71	0.76	0.12	0.19	0.46	0.09	0.28
Fe	[mg/g]	91.58	36.87	33.21	36.70	31.18	28.02	5.15	4.03	6.29	3.90	4.35
Co	[µg/g]	32.18	12.56	10.80	12.40	10.05	9.34	1.59	1.28	2.88	1.21	1.90
Ni	[µg/g]	113.94	43.11	127.74	51.98	83.08	99.72	7.86	4.94	8.64	11.25	3.72
Cu	[µg/g]	749.17	242.37	333.15	323.86	213.06	356.40	41.26	29.11	125.52	32.40	55.81
Zn	[mg/g]	3.48	1.43	1.28	1.51	1.20	1.09	0.23	0.19	0.93	0.18	0.23
As	[µg/g]	16.05	6.60	5.60	6.31	5.12	4.76	1.08	0.90	1.35	0.79	0.91
Zr	[µg/g]	175.66	56.92	47.76	57.30	44.77	40.97	4.50	3.74	6.41	3.83	4.83
Mo	[µg/g]	39.92	16.40	14.36	15.49	13.23	11.39	1.37	1.07	2.04	1.04	1.25
Rh	[µg/g]	n.a.	<0.01	<0.01	<0.01	<0.01	<0.01	<0.01	<0.01	<0.01	<0.01	<0.01
Pd	[µg/g]	0.29	<0.01	0.07	0.09	0.05	0.08	<0.01	0.01	0.02	0.01	0.01
Cd	[µg/g]	1.62	0.68	0.50	0.67	0.50	0.53	0.09	0.08	0.24	0.07	0.10
Sb	[µg/g]	106.48	39.35	37.22	40.49	34.93	31.24	3.85	3.29	4.64	3.28	4.02
Ba	[µg/g]	675.94	261.07	234.40	249.29	219.58	217.29	36.88	27.46	40.66	27.38	67.25
La	[µg/g]	31.69	10.78	9.43	10.06	8.89	7.84	1.36	1.07	1.66	1.00	1.15
Ce	[µg/g]	68.29	23.50	20.50	21.85	19.33	16.95	2.96	2.30	3.62	2.19	2.51
W	[µg/g]	10.38	2.85	2.40	2.16	2.41	2.13	0.35	0.32	0.61	0.30	0.32
Pt	[µg/g]	0.28	0.08	n.a.	<0.01	0.03	0.01	0.01	0.01	0.24	0.01	0.02
Pb	[µg/g]	213.92	101.59	87.72	91.09	81.89	69.42	15.97	12.16	15.54	11.42	11.89

b

Sample		S2										
Size fraction		125µm	10µm					1µm				
Extractant		UPW	UPW	SPP	FL70	SOx	SDS	UPW	SPP	FL70	SOx	SDS
Ti	[mg/g]	4.50	0.96	0.98	1.00	0.95	0.66	0.11	0.11	0.05	0.14	0.08
Cr	[µg/g]	349.99	86.08	91.34	89.50	80.63	56.72	8.98	10.88	4.49	10.97	7.13
Mn	[mg/g]	2.11	0.51	0.62	0.66	0.51	0.46	0.08	0.19	0.17	0.10	0.11
Fe	[mg/g]	64.41	19.35	20.80	21.03	19.06	13.65	2.60	3.23	1.40	3.21	1.82
Co	[µg/g]	20.55	5.51	5.79	6.30	5.37	4.15	0.82	1.07	0.94	1.06	0.75
Ni	[µg/g]	71.97	19.78	18.98	n.a.	2.14	n.a.	3.84	14.13	n.a.	7.45	4.60
Cu	[µg/g]	429.11	159.84	178.75	203.10	157.66	137.91	28.97	48.38	42.33	46.94	53.48
Zn	[mg/g]	3.58	1.20	1.31	1.42	1.18	0.91	0.20	0.28	0.19	0.25	0.17
As	[µg/g]	10.60	3.14	3.62	3.56	3.24	2.12	0.56	0.74	0.28	0.77	0.36
Zr	[µg/g]	139.64	34.30	31.88	34.23	31.11	20.24	2.60	3.09	1.19	3.37	3.49
Mo	[µg/g]	31.88	8.65	9.11	9.15	8.37	5.68	0.93	1.03	0.40	1.07	0.68
Rh	[µg/g]	n.a.	<0.01	<0.01	<0.01	<0.01	<0.01	<0.01	<0.01	<0.01	<0.01	<0.01
Pd	[µg/g]	0.52	<0.01	0.04	0.04	0.04	0.03	<0.01	0.01	<0.01	0.01	0.01
Cd	[µg/g]	0.96	0.22	0.24	0.24	0.20	0.17	0.03	0.04	0.18	0.04	0.23
Sb	[µg/g]	65.39	20.03	22.97	22.91	20.99	14.47	1.81	2.39	1.20	2.41	1.63
Ba	[µg/g]	536.35	134.77	142.06	140.54	132.51	93.32	18.19	21.71	9.19	21.96	23.47
La	[µg/g]	26.16	5.68	5.93	5.93	5.46	3.69	0.71	0.87	0.34	0.86	0.52
Ce	[µg/g]	58.06	12.24	12.65	12.62	11.67	8.04	1.54	1.87	0.73	1.85	1.38
W	[µg/g]	22.13	1.88	2.01	1.50	1.81	1.22	0.28	0.33	0.05	0.34	2.21
Pt	[µg/g]	0.16	0.02	n.a.	n.a.	<0.01	<0.01	0.02	<0.01	<0.01	0.01	0.01
Pb	[µg/g]	112.29	41.41	43.95	40.86	39.61	27.40	6.88	8.32	4.97	8.07	5.07

Table.S4.c.d. Concentrations in digested sediment dispersions normalized per gram of 125um. Determined with conventional ICP-MS.

c

Sample		S3										
Size fraction		125µm	10µm					1µm				
Extractant		UPW	UPW	SPP	FL70	SOx	SDS	UPW	SPP	FL70	SOx	SDS
Ti	[mg/g]	4.06	0.49	0.66	0.68	0.65	0.47	0.07	0.10	0.09	0.08	0.10
Cr	[µg/g]	353.48	43.09	60.75	56.24	59.49	39.42	5.75	9.26	8.23	6.68	8.09
Mn	[mg/g]	1.74	0.26	0.45	0.44	0.36	0.32	0.06	0.19	0.25	0.06	0.13
Fe	[mg/g]	53.37	9.27	13.24	11.61	12.49	8.96	1.53	2.49	2.24	1.78	2.06
Co	[µg/g]	15.89	2.77	3.87	3.65	3.65	2.96	0.50	0.89	1.11	0.61	0.84
Ni	[µg/g]	57.82	5.85	9.65	n.a.	n.a.	n.a.	2.12	3.23	1.66	3.89	3.68
Cu	[µg/g]	374.98	50.38	117.74	114.89	98.27	107.00	18.01	34.22	61.94	20.13	60.00
Zn	[mg/g]	1.72	0.41	0.59	0.56	0.54	0.43	0.08	0.14	0.23	0.09	0.16
As	[µg/g]	8.49	1.64	2.19	2.04	2.04	1.58	0.29	0.55	0.50	0.40	0.42
Zr	[µg/g]	132.41	14.30	21.36	22.23	21.25	13.53	1.47	2.51	2.16	1.83	3.28
Mo	[µg/g]	19.24	4.02	5.50	4.93	5.28	3.50	0.73	0.86	0.77	0.78	0.78
Rh	[µg/g]	n.a.	<0.01	<0.01	<0.01	<0.01	<0.01	<0.01	<0.01	<0.01	<0.01	<0.01
Pd	[µg/g]	0.18	<0.01	0.03	0.03	0.03	0.02	<0.01	0.01	0.01	0.01	0.01
Cd	[µg/g]	0.53	0.13	0.15	0.17	0.17	0.13	0.02	0.04	0.11	0.03	0.14
Sb	[µg/g]	46.57	10.27	15.84	15.83	15.06	10.22	1.34	2.30	1.91	1.71	1.86
Ba	[µg/g]	437.63	68.97	95.54	85.49	90.77	72.17	11.75	17.20	15.11	12.82	26.74
La	[µg/g]	29.32	2.86	4.04	3.61	3.79	2.60	0.43	0.69	0.61	0.48	0.59
Ce	[µg/g]	62.33	6.26	8.60	7.70	8.09	5.42	0.94	1.48	1.32	1.17	1.80
W	[µg/g]	7.39	0.82	1.15	0.68	1.22	0.74	0.15	0.24	0.16	0.19	4.25
Pt	[µg/g]	0.09	<0.01	n.a.	n.a.	<0.01	n.a.	<0.01	<0.01	<0.01	<0.01	0.01
Pb	[µg/g]	84.88	22.62	31.85	25.53	28.56	20.93	4.83	7.35	6.58	5.16	5.73

d

Sample		SRB									
Size fraction		10µm					1µm				
Extractant		UPW	SPP	FL70	SOx	SDS	UPW	SPP	FL70	SOx	SDS
Ti	[mg/g]	0.26	0.73	0.13	0.42	0.15	0.05	0.10	0.05	0.12	0.04
Cr	[µg/g]	7.60	19.88	7.75	12.50	4.50	2.88	6.19	1.51	7.07	1.92
Mn	[mg/g]	0.05	0.23	0.23	0.16	0.04	0.01	0.07	0.08	0.09	0.02
Fe	[mg/g]	2.48	6.89	2.74	4.26	1.44	0.99	2.18	0.72	2.51	0.67
Co	[µg/g]	1.11	3.28	1.57	2.10	0.68	0.36	0.81	0.75	1.07	0.26
Ni	[µg/g]	4.12	10.11	4.05	7.41	2.20	1.65	2.55	0.90	4.31	0.94
Cu	[µg/g]	6.27	13.86	10.00	10.89	3.47	3.37	3.12	1.81	7.38	1.91
Zn	[mg/g]	0.03	0.07	0.01	0.08	0.01	0.03	0.01	0.02	0.01	0.00
As	[µg/g]	0.72	2.06	0.91	1.26	0.61	0.26	0.93	0.36	0.76	0.35
Zr	[µg/g]	5.24	13.76	6.76	8.11	2.95	1.27	2.62	0.85	3.08	0.77
Mo	[µg/g]	0.15	0.26	0.17	0.25	0.02	0.09	0.11	0.06	0.15	n.a.
Rh	[µg/g]	<0.01	<0.01	<0.01	<0.01	<0.01	0.01	<0.01	<0.01	<0.01	<0.01
Pd	[µg/g]	0.01	0.01	<0.01	<0.01	<0.01	<0.01	<0.01	<0.01	<0.01	<0.01
Cd	[µg/g]	0.03	0.08	0.06	0.08	<0.01	0.03	0.05	<0.01	0.06	0.00
Sb	[µg/g]	0.33	0.99	0.48	0.51	0.17	0.29	0.50	0.01	0.43	0.09
Ba	[µg/g]	33.52	80.38	25.67	50.06	20.67	11.56	21.12	6.87	24.27	8.54
La	[µg/g]	2.33	5.70	1.49	3.55	1.47	0.60	1.11	0.44	1.40	0.41
Ce	[µg/g]	4.99	12.16	3.35	7.63	3.07	1.35	2.61	1.02	3.17	0.90
W	[µg/g]	0.23	0.55	0.15	0.33	0.14	0.06	0.12	0.06	0.12	0.03
Pt	[µg/g]	0.01	0.01	<0.01	0.01	0.02	0.01	<0.01	<0.01	<0.01	0.01
Pb	[µg/g]	4.12	11.94	8.28	8.24	2.49	1.94	4.38	2.56	5.73	1.30

Table.S5. Concentration in ultra filtrated sediment suspensions (30kDa). Determined with concentional ICP-MS.

a

30kDa	S1					
		UPW	SPP	SOx	SDS	FL70
Ti	[µg / L]	n.a.	n.a.	n.a.	n.a.	n.a.
Cr	[µg / L]	n.a.	n.a.	n.a.	n.a.	n.a.
Mn	[µg / L]	n.a.	0.16	n.a.	78.42	107.95
Fe	[µg / L]	n.a.	n.a.	n.a.	n.a.	194.85
Co	[µg / L]	n.a.	n.a.	n.a.	0.40	2.30
Ni	[µg / L]	n.a.	n.a.	n.a.	n.a.	n.a.
Cu	[µg / L]	4.04	28.26	20.31	14.39	114.57
Zn	[µg / L]	n.a.	285.74	n.a.	71.38	1029.44
As	[µg / L]	0.57	3.08	n.a.	n.a.	0.38
Zr	[µg / L]	n.a.	n.a.	n.a.	n.a.	n.a.
Mo	[µg / L]	n.a.	2.22	1.28	n.a.	0.93
Rh	[µg / L]	n.a.	n.a.	n.a.	n.a.	n.a.
Pd	[µg / L]	n.a.	n.a.	n.a.	n.a.	n.a.
Cd	[µg / L]	n.a.	n.a.	n.a.	n.a.	0.42
Sb	[µg / L]	n.a.	n.a.	n.a.	n.a.	n.a.
Ba	[µg / L]	n.a.	n.a.	n.a.	n.a.	n.a.
La	[µg / L]	n.a.	n.a.	n.a.	n.a.	n.a.
Ce	[µg / L]	n.a.	n.a.	n.a.	n.a.	n.a.
W	[µg / L]	n.a.	0.63	0.74	n.a.	n.a.
Pt	[µg / L]	n.a.	n.a.	n.a.	n.a.	n.a.
Pb	[µg / L]	n.a.	n.a.	n.a.	n.a.	n.a.

b

30kDa	S2					
		UPW	SPP	SOx	SDS	FL70
Ti	[µg / L]	n.a.	n.a.	n.a.	n.a.	n.a.
Cr	[µg / L]	n.a.	n.a.	n.a.	n.a.	n.a.
Mn	[µg / L]	n.a.	10.67	n.a.	32.61	1282.76
Fe	[µg / L]	n.a.	n.a.	n.a.	n.a.	1250.48
Co	[µg / L]	n.a.	0.51	n.a.	n.a.	6.67
Ni	[µg / L]	n.a.	n.a.	n.a.	n.a.	n.a.
Cu	[µg / L]	39.91	131.73	70.91	8.08	346.78
Zn	[µg / L]	n.a.	45.35	n.a.	46.23	1830.36
As	[µg / L]	n.a.	3.85	1.91	0.38	0.38
Zr	[µg / L]	n.a.	n.a.	n.a.	n.a.	n.a.
Mo	[µg / L]	4.26	7.02	9.25	n.a.	1.18
Rh	[µg / L]	n.a.	n.a.	n.a.	n.a.	n.a.
Pd	[µg / L]	n.a.	n.a.	n.a.	n.a.	n.a.
Cd	[µg / L]	n.a.	n.a.	n.a.	n.a.	1.54
Sb	[µg / L]	n.a.	n.a.	n.a.	n.a.	n.a.
Ba	[µg / L]	n.a.	n.a.	n.a.	n.a.	n.a.
La	[µg / L]	n.a.	n.a.	n.a.	n.a.	n.a.
Ce	[µg / L]	n.a.	n.a.	n.a.	n.a.	n.a.
W	[µg / L]	n.a.	1.62	0.95	n.a.	n.a.
Pt	[µg / L]	n.a.	n.a.	n.a.	n.a.	n.a.
Pb	[µg / L]	n.a.	n.a.	n.a.	n.a.	13.03

c

30kDa	S3					
		UPW	SPP	SOx	SDS	FL70
Ti	[µg / L]	n.a.	n.a.	n.a.	n.a.	n.a.
Cr	[µg / L]	n.a.	n.a.	n.a.	n.a.	n.a.
Mn	[µg / L]	n.a.	n.a.	n.a.	77.45	3223.61
Fe	[µg / L]	n.a.	n.a.	n.a.	n.a.	3419.12
Co	[µg / L]	n.a.	n.a.	n.a.	0.43	19.77
Ni	[µg / L]	n.a.	n.a.	n.a.	n.a.	36.96
Cu	[µg / L]	14.42	24.64	28.84	193.88	1575.89
Zn	[µg / L]	n.a.	n.a.	n.a.	115.35	5935.59
As	[µg / L]	n.a.	n.a.	0.56	n.a.	n.a.
Zr	[µg / L]	n.a.	n.a.	n.a.	n.a.	n.a.
Mo	[µg / L]	7.06	2.21	7.94	n.a.	11.69
Rh	[µg / L]	n.a.	n.a.	n.a.	n.a.	n.a.
Pd	[µg / L]	n.a.	n.a.	n.a.	n.a.	n.a.
Cd	[µg / L]	n.a.	n.a.	n.a.	n.a.	3.32
Sb	[µg / L]	n.a.	n.a.	n.a.	n.a.	n.a.
Ba	[µg / L]	n.a.	n.a.	n.a.	n.a.	n.a.
La	[µg / L]	n.a.	n.a.	0.20	n.a.	n.a.
Ce	[µg / L]	n.a.	n.a.	n.a.	n.a.	n.a.
W	[µg / L]	n.a.	n.a.	n.a.	n.a.	0.66
Pt	[µg / L]	n.a.	n.a.	n.a.	n.a.	n.a.
Pb	[µg / L]	n.a.	n.a.	n.a.	n.a.	29.19

d

30kDa	SRB					
		UPW	SPP	SOx	SDS	FL70
Ti	[µg / L]	n.a.	n.a.	n.a.	n.a.	n.a.
Cr	[µg / L]	n.a.	n.a.	n.a.	n.a.	n.a.
Mn	[µg / L]	n.a.	n.a.	n.a.	n.a.	98.36
Fe	[µg / L]	n.a.	n.a.	n.a.	n.a.	2248.12
Co	[µg / L]	n.a.	n.a.	n.a.	n.a.	13.08
Ni	[µg / L]	n.a.	n.a.	n.a.	n.a.	n.a.
Cu	[µg / L]	n.a.	15.62	16.04	n.a.	77.28
Zn	[µg / L]	n.a.	n.a.	n.a.	n.a.	482.08
As	[µg / L]	0.39	10.58	1.52	1.54	1.13
Zr	[µg / L]	n.a.	n.a.	n.a.	n.a.	n.a.
Mo	[µg / L]	n.a.	1.38	1.60	0.79	n.a.
Rh	[µg / L]	n.a.	n.a.	n.a.	n.a.	n.a.
Pd	[µg / L]	n.a.	n.a.	n.a.	n.a.	n.a.
Cd	[µg / L]	n.a.	n.a.	n.a.	n.a.	0.48
Sb	[µg / L]	n.a.	n.a.	21.52	n.a.	n.a.
Ba	[µg / L]	n.a.	n.a.	n.a.	n.a.	n.a.
La	[µg / L]	n.a.	n.a.	n.a.	n.a.	0.45
Ce	[µg / L]	n.a.	n.a.	n.a.	n.a.	1.00
W	[µg / L]	n.a.	n.a.	n.a.	n.a.	n.a.
Pt	[µg / L]	n.a.	n.a.	n.a.	n.a.	n.a.
Pb	[µg / L]	n.a.	n.a.	n.a.	n.a.	81.29

Table.S6. Concentration in ultra filtrated runoff water suspensions (30kDa). Determined with concentional ICP-MS.

e	30kDa	W2		W3	
		UPW	SPP	UPW	SPP
Ti	[µg / L]	n.a.	n.a.	n.a.	n.a.
Cr	[µg / L]	n.a.	6.53	n.a.	n.a.
Mn	[µg / L]	217.48	60.68	18.99	8.14
Fe	[µg / L]	n.a.	523.06	n.a.	144.61
Co	[µg / L]	1.75	0.97	n.a.	n.a.
Ni	[µg / L]	n.a.	n.a.	n.a.	n.a.
Cu	[µg / L]	42.43	60.41	47.98	37.53
Zn	[µg / L]	331.44	116.08	112.01	87.89
As	[µg / L]	0.76	2.34	n.a.	n.a.
Zr	[µg / L]	n.a.	n.a.	n.a.	n.a.
Mo	[µg / L]	4.71	4.54	2.34	1.26
Rh	[µg / L]	n.a.	n.a.	n.a.	n.a.
Pd	[µg / L]	n.a.	n.a.	n.a.	n.a.
Cd	[µg / L]	n.a.	n.a.	n.a.	n.a.
Sb	[µg / L]	n.a.	22.23	n.a.	n.a.
Ba	[µg / L]	n.a.	n.a.	n.a.	n.a.
La	[µg / L]	n.a.	n.a.	n.a.	n.a.
Ce	[µg / L]	n.a.	n.a.	n.a.	n.a.
W	[µg / L]	n.a.	0.72	n.a.	n.a.
Pt	[µg / L]	n.a.	n.a.	n.a.	n.a.
Pb	[µg / L]	n.a.	n.a.	n.a.	n.a.

Table.S7. Dissolved anion and cation concentrations in road runoff water samples determined by IC and ICP-OES.

		W2	W3
F^-	[mg / L]	0.09	0.05
Cl^-	[mg / L]	29.91	34.69
NO_3^-	[mg / L]	2.23	27.95
SO_4^{2-}	[mg / L]	13.20	12.22
Na	[mg / L]	225.72	272.75
Mg	[mg / L]	4.70	22.55
Al	[mg / L]	0.09	0.03
Si	[mg / L]	47.69	16.77
K	[mg / L]	190.34	8.97
Ca	[mg / L]	497.96	273.85
Cr	[µg / L]	1.70	1.60
Mn	[µg / L]	8.10	4.20
Fe	[mg / L]	0.18	0.06
Ni	[µg / L]	4.00	3.80
Cu	[µg / L]	58.10	71.70
Zn	[µg / L]	932.80	207.50
Sr	[µg / L]	59.30	31.70
Cd	[µg / L]	n.a	n.a
Ba	[µg / L]	58.20	25.20
Pb	[µg / L]	n.a	0.2

Table.S8.a Concentrations of trace metal sand Al, Fe associations in sediment suspensionsnormalized per gram of 125µm stock fraction.Determined with ICP-TOFMS.

a S1

	Total			with Al			without Al			without Al and Fe		
[ug/g]	UPW	SPP	FL70	UPW	SPP	FL70	UPW	SPP	FL70	UPW	SPP	FL70
Al	282.24	149.98	216.50	282.24	149.98	216.50	n.D.	n.D.	n.D.	n.D.	n.D.	n.D.
Ti	18.89	11.76	25.24	8.72	3.16	4.13	10.17	8.60	21.12	9.11	7.15	19.02
Cr	2.12	0.94	2.38	0.85	0.27	0.31	1.27	0.67	2.08	0.30	0.26	0.94
Mn	9.92	7.46	1.85	6.13	2.79	0.68	3.79	4.67	1.17	1.39	2.79	0.43
Fe	759.53	421.30	516.77	454.21	208.55	239.17	305.32	212.75	277.59	n.D.	n.D.	n.D.
Co	0.06	0.00	0.02	0.02	n.D.	0.01	0.04	0.00	0.01	0.03	0.00	0.01
Ni	0.11	0.07	0.02	0.04	0.02	n.D.	0.07	0.05	0.02	0.04	0.05	0.02
Cu	1.88	0.96	1.43	1.05	0.30	0.30	0.83	0.67	1.13	0.16	0.14	0.94
Zn	7.05	3.54	6.32	4.17	1.82	2.84	2.88	1.72	3.48	0.46	0.36	1.39
As	n.D.	0.02	0.01	n.D.	n.D.	n.D.	n.D.	0.02	0.01	n.D.	n.D.	0.01
Zr	0.64	0.62	1.24	0.18	0.09	0.17	0.46	0.53	1.06	0.33	0.41	0.96
Mo	0.02	0.01	0.09	n.D.	0.01	0.02	0.02	n.D.	0.07	0.01	n.D.	0.05
Rh	0.01	n.D.	0.01	n.D.	n.D.	n.D.	0.01	n.D.	0.01	0.01	n.D.	0.01
Pd	0.02	n.D.	n.D.	0.02	n.D.	n.D.	n.D.	n.D.	n.D.	n.D.	n.D.	n.D.
Ag	n.D.	0.00	n.D.	n.D.	0.00	n.D.	n.D.	n.D.	n.D.	n.D.	n.D.	n.D.
Cd	n.D.	n.D.	n.D.	n.D.	n.D.	n.D.	n.D.	n.D.	n.D.	n.D.	n.D.	n.D.
Sb	0.51	0.34	0.48	0.20	0.08	0.05	0.32	0.26	0.43	0.06	0.11	0.17
Te	0.07	0.03	0.01	0.01	n.D.	n.D.	0.06	0.03	0.01	0.06	0.03	0.01
Ba	0.61	3.29	0.39	0.50	0.41	0.23	0.11	2.88	0.16	0.01	2.85	0.12
La	0.08	0.22	0.21	0.03	0.08	0.02	0.06	0.14	0.18	0.05	0.12	0.17
Ce	0.48	0.64	0.60	0.25	0.16	0.10	0.23	0.48	0.50	0.19	0.42	0.45
W	0.01	0.00	0.01	0.00	0.00	n.D.	0.01	n.D.	0.01	0.01	n.D.	0.01
Pt	0.02	0.01	0.00	n.D.	n.D.	n.D.	0.02	0.01	0.00	0.01	0.01	0.00
Pb	3.43	1.98	1.36	1.90	0.84	0.45	1.53	1.14	0.92	0.38	0.41	0.28

Table.S8.b Concentrations of trace metals and Al, Fe associations in sediment suspensionsnormalized per gram of 125µm stock fraction.Determined with ICP-TOFMS.

b S2

	Total			with Al			without Al			without Al and Fe		
	UPW	SPP	FL70	UPW	SPP	FL70	UPW	SPP	FL70	UPW	SPP	FL70
Al	195.21	165.70	108.30	195.21	165.70	108.30	n.D.	n.D.	n.D.	n.D.	n.D.	n.D.
Ti	27.10	22.29	6.68	7.95	5.83	2.04	19.15	16.45	4.64	16.83	14.15	3.96
Cr	1.26	1.93	0.64	0.61	0.40	0.25	0.65	1.53	0.39	0.39	0.91	0.16
Mn	4.44	5.05	1.21	1.81	2.56	0.74	2.62	2.49	0.47	1.58	1.40	0.15
Fe	562.05	459.08	274.34	316.91	221.73	165.84	245.15	237.35	108.50	n.D.	n.D.	n.D.
Co	0.03	0.05	0.00	0.01	0.03	0.00	0.01	0.02	n.D.	0.01	0.02	n.D.
Ni	n.D.	0.08	0.02	n.D.	0.02	n.D.	n.D.	0.06	0.02	n.D.	0.03	0.01
Cu	1.35	1.20	0.20	0.62	0.45	0.08	0.73	0.75	0.12	0.27	0.28	0.08
Zn	5.37	2.87	1.78	3.08	1.50	1.22	2.29	1.36	0.56	0.89	0.51	0.19
As	0.00	0.01	n.D.	n.D.	n.D.	n.D.	0.00	0.01	n.D.	0.00	0.01	n.D.
Zr	0.70	1.10	0.27	0.15	0.15	0.06	0.55	0.95	0.21	0.44	0.90	0.16
Mo	0.06	0.06	0.02	0.01	0.01	0.01	0.04	0.05	0.01	0.02	0.04	n.D.
Rh	0.00	0.00	0.00	0.00	n.D.	n.D.	n.D.	0.00	0.00	n.D.	0.00	0.00
Pd	n.D.	0.02	n.D.	n.D.	n.D.	n.D.	n.D.	0.02	n.D.	n.D.	n.D.	n.D.
Ag	0.00	n.D.	n.D.	0.00	n.D.	n.D.	n.D.	n.D.	n.D.	n.D.	n.D.	n.D.
Cd	n.D.	n.D.	n.D.	n.D.	n.D.	n.D.	n.D.	n.D.	n.D.	n.D.	n.D.	n.D.
Sb	0.51	0.62	0.18	0.16	0.06	0.07	0.35	0.56	0.11	0.18	0.31	0.02
Te	0.02	n.D.	0.01	n.D.	n.D.	n.D.	0.02	n.D.	0.01	0.01	n.D.	0.01
Ba	0.32	0.41	0.17	0.25	0.26	0.16	0.06	0.15	0.01	0.04	0.12	0.00
La	0.12	0.15	0.05	0.04	0.03	0.02	0.08	0.12	0.02	0.07	0.11	0.02
Ce	0.42	0.47	0.16	0.17	0.13	0.07	0.25	0.34	0.09	0.23	0.29	0.07
W	0.02	0.01	0.00	0.00	n.D.	0.00	0.02	0.01	0.00	0.02	0.00	0.00
Pt	0.03	0.08	n.D.	0.00	n.D.	n.D.	0.03	0.08	n.D.	0.03	0.08	n.D.
Pb	1.81	1.34	0.78	0.89	0.62	0.45	0.92	0.73	0.33	0.34	0.28	0.05

Table.S8.c Concentrations of trace metal sand Al, Fe associations in sediment suspensionsnormalized per gram of 125µm stock fraction.Determined with ICP-TOFMS.

C S3

	Total			with Al			without Al			without Al and Fe		
[ug/g]	UPW	SPP	FL70	UPW	SPP	FL70	UPW	SPP	FL70	UPW	SPP	FL70
Al	96.76	324.79	154.85	96.76	324.79	154.85	n.D.	n.D.	n.D.	n.D.	n.D.	n.D.
Ti	9.33	30.08	18.56	4.05	12.81	5.17	5.28	17.26	13.39	4.43	14.07	11.93
Cr	0.64	2.11	1.09	0.34	0.99	0.37	0.30	1.12	0.71	0.14	0.61	0.47
Mn	4.84	27.92	12.32	2.16	10.76	4.84	2.68	17.16	7.48	1.15	11.65	4.96
Fe	301.79	618.16	389.76	178.26	342.58	219.06	123.53	275.58	170.70	n.D.	n.D.	n.D.
Co	0.01	0.04	0.03	0.01	0.01	0.01	0.00	0.03	0.02	n.D.	0.03	0.01
Ni	0.04	0.12	0.07	0.03	n.D.	0.01	0.01	0.12	0.06	n.D.	0.09	0.04
Cu	0.64	4.52	0.81	0.29	2.13	0.23	0.35	2.38	0.58	0.08	0.95	0.36
Zn	2.62	16.81	2.88	1.72	10.28	1.67	0.90	6.53	1.22	0.12	2.12	0.40
As	n.D.	n.D.	0.01	n.D.	n.D.	n.D.	n.D.	n.D.	0.01	n.D.	n.D.	n.D.
Zr	0.45	0.50	0.69	0.11	0.09	0.15	0.34	0.41	0.54	0.26	0.35	0.43
Mo	0.03	0.07	0.04	0.01	0.05	0.01	0.02	0.03	0.03	0.02	n.D.	0.03
Rh	0.00	n.D.	0.01	n.D.	0.00	0.00	0.00	0.00	0.00	0.00	0.00	0.00
Pd	n.D.	n.D.	0.01	n.D.	n.D.	n.D.	n.D.	n.D.	0.01	n.D.	n.D.	n.D.
Ag	n.D.	0.00	0.00	n.D.	0.00	n.D.	n.D.	n.D.	0.00	n.D.	n.D.	0.00
Cd	n.D.	0.03	n.D.	n.D.	0.00	n.D.	n.D.	0.02	n.D.	n.D.	0.00	n.D.
Sb	0.30	1.03	0.47	0.07	0.25	0.09	0.23	0.78	0.38	0.06	0.43	0.10
Te	0.02	n.D.	0.01	n.D.	0.00	n.D.	0.02	n.D.	0.01	0.02	n.D.	0.01
Ba	0.28	0.63	0.36	0.23	0.47	0.21	0.05	0.16	0.15	0.01	0.13	0.14
La	0.04	0.10	0.18	0.01	0.06	0.02	0.03	0.04	0.16	0.03	0.03	0.15
Ce	0.22	0.27	0.54	0.08	0.15	0.10	0.14	0.12	0.43	0.14	0.11	0.41
W	0.00	0.03	0.01	0.00	0.02	n.D.	0.00	0.01	0.01	0.00	0.01	0.00
Pt	0.00	n.D.	0.00	n.D.	n.D.	n.D.	0.00	n.D.	0.00	0.00	n.D.	0.00
Pb	1.12	2.62	1.13	0.62	1.50	0.55	0.50	1.12	0.59	0.11	0.49	0.23

Table.S8.d Concentrations of trace metal sand Al, Fe associations in sediment suspensionsnormalized per gram of 125µm stock fraction.Determined with ICP-TOFMS.

d SRB

	Total			with Al			without Al			without Al and Fe		
[ug/g]	UPW	SPP	FL70	UPW	SPP	FL70	UPW	SPP	FL70	UPW	SPP	FL70
Al	87.00	104.09	79.70	87.00	104.09	79.70	n.D.	n.D.	n.D.	n.D.	n.D.	n.D.
Ti	8.48	15.55	6.18	1.37	1.16	0.77	7.11	14.39	5.41	6.84	13.63	4.89
Cr	0.13	0.23	0.09	0.02	0.03	0.02	0.11	0.20	0.08	0.06	0.19	0.05
Mn	0.68	1.25	1.31	0.15	0.35	0.54	0.53	0.90	0.77	0.07	0.45	0.20
Fe	97.40	150.42	92.68	40.72	58.49	41.97	56.67	91.94	50.71	n.D.	n.D.	n.D.
Co	0.01	0.02	0.03	n.D.	0.01	0.01	0.01	0.01	0.02	0.01	0.00	0.01
Ni	n.D.	0.04	n.D.	n.D.	n.D.	n.D.	n.D.	0.04	n.D.	n.D.	0.04	n.D.
Cu	0.01	0.03	0.03	0.00	n.D.	n.D.	0.01	0.03	0.03	0.00	0.03	0.03
Zn	0.09	0.18	0.07	0.02	0.05	0.02	0.06	0.13	0.05	0.02	0.11	0.03
As	n.D.	n.D.	n.D.	n.D.	n.D.	n.D.	n.D.	n.D.	n.D.	n.D.	n.D.	n.D.
Zr	0.23	1.08	0.25	0.02	0.06	0.03	0.21	1.03	0.22	0.19	0.93	0.21
Mo	n.D.	n.D.	n.D.	n.D.	n.D.	n.D.	n.D.	n.D.	n.D.	n.D.	n.D.	n.D.
Rh	0.01	0.00	0.01	n.D.	n.D.	n.D.	0.01	0.00	0.01	0.01	0.00	0.01
Pd	n.D.	n.D.	n.D.	n.D.	n.D.	n.D.	n.D.	n.D.	n.D.	n.D.	n.D.	n.D.
Ag	n.D.	n.D.	n.D.	n.D.	n.D.	n.D.	n.D.	n.D.	n.D.	n.D.	n.D.	n.D.
Cd	n.D.	n.D.	n.D.	n.D.	n.D.	n.D.	n.D.	n.D.	n.D.	n.D.	n.D.	n.D.
Sb	0.00	0.01	0.00	n.D.	n.D.	n.D.	0.00	0.01	0.00	n.D.	0.00	0.00
Te	n.D.	0.03	0.02	n.D.	n.D.	n.D.	n.D.	0.03	0.02	n.D.	0.03	0.02
Ba	0.12	0.20	0.07	0.05	0.06	0.00	0.07	0.14	0.06	0.07	0.14	0.06
La	0.22	0.56	0.17	0.02	0.02	0.02	0.20	0.53	0.15	0.19	0.52	0.14
Ce	0.57	1.28	0.45	0.08	0.08	0.07	0.49	1.20	0.38	0.46	1.16	0.34
W	n.D.	0.01	n.D.	n.D.	0.00	n.D.	n.D.	0.00	n.D.	n.D.	0.00	n.D.
Pt	0.04	0.04	0.00	0.00	n.D.	n.D.	0.04	0.04	0.00	0.03	0.04	0.00
Pb	0.15	0.42	0.15	0.03	0.10	0.04	0.12	0.32	0.11	0.07	0.24	0.05

Table.S9.a Concentrations of trace metals and Al, Fe associations in runoff water suspensions.Determined with ICP-TOFMS.

a W2

	Total		with Al		without Al		without Al and Fe	
[ug/L]	UPW	SPP	UPW	SPP	UPW	SPP	UPW	SPP
Al	87.29	93.66	87.29	93.66	n.D.	n.D.	n.D.	n.D.
Ti	18.22	14.96	1.27	1.59	16.95	13.37	15.88	12.08
Cr	2.05	2.09	0.20	0.24	1.85	1.85	1.47	1.00
Mn	1.58	2.37	0.17	0.17	1.41	2.19	0.95	1.97
Fe	228.49	224.38	69.52	75.92	158.97	148.46	n.D.	n.D.
Co	0.03	0.09	0.00	0.00	0.03	0.08	0.02	0.08
Ni	0.25	0.11	n.D.	0.01	0.25	0.11	0.23	0.06
Cu	2.24	1.90	0.20	0.28	2.05	1.61	1.34	1.04
Zn	3.37	1.62	0.67	0.47	2.70	1.16	1.80	0.90
As	0.00	0.02	n.D.	n.D.	0.00	0.02	n.D.	0.01
Zr	1.30	1.27	0.15	0.09	1.15	1.18	1.02	1.03
Mo	0.12	0.08	0.01	0.01	0.11	0.07	0.05	0.04
Rh	0.00	0.00	n.D.	n.D.	0.00	0.00	0.00	0.00
Pd	0.01	0.02	n.D.	n.D.	0.01	0.02	0.01	0.02
Ag	0.00	0.00	n.D.	n.D.	0.00	0.00	0.00	0.00
Cd	n.D.	n.D.	n.D.	n.D.	n.D.	n.D.	n.D.	n.D.
Sb	0.78	0.65	0.05	0.04	0.73	0.60	0.53	0.42
Te	n.D.	0.00	n.D.	n.D.	n.D.	0.00	n.D.	0.00
Ba	1.26	0.30	0.18	0.11	1.08	0.19	0.91	0.16
La	0.29	0.31	0.02	0.05	0.26	0.26	0.25	0.26
Ce	0.83	0.93	0.06	0.12	0.77	0.81	0.75	0.77
W	0.03	0.01	n.D.	n.D.	0.03	0.01	0.02	0.01
Pt	0.01	0.02	0.00	0.00	0.01	0.02	0.01	0.02
Pb	1.07	0.91	0.17	0.18	0.89	0.73	0.53	0.40

Table.S9.b Concentrations of trace metals and Al, Fe associations in runoff water suspensions.Determined with ICP-TOFMS.

b W3

	Total		with Al		without Al		without Al and Fe	
[ug/L]	UPW	SPP	UPW	SPP	UPW	SPP	UPW	SPP
Al	52.94	8.85	52.94	8.85	n.D.	n.D.	n.D.	n.D.
Ti	3.42	0.51	1.95	0.12	1.47	0.39	1.21	0.17
Cr	0.52	0.10	0.25	0.06	0.28	0.05	0.06	0.02
Mn	0.90	0.27	0.47	0.10	0.44	0.17	0.05	0.08
Fe	190.38	16.57	115.54	9.44	74.85	7.13	n.D.	n.D.
Co	0.06	0.01	0.06	0.00	0.00	0.00	0.00	0.00
Ni	0.01	0.01	0.01	n.D.	n.D.	0.01	n.D.	0.01
Cu	0.78	0.09	0.26	0.04	0.53	0.05	0.08	0.03
Zn	0.95	0.25	0.58	0.07	0.37	0.18	0.09	0.13
As	n.D.	0.00	n.D.	n.D.	n.D.	0.00	n.D.	n.D.
Zr	0.22	0.01	0.15	0.00	0.07	0.01	0.05	0.01
Mo	0.03	0.00	0.00	n.D.	0.03	0.00	0.01	0.00
Rh	0.00	0.00	0.00	n.D.	0.00	0.00	0.00	0.00
Pd	0.00	n.D.	0.00	n.D.	n.D.	n.D.	n.D.	n.D.
Ag	n.D.	n.D.	n.D.	n.D.	n.D.	n.D.	n.D.	n.D.
Cd	n.D.	n.D.	n.D.	n.D.	n.D.	n.D.	n.D.	n.D.
Sb	0.13	0.01	0.04	0.00	0.09	0.01	0.00	0.01
Te	0.01	0.01	0.00	n.D.	0.01	0.01	0.01	0.01
Ba	0.10	0.02	0.08	0.02	0.02	0.00	0.02	0.00
La	0.03	0.00	0.02	0.00	0.01	0.00	0.01	0.00
Ce	0.08	0.01	0.04	0.00	0.04	0.01	0.03	0.00
W	0.00	0.00	0.00	n.D.	0.00	0.00	n.D.	n.D.
Pt	0.00	0.00	0.00	n.D.	0.00	0.00	0.00	0.00
Pb	0.73	0.07	0.47	0.04	0.26	0.04	0.03	0.00

Fig.S1. SEM images from 1µm fraction S2extracted wit UPW

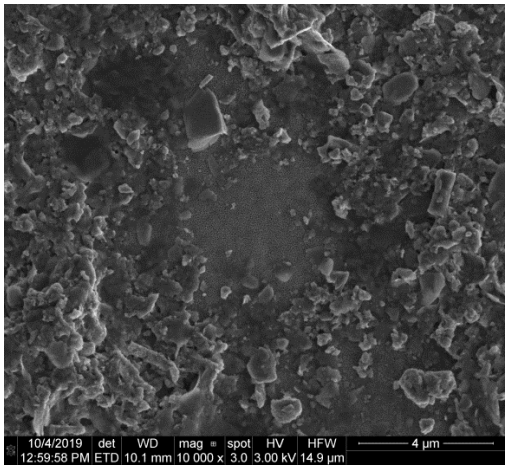

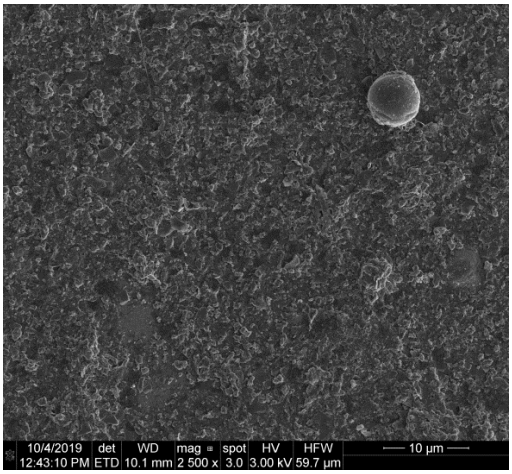

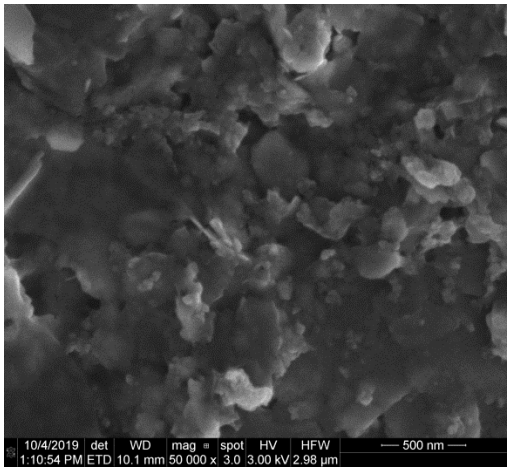

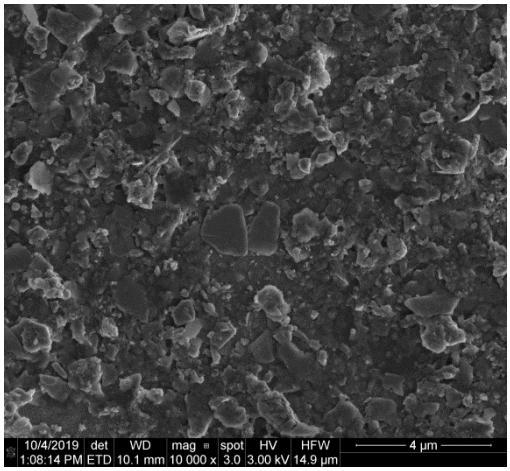

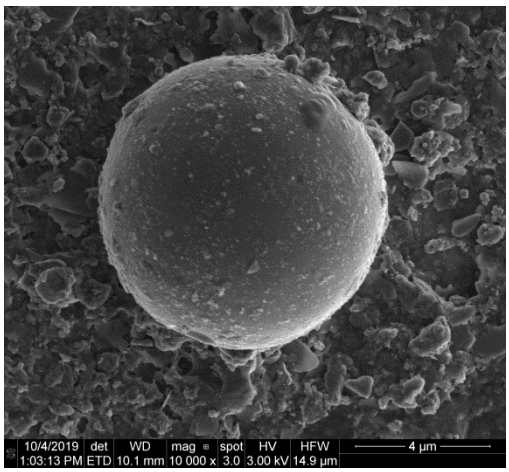

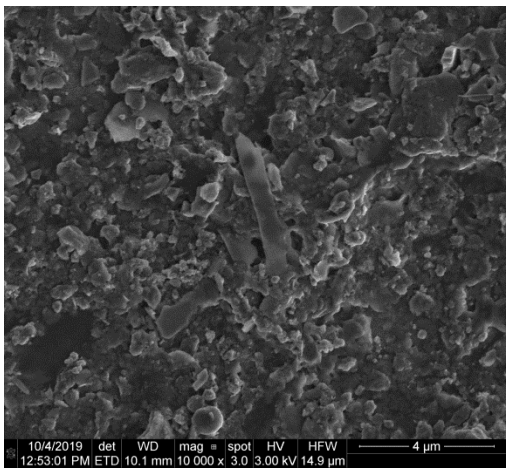

Fig.S2. SEM images from 1µm fraction S2extracted wit SPP